JIMMA UNIVERSTY

JIMMA INSTITUTE OF TECHNOLOGY

SCHOOL OF GRADUATE STUDIES

FACULTY OF CIVIL AND ENVIRONMENTAL ENGINEERING

GEOTECHNICAL ENGINEERING CHAIR

GEOTECHNICAL INVESTIGATION OF LAND SLIDE AND GEOPHYSICAL TECHNIQUES: A CASE OF TULLU GOLA, WEST ARSI ZONE, OROMIYA, ETHIOPIA

A Thesis Submitted to the School of Graduate Studies of Jimma University, Jimma Institute of Technology, Faculty of Civil and Environmental Engineering in Partial Fulfillment of the Requirements for the Degree of Masters of Science in Geotechnical Engineering.

BY: TADESSE GEMECHU TELILA

July, 2022

Jimma, Ethiopia

JIMMA UNIVERSTY
JIMMA INSTITUTE OF TECHNOLOGY
SCHOOL OF GRADUATE STUDIES
FACULTY OF CIVIL AND ENVIRONMENTAL ENGINEERING
GEOTECHNICAL ENGINEERING CHAIR

GEOTECHNICAL INVESTIGATION OF LAND SLIDE AND GEOPHYSICAL TECHNIQUES: A CASE OF TULLU GOLA, WEST ARSI ZONE, OROMIYA, ETHIOPIA

A Thesis Submitted to the School of Graduate Studies of Jimma University, Jimma Institute of Technology, Faculty of Civil and Environmental Engineering in Partial Fulfillment of the Requirements for the Degree of Masters of Science in Geotechnical Engineering

BY: TADESSE GEMECHU TELILA

ADVISOR: - FEKADU FUFA (DR.-ING. ASSOC. PROF.)

CO-ADVISOR:- Mr.TEWODROS TSEGAYE (MSc)

July, 2022
Jimma, Ethiopia

DECLARATION

I hereby declare that all information in this document has been obtained and presented in accordance with academic rules and ethical conduct. I also declare that, as required by these rules and conduct, I have fully cited and referenced all material and results in this my thesis title of " Geotechnical Investigation of landslide and Geophysical Techniques: A Case of Tullu Gola, West Arsi zone, Oromiya, Ethiopia" .

TADESSE GEMECHU TELILA	_____	_____
Name	**Signature**	**Date**

This thesis has been submitted for examination with my approval to University supervisors

Dr.Ing FEKADU FUFA (Dr.-Ing.Assoc.Prof.)	_____	_____
Main Advisor	**Signature**	**Date**
Mr.TEWODROS TSEGAYE (MSc)	_____	_____
Co-Advisor	**Signature**	**Date**
Dr. BISRAT GISSILA (PhD)	_____	_____
External Examiner	**Signature**	**Date**
Mr. CHEMEDA ALEMU (MSc)	_____	_____
Internal Examiner	**Signature**	**Date**
Dr.Alemineh Sorsa (PhD)	_____	_____
Chair Person	**Signature**	**Date**

ACKNOWLEDGEMENTS

Above all, I thank God, my creator, for His support throughout my life, up to this point. I would like to extend my sincere thanks and appreciation, especially to my advisor, Fekadu Fufa (Dr.-Ing. Assoc. Prof.) and co-advisor, Mr. Tewodros Tsegaye (MSc.), for their guidance throughout the making of this thesis. I wish to acknowledge the advice and encouragement I received from them. I am grateful to my beloved family. Their encouragement and support inspired me to pursue my studies and assisted me in overcoming obstacles along the way.

ABSTRACT

Landslides are one of the most destructive natural dangers, and they have a direct and indirect impact on a variety of human activities. On May 18, 2018, a landslide occurred in Tullu Gola Peasant Association, Nansabo district, West Arsi Zone, Oromiya Regional National State. The landslide destroyed more than 15ha of land, four dwelling houses, trees mixed with coffee, cultivated land, a dry-weather road, animals, grassland, and a tiny spring, as well as disrupting Tullu Gola's socio-economic operations. Therefore, the purpose of this work was to determine the causes of landslides by employing geotechnical conditions and geophysical techniques. Slope stability analysis of the research area was done using the finite element method (PLAXIS 2D version 8.2). To determine subsurface conditions, geophysical methods were conducted. Soil samples were taken from the top, right, left, and bottom of the slopes. The soil type of the study was dominated by fine-grained soils (silty), which was expected to be one of the triggering factors, especially during the rainy season. On May 18, 2010, this entry was published. The triggering factors that initiated the landslide, in addition to soil type, were heavy rainfall, deforestation, and various streams found along the landslide affected area. The landslide of the study area was also caused by inherent unstable geological structures, elevation, and steepness of slope. The factor of safety obtained in the affected area (the top side of the slope) was 0.62; in the same way, the factor of safety for the right side of the slope was around 1, which is in the range of an unstable slope. Remedial measures to mitigate landslide risk could be proper slope drainage to reduce water penetration, transferring dangerous settlement and leaving landslide alone (environment preserve, park), and stream train by gabion, which can be located at the higher and lower ends of the research area. Hence, the soil type of the study area was dominated by fine-grained soils and they influenced the occurrence of mass movement in the study area during the rainy season. The geomorphological conditions also play a great role in the stability problem of the study area. Stability conditions on the slope also exist in unstable conditions. Provision of surface drainage and engineering structures like gabion walls were forwarded as remedial measures to safeguard future failures of the slope of the study area.

Key words: *FEM; Geotechnical Conditions; Landslide; PLAXIS 2D; Slope Stability*

TABLE OF CONTENTS

Contents **Pages**

LIST OF TABLES

LISTS OF FIGURES

ACRONYMS

ASTM	American Society for Testing and Material
B.S.T.P-2	Bottom Side Test Pit Two
C	Cohesion
DEM	Demographic Elevation Model
EP	Electrical Profiling
ERT	Electrical Resistivity Tomography
ERA	Ethiopian Road Authority
F.S.	Factor of Safety
GIS	Geographic Iinformation System
GPS	Global Positioning System
GWT	Ground Water Table
Ha	Hectare
ϕ	Internal Angle of Friction
LS	Landslide
LULC	Land Use/Land Cover
L.S.T.P-1	Left Side Test Pit One
LL	Liquid Limit
MER	Main Ethiopian Rift
NE	North East
PI	Plasticity Index
PL	Plastic Limit
R.S.T.P-4	Right Side Test Pit Four
SE	South East
T.S.T.P-3	Top Side Test Pit Three
UCS	Unconfined Compressive Strength
USCS	Unified Soil Classification System
VES	Vertical Electrical Sounding

SYMBOL

(°)	Degree
gm/cm^3	Bulk Density
kN/m^3	Cohesion Pressure
gm/cm^3	Dry Density
m	Diameter of Sample
hrs	Time
°C	Temperature
Kpa	Cohesion pressure
cm/s	Permeability
g	Mass of sample
m	Height of Sample
kN/m3	Saturated unit weight
kN/m3	Unsaturated unit weight
Mpa	Triaxial Loading Stiffness Reference (E^{ref}_{50})
Mpa	Oedometer Loading Stiffness Reference (E^{ref}_{oed})
Mpa	Triaxial Unloading and Reloading Stiffness Reference
m/day	Permeability
kg/m3	Density of soil
kPa	Unconfined Compressive StrengthResistivity
ohm-m	Resistivity
Ml	Volume of Sample in Water
Cm3	Initial Volume of Sample

FORMULAE

- $E_{oed} = Eoed^{ref}(\frac{c\cos\phi - \sigma 1\sin\phi}{c\cos\phi + prefsin\phi})^{m}$
- $k_o^{NC} = 1 - \sin\phi$
- $E_{ur}^{ref} = 3\ E^{ref}_{50}$
- $E^{ref}_{50} = \frac{50\%\sigma}{50\%\varepsilon}$
- Cc(compression Index) = $0.2343[\frac{LL(\%)}{100}]Gs$
- Cs(swelling Index) = $\frac{(e3-e4)}{log\frac{\sigma 4}{\sigma 3}}$
- K(permeability) = $\frac{Rtalog\frac{ho}{h1}}{At}$
- OCR = $\frac{\sigma' c}{\sigma'}$
- W(water content) = $\frac{Mw}{Ms}$*100
- Gs(specific gravity) = $\frac{Ms}{Vs\rho w}$
- PI(Plasticity Index) = LL – PL
- FS(Free Swelling) = $\frac{(Vf-Vo)}{Vo}$*100
- Unit weight (γ)= $\frac{W}{V} = (\frac{G_S + S_e}{1+e})\ \gamma_w$
- Dry unit weight (S=0) = $\frac{w_s}{V} = (\frac{G_S}{1+e})\ \gamma_w = \frac{\gamma}{1+w} = G_s\gamma_w(1\text{-}n)$
- Saturared unit weight (S=1); $\gamma_{Sat} = (\frac{G_S + e}{1+e})\ \gamma_w$

CHAPTER ONE
INTRODUCTION

1.1. Background

Natural disasters such as landslides are common around the world and are caused by geological and geomorphologic processes (F.Mahler et al. 2012). Numerous natural phenomena, such as torrential downpours, snowmelt, groundwater inundation and drainage, erosion, earthquakes, volcanic activity, and modification of the terrain, can cause it to start. Landslide hazards are brought on by human-caused activities such as deforestation and building operations like excavation (Hamza and Raghuvanshi, 2017).

The main contributing factors to previous landslides in Ethiopia in the past have been geomorphological factors like elevation, slopes, aspects, soil infiltration capacity, surface excavations, and rainfall; complex and fragile geology with increased human activities like building roads on mountains; land use and land cover change; and heavy rain (Woldearegay et al., 2004; Woldearegay, 2013; Abebe et al., 2010). A variety of initiating and triggering variables are linked to the movement of landslides. Rainfall, shifting groundwater levels, shifting slope geometry, and geological formations are a few of these variables. It's crucial to have a combination of heavy rains, steep terrain, and soil conditions (Liu, Zheng, and Hu, 2013). Volcanic activity has shaped the landscape in the Tullu Gola Peasant Association Nansabo District. Precambrian basement, Mesozoic sedimentary rocks, and Cenozoic volcanic rocks form the foundation of the Tullu Gola that was discovered in the Nansabo District (Abebeet al., 2010). The unconformable sedimentary and volcanic rocks are deposited on top of the Precambrian rocks. A plateau was created in a series of terraces as a result of several eruptions. Erosion has changed the landscape in modern times. At the highest points of the relief, the cones and domes are still discernible. Rivers have carved out a number of imposing canyons lower in the landscape.

The slide area caused a deep hole, cracked and uprooted trees, blocked stream drainage pipes on both the surface and below ground, and destroyed cow grazing pasture (Lollino et al., 2015). The hills are primarily convex in shape. This can occasionally be a result of an old lava flow, but it can also be the result of past landslide activity. Large rock fragments raised by plows in the field indicate that these hills were formed by landslides. On May 18, 2018, a rapid landslide occurred

in the Tullu Gola Peasant Association in the Nansabo district of the West Arsi Zone of the Oromiya Regional National State, destroying more than 10 acres of land under persistent, heavy rain. The local topography makes the area vulnerable to erosion and subsurface scarring, which sets up the necessary conditions for surface runoff to enter weak areas and start land slides. By using prior fieldwork and soil laboratory testing experiments, this study will conduct a geotechnical and geophysical approach examining the causes of landslides in the area and assigning the proposal to minimize the problem.

1.2. Statement of the Problem

One of the most significant environmental issues on the globe is landslides. According to a number of sources, from 2004 to 2016, there were 55,997 fatalities worldwide due to land slide threats (Patra and Devi, 2018). Several studies conducted in various regions of Ethiopia revealed that landslides were responsible for disasters in the northern highlands (Dessie areas, Shale hill slopes, Tigray, Tekeze areas), central highlands (Abay basin, Jimma basin, West Shoa, Tarmaber and surroundings), southern regions (Gilgel GibeII, Sodo Shone area, and Wondo Genet), as well as a number of locations along the Ethiopian margins (Woldearegay

In various regions of Ethiopia between 1993 and 1998, 300 lives were lost, 200 homes were destroyed, a 100-kilometer road was damaged, and more than 500 hectares of agricultural land were destroyed (Ali, Tiruneh et al., 2017). More than 135 human deaths, 1450 destroyed homes, 6,500 people uprooted, more than 2000 hectares of land damaged, more than 100 km of asphalt roads damaged, and 1.5 million dollars worth of resource damage were all reported between 1999 and 2008. (Woldearegay, 2013; Yifru and Ayehu, 2017).

In the southern part of Ethiopia, a landslide danger brought on by the torrential rains during the summer of 2018 resulted in 12 homes being damaged, more than 6 hectares of land being damaged, 23 human fatalities, 15 human injuries, and over 30 domestic animal deaths (Kabeta and Teshager, 2020). In 2017, the sliding of landfills caused more than 30 fatalities in Addis Abeba. According to Woldearegay (2013), landslide disasters in Ethiopia may be more severe than what has been documented because many of them have gone unreported unless they have affected areas that depend on the government for vital support. Landslide-related hazards are causing severe worries among Ethiopians in general as well as among planners and decision-makers at different levels of government.

A sudden landslide in 2018 destroyed more than 15 hectares in the West Arsi zone, Nansabo District, and Tullu Gola Peasant Association. The West Arsi zone is situated in southern Ethiopia, 415 kilometers from Addis Abeba, the country's capital. The research area features ponds, a creek that runs between the sliding zones, some trees, grass, and coffee. As a result, there is a landslide risk in this location. A total of 50 livestock, 100 hens, 100 goats, and 24 people perished. About 10 acres of agriculture were destroyed, along with the displacement and homelessness of twenty Abbaa warra. In the study region, landslides rendered a total of 15 hectares of land unusable. This research was carried out in order to better understand the causes of landslides in the case study area utilizing geotechnical and geophysical approaches.

1.3. Objective

1.3.1. General objective

The main objective of this research work is to investigate the causes of landslide in Tullu Gola Peasant Association using geotechnical investigation and geophysical techniques.

1.3.2. Specific Objectives

Specific objectives of the study are:

1. To investigate the geotechnical characteristics of the soils of the study area;
2. To figure out what the most common causes of landslides are in the study area;
3. To find out how deep the groundwater table is ; and
4. To suggest possible remedial measures to minimize the risk of the occurrence of landslides in the study area;

1.4. Research Questions

The research questions that the researcher had required to be answered were as follows:

1. What is the geotechnical characterization of the soil of the study area?
2. What are the most common causes of landslides are in the study area?
3. At what depth the Groundwater table found?
4. What are the possible remedial measures that might be applied in order to alleviate the landslide problems?

1.5. Significance of the Study

The study's main contribution is to the communities' early preparation for the negative effects of landslides. It is used to identify the elements that cause a slope to shift and to provide information about a region that is prone to sliding. Additionally, all currently employed engineers, graduate students, and decision-makers will use this research as a starting point as they continue to look into the factors that trigger landslides and evaluate slope stability.

1.6. Scope of the Study

The goal of the study is to evaluate the causes of landslides and set the parameters for a slope stability analysis of the area using field test equipment, visual observation, GPS, and geophysical and geotechnical laboratory tests. Consolidation, Triaxial, Atterberg limit, moisture content, specific gravity, grain size, wet sieve analysis, hydrometer analysis, permeability, unconfined compression strength, and swelling free lab tests were among the tests that were carried out. We used both the disturbed and undisturbed samples. The applications selected for the issue's evaluation and analysis were Arc GIS 10.3 and Plaxis-2D. Arc GIS 10.3 was used for delineation. It has several easy-to-use built-in capabilities and can produce a derivative map from the DEM. Vertical electrical sound testing and resistivity profiling were analyzed using the programs Res2dinvx64 and Win Resist, respectively. The program's user-friendly graphical user interface makes it simple for users to generate a geometric model and finite element mesh. Utilizing characteristics from geotechnical laboratory test results as input for the Plaxis-2D software tool, a safety factor was generated.

1.7. Limitations

The research has the following limitations:

1. Despite the study's positive contribution to the scant body of knowledge on landslides in Ethiopia, topographical changes made it challenging to expand the study's scope and conduct enough field tests.
2. Due to the unfavorable area for sampling, it was difficult to get random transport access to go slide area and receive data.
3. Due to the gorge, it was dangerous as we wanted to take the sample and work with geophysics.

1.8. Structure of the Thesis

This thesis was divided into five chapters, each of which contains the following information: The first chapter is an introductory chapter that provides an outline of the research and the topic area. The literature review in Chapter 2 is about landslide occurrences, affecting factors, and mitigation techniques; Chapter 3 is about materials and methods; Chapter 4 is about the results and discussion; and Chapter 5 is about the study's conclusions and recommendations.

CHAPTER TWO
LITERATURE REVIEW

2.1. General

A landslide (LS) is described as the movement of a mass of rock, debris, or earth down a slope (Cruden, 2003). They are a major issue around the world, taking thousands of lives every year (Patra and Devi, 2018). Due to high rates of precipitation and weathering, especially in areas with steep topography and tectonic activity, many regions, especially in the tropics, are severely influenced by LS (Highland and Bobrowsky, 2008). In addition, LS risk in the tropics is probably going to increase in the near future due to growing demographic pressure, deforestation, and changes in land use (Lollino et al., 2015), as well as climate change (Guerra et al., 2017).

Additionally, the bulk of LS-related deaths take place in countries in the Global South, the majority of which are tropical (Mr. Digvijay P. Salunkhe et al., 2017). In addition, LS may have a severe negative influence on people in tropical developing nations because of their high economic, social, political, and cultural sensitivity (Yifru and Ayehu, 2017). Mountainous areas are subject to mass movements because of triggering and preparatory or conditional causal factors. The external stimuli (such as rain, tremors, and land use) that actually cause mass movements to start are referred to as initiating causal factors.

Slope instability, in contrast, is brought on by conditional variables such as topography, soils, weathering, and geology. In 2011, anthropogenic activities in mountainous areas frequently produce unstable spots in the earth's composition on hill slopes (Hulagabali, Gudissa, and Ararsa, 2008). With regards to various landslides, weather might be a problematic problem. Extreme weather conditions, such as extended or heavy rain, can result in landslides, which can be risky (McColl, 2015). Sliding happens when shear stress is greater than shear strength. Under typical conditions, the balance between shear stress and shear strength is maintained (Liu, Zheng, and Hu, 2013).

2.2. Types of Landslides

The term "landslide" has been defined in many different ways, and each definition classifies it according to its study objectives. Abebe et al. (2010) provide a thorough assessment of the materials on which landslides occur and the types of landslides related with them in northern Ethiopia in their paper on landslides in the Ethiopian highlands and the rift edge. According to the authors, there are five different types of landslides. The first type of landslide is modeled on hard bedrock, such as basalt, and happens on steep slopes. Fast mass movement in this area in the environment is frequently associated with rock slides, topples, and collapses.

The second category of quick landslides—debris slides and earth flows—and the steep slopes on weathered pyroclastic and volcanic agglomerates are connected. Rapid collapse phenomena like slumps, which are frequent in the alluvial banks of deeply incised rivers, are the third type of slope morphology. The fourth type of landslide forms on clayey materials. These clay minerals arise from volcanic bedrock or sedimentary deposits. The fourth type of landslide often follows several generations of landslide activity in the landscape. In the final group, clayey formations are covered by thick layers of hard rock (Abebe et al., 2010a). The four types of landslides described by Cruden (2003) are further described below.

The following types and modes of movement distinguish various types of landslides.

2.2.1. Falls

The fastest kind of landslide, called a fall, begins on cliffs or steep slopes and descends either vertically or at a sharp angle. Falls range from small streams of dirt or stones to the abrupt shearing of a significant portion of a rock face. Falls, as defined by Highland and Bobrowsky (2008), are the abrupt movement of large geological masses, such as rocks and boulders, that separate from the cliffs or steep slopes. According to Gaurina-Medjimurec (2014), a region's susceptibility to rock fall is mostly determined by the location and direction of cracks, bedding, and other geological discontinuities. The main locations for rock fall are stream banks, highway and railroad cuts, abandoned mine and quarry regions, and other human-made steep slopes.

2.2.2. Slumps

A slump is a slide that has a downward rotating component and travels along a concave shear surface with a base movement that is greater than the top movement. The most frequent causes of slumps are: a rise in moisture content, which reduces strength; (ii) removal of support at a slope's toe; (iii) addition of material at a slope's top; and (iv) the creation of a cut or filled slope that is too steep for the materials involved to be stable. Slump collapse frequently happens in uniformly thick soils and worn rock, but it can also happen in bed rock (Cruden and Varnes, 1996).

2.2.3. Topples

Generally speaking, the failure is determined by the fracture pattern in rock caused by abrupt falling, sliding, bouncing, and rolling. A topple is the tilting of a rock without collapse, or by the forward rotation of rocks about a pivot point at a quick rate of movement. These blocks or columns are typically identified by the junction of joints or other fractures, and erosion frequently disturbs their basal stability (Highland and Bobrowsky, 2008).

2.2.4. Slides

A slide is the mass movement of soil or rock that occurs as a coherent unit by slipping along one or more failure surfaces. According to Highland and Bobrowsky (2008), the two major types of slides are rotational and translational slides. Rotational slides are in which the surface rupture is curved concavely upward and the slide movement is roughly rotational about the axis that is parallel to the ground surface and transverse across the slide(Kabeta and Teshager, 2020). A translational slide is a landslide mass which moves along a roughly planar surface with little rotation or backward tilting.

2.2.5. Flow

A mass movement known as a flow has a disorganized, chaotic, and turbulent internal structure (Highland and Bobrowsky, 2008). In a sediment flow, the rock and/or soil that are involved are combined with air or water, which gives the flow a lubricating effect. Granular sediment flows are defined as having less than 20% water content and slurry sediment flows as having between 20% and 40% water content. Both granular and slurry flows have the ability to pick up debris as

they go down a slope or channel; if enough foreign material gathers, the flow may be referred to as a debris flow.

According to Highland and Bobrowsky (2008), there are five sorts of flows that are distinct from one another. These are: Is Debris flow: this rapid mass movement is made up of air, water, loose soil, rocks, organic matter, and organic matter that has been mobilized as slurry and is flowing down the slope. Debris flows frequently result from other forms of landslides that happen on steep slopes, are practically wet, and contain a significant amount of debris the size of silt and sand. (ii) Debris Avalanche: This is a type of highly rapid to very quick debris flow. (iii) Earth flow: This type of flow is elongated and typically occurs on moderate slopes and in saturated conditions in materials with fine grains or rocks containing clay. (iv) Mud flows: These are earth flows that are moist enough to move quickly and contain at least 50% sand, silt, and clay-sized particles. (v) Creep: The gradual, continuous downward movement of soil or rock that forms slopes. Shear stress that is large enough to create permanent deformation but not enough to cause shear collapse is what causes movement. Tree trunks that are curled, fences or retaining walls that are bowed, poles or fences that are skewed, and minor soil ripples or ridges are all signs of creep. In addition to the categories of landslide types already mentioned, toppling and lateral spread (J.Crozier, 2004).

Table 2-1: Landslide classification after (Misilimba, 2007)

<table>
<tr><th colspan="3" rowspan="3">Type of movement</th><th colspan="3">Type of material</th></tr>
<tr><td rowspan="2">Bedrock</td><td colspan="2">Engineering soils</td></tr>
<tr><td>Predominantly coarse</td><td>Predominantly fine</td></tr>
<tr><td colspan="3">Falls</td><td>Rock fall</td><td>Debris fall</td><td>Earth fall</td></tr>
<tr><td colspan="3">Topples</td><td>Rock topple</td><td>Debris topple</td><td>Earth topple</td></tr>
<tr><td>Slides</td><td>Rotational</td><td>Few units</td><td>Rock slump</td><td>Debris slump</td><td>Earth slump</td></tr>
<tr><td></td><td>Translational</td><td>Many units</td><td>Rock slide</td><td>Debris slide</td><td>Earth slide</td></tr>
<tr><td colspan="3">Lateral spreads</td><td>Rock spread</td><td>Debris spread</td><td>Earth spread</td></tr>
<tr><td colspan="3">Flows</td><td>Rock flow</td><td>Debris flow</td><td>Earth flow</td></tr>
<tr><td colspan="3">Complex</td><td colspan="3">Combination of two or more principle type of movements.</td></tr>
</table>

2.3. Causes Triggering Landslides

2.3.1. Effect of Slope Steepness

Shear stress, also known as the tangential component of gravity, rises on steeper slopes while the perpendicular component of gravity falls. Shear strength, which comprises frictional resistance and cohesiveness among the constituent particles, refers to the forces preventing motion down the slope. The slope collapses when the shear stress exceeds the shear strength (Kabeta and Teshager, 2020).

2.3.2. Geotechnical Properties of Soils

A quantitative assessment of soil shear strength is necessary for evaluations of slope stability using limiting equilibrium techniques (Geertsema, Highland, and Vaugeouis, 2009). This sheds light on crucial engineering properties that affect slope stability and how these properties relate to other aspects of soil attributes (Azeze, 2020). The stability of both natural and man-made hill slopes is governed by a fundamental feature called soil shear strength (Coutinho and Da Silva, 2013). It is not a unique value, though, because loading, unloading, and water content in particular all have a significant impact. The basic definition of the shear strength of soil material is a function of three shear strength parameters: normal stress on the slip surface (NSS), cohesion (C), and internal angle of friction (IAF).

Soil cohesiveness is decreased as soil moisture is increased. Soil strength decreases as suction decreases. Drawing water out of soil is known as suction. The internal angle of friction is especially significant in low cohesion soils, where rooting strength and cohesion are augmented in field soils (Fisseha and Mewa, 2016). Sands are true cohesion-less soils with a single-grained structure whose shear strength is primarily derived from granular friction and grain interlocking. Cohesive soils' significant characteristic of shrinkage has an impact on the stability of the slope. The possibility of shrinking and expanding is higher in expansive clays (such as montmorillonite and vermiculite) than in non-expanding clays (kaolinite). Smaller particle size and a higher plasticity index cause more drying-related shrinking (Gaurina-Medjimurec, 2014).

2.3.2.1. Swelling and Shrinkage of Soil Particles

Msilimba (2012) Mention how the expansion and contraction of water or soil in pore spaces and bedrock fissures may result in slope failure. The triggering of a landslide is triggered by the

expansion and contraction of soil particles. When there is humidity, soil particles grow; when there is less moisture in the soil, they contract. This is what causes a landslide to occur.

2.3.3. The Effect of water

Water has a significant role in the mass waste process. Water will either cause material to slip downward like a liquid or help hold it together, increasing its angle of repose (Duan, Chen, and Niu, 2019). Water serves as a lubricant or a glue in mass waste. Water may strengthen materials in small amounts. Because the tiny layer of water that separates the particles enhances the strain holding them together, slightly damp particles have a larger angle of repose. Sand serves as a good illustration of this process. Sand that is dry is not very cohesive. Dry sand cannot be used to build very tall sand castles (Gaurina-Medjimurec, 2014). One constructed of slightly moistened sand will do, though. But if you add too much water, the sand will get soggy and the castle will crumble. Water saturation causes a material's angle of repose to slightly decrease and the tendency for the material to flow like a liquid. This happens because the extra water completely envelops the material's particles, removing the frictional contact that binds them together (Broothaertset al., 2012).

Additional water adds to the mass of the material on a slope. Weight and mass are measures of how much matter is in an object and how much force gravity is exerting on it, respectively. The mass of an object determines how much gravitational force there will be; the heavier the object, the more force there will be. The force of gravity acting on a piece of material on a slope will grow as its mass does. Waterlogged material is subject to significant shear stress and will slide or flow down a slope under that force of gravity since there is little to no friction between its particles.

2.3.4. Human Activities

2.3.4.1. Vegetation Cover Destruction

Landslides are influenced by a variety of variables, though deforestation speeds up mass movement (Nelson, 2013). For instance, huge landslides tend to occur where mature, vigorous vegetation is present. Even though a region may have experienced deforestation, this is frequently partially countered by recolonization (Liu et al., 2017). Deforestation techniques and subsequent ground treatment have an impact on the degree and rate of strength loss (Ortigao, Sayao, and Sayao, 2004). On steep jointed rock, the vegetation cover could constitute an unstable force.

Global warming will affect the economy, agriculture and forestry practices, land usage and cover, and many other factors. These changes may also alter the frequency and activity of landslides, altering the danger and hazard associated with them (Patra and Devi, 2018). Because they are significantly influenced by human activities including poor land use practices, deforestation, and overgrazing, there is now "little confidence in estimates of an anthropogenic effect on occurrences like shallow landslides in temperate and tropical regions" (Radbruch-Hall and Varnes, 1976).

2.3.4.2. Infrastructure Development

The stability of slopes can be significantly impacted by earthwork operations involving huge land surfaces in hilly environments. The removal of lateral supports by excavation for road construction, dam construction, housing, and farming is a notable interference (Reichenbach et al., 2014). Landslides can also be caused by other human activities that cause the ground to vibrate.

2.3.5. Geomorphic Factors

The values of the curvature can be used to describe the topography's shape. If the surface at that raster cell is upward concave, the curvature is negative; if it is upward convex, the curvature is positive. Curvature will be zero if the surface is flat. As the negative curvature value increases, so does the likelihood of a landslide. The value is higher in hilly and mountainous locations and lower in flat areas, according to topographic type (Mersha and Meten, 2020).

Gradient of the slope: As the gradient of the slope increases, the shear stress rises as a result of the gravitational impact, enhancing material movement down the slope. Mengistu and Senamaw (2020) assert that slope gradient is the primary cause of mass movement, particularly for shallow landslides. The key causal factor in most landslide assessments is the slope gradient (Mia, Sultana 2016).

The slope's aspect is the direction that it is facing. Through differential evaporation, it has a significant impact on hydrological processes, which in turn influences weathering and root development, especially in dry areas (McColl, 2015). Aspect and bedrock structure are intimately connected, especially in metamorphic rocks. On slope aspects parallel to the direction of foliation and lineation planes, rock failures are frequent (Mia, Sultana, and Paul, 2016).

Table 2-2: Causes of Landslides (Choi and Cheung, 2013)

External Causes	Internal Causes
1. Geometrical change ➢ Height ➢ Gradient ➢ Slope length	**1.**Progressive Failure (internal response to unloading) ✓ Expansion and swelling ✓ Fissuring ✓ Straining, softening ✓ Stress concentration
2.Loading ➢ Natural ➢ Man-induced	**2.**Weathering ✓ Physical property changes ✓ Chemical changes
3. Unloading ➢ Natural ➢ Man-induced	3. Seepage erosion ✓ Removal of cements ✓ Removal of fine particles
4. Shocks and Vibrations ➢ Single ➢ Multiple/continuous	4. Water regime change ✓ Saturation ✓ Rise in water table ✓ Excess pressures ✓ Draw down

2.3.6. Hydrologic Factor

A significant factor in landslide initiation is hydrology (Wang and Sassa, 2003). Precipitation (spatial and temporal distribution of rainfall), water recharging into soil (and the potential for overland flow), later and vertical movement within the regolith, evapo-transpiration, and interception are some of the most important hydrologic processes in this regard (Duan, Chen, and Niu, 2019).

An increase in precipitation total is anticipated to lead to wetter antecedent conditions, which can have a number of detrimental effects on slope instability, including less rain being needed to reach a critical level that can cause a slope to fail and (ii) a higher water table reducing shear strength, decreasing soil suction and cohesion, and increasing the weight (wet density) of the slope materials, all of which work to increase the risk of failure (Gaurina-Medjimurec, 2014).

2.3.7. Geological Conditions

Potentially weak planes in a slope include geological features such as bedding, joints, foliation, cleavage, faults, and schistosity (Girmaet al., 2015). Their strength is typically lower than that of the nearby solid rock. Slope instability is also caused by the region's tectonic setting, which fractures. Since fault and fracture zones are weak zones, they can be advantageous planes of weakness where failures take place. Understanding their orientation in relation to the slope angle, direction, and strength along such potential weak planes is crucial (Sidle and Ochiai, 2006). Furthermore, Highland and Bobrowsky (2008) suggest that slope stability is significantly influenced by the degree of fracture and shearing.

2.3.8. Weathering of the Slope Forming Materials

Weathering is a continuous background process that degrades material strength over time (Guerra et al., 2017). It is seldom the direct cause of land slides, though. The initial mineralogy, the kind of climate, and the biological habitat all affect weathering. Indirectly, weathering also contributes to slope failure by increasing permeability and pore water pressure (Hamza and Raghuvanshi, 2017).

2.3.9. Seismicity and other Vibrations

Earthquakes cause a shearing stress and a decrease in the slope material's resistance, which both lower stability. According to McColl (2015), there are three main effects of earthquake wave propagation: the direct mechanical effect of horizontal acceleration, which temporarily increases shearing stress; the cyclic loading, which weakens inter-particle bonding and results in liquefaction; and the reduction in inter-granular bonding by sudden shock, regardless of the degree of saturation.

2.4. Classification of Condition of Slopes

Slopes can be classified into three categories based on (Symposium, 2018). (1) Stable slopes are ones that have a high enough margin of stability to withstand any destabilizing factors. (3) Actively unstable slopes are those that move continuously or intermittently due to destabilizing forces. Two (2) marginally stable slopes are those that may eventually collapse as a result of the destabilizing force reaching a critical degree of activity.

2.5. Ground Investigations

According to Tsige, Quezon, and Woldearegay (2017), additional investigation of an existing slope or the site on which a slope is to be created is necessary in order to gather crucial drilling data. This information will provide details on the strata, moisture content, and degree of standing water. The parameter values required for the study must be established before a geotechnical analysis can be carried out. These are internal friction angle, cohesiveness, and unit weight.

2.5.1. Geotechnical Parameters

The parameter values required for the study must be determined before a geotechnical analysis can be carried out (Choi and Cheung, 2013). Unit weight, cohesion, and angle of internal friction are those variables.

2.5.2. Type of Soil

Soils, or more accurately, earth materials, are categorized by geotechnical engineers according to their slope stability, foundation support, or suitability as a construction material (Broothaerts et al., 2012). Based on a few straightforward laboratory or field experiments, these systems are intended to forecast some of the engineering qualities and behavior of a given soil.

2.5.3. Geophysical Survey

Many geophysical surveys can be conducted to comprehend the earth's surface. Electrical resistivity is the one geophysical survey out of the others (Marwa Mostafa, Amr Radwan, 2016). The goals of geophysical investigations are to measure the depth of the water table, the potential aquifer depth, the geologic unit's fracture zone, the potential location of ground water, and the various resistivity zones. Determine the electrical resistivity layer in relation to the geologic unit beneath the earth, identify different electrical resistivity layers of the geologic formation and structure beneath the earth, and determine weak zones with depth underground. You can also use the resistivity values of the area to determine the direction of ground water flow based on the structures you see along the study's path. The two main types of electrical resistivity are profiling and VES (vertical electrical sounding). In order to identify subsurface anomalies, geophysics uses non-intrusive methods rather than destructive excavation (Marwa Mostafa, Amr Radwan, 2016). A resistivity survey is conducted in order to ascertain the distribution of subsurface resistivity from measurements of potential difference, or voltage, taken on the ground surface. Based on the presumption that subsurface geological materials exhibit a wide range of resistivity

values and that geological boundaries can be recognized based on measurements of resistivity, the electrical resistivity technique was developed (Marwa Mostafa, Amr Radwan, 2016). Surface voltage measurements after injecting current via two electrode pairs can identify a target of interest if its electrical resistivity contrast with the surrounding material is sufficiently large (Marwa Mostafa, Amr Radwan, 2016).

Depending on how far apart the current and potential electrodes are in the survey, resistivity values are connected to different depths and can be understood in terms of a lithologic or geohydrology model of the subsurface (Figure 2.1).

One of the most common geophysical research techniques used to ascertain the soil's subsurface condition is electrical resistivity tomography (ERT). ERT is widely employed in studies of geohazards and geophysical investigations of soils at shallow depths. (Marwa Mostafa, Amr Radwan, 2016).

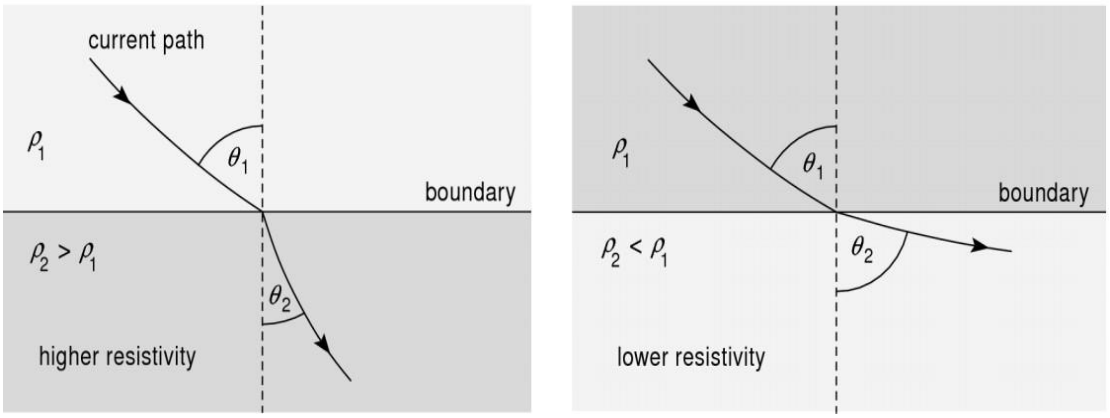

Figure 2-1 Geophysical resistivity investigation method (Lollino et al., 2015)

Analysis of the lateral (imaging) and vertical fluctuations in subsurface moisture content and nearby geology was part of the geophysical resistivity assessment of the subsurface conditions. Different minerals and rocks have various particular resistivity values (Table 2.3).

Table 2-3:Specific resistivity of various rocks and minerals (Marwa Mostafa, Amr Radwan, 2016)

S/N	Rock type/Material	Specific Resistivity (ohm-m)
1	Clay, marl, rich	3 - 30
2	Clay, marl, meager	10 - 40
3	Clay, sandy, silt	25 – 150
4	Sand, with clay	50 - 300
5	Sand, gravel in ground water	200-400
6	Sand, gravel, dry	800 - 5000
7	Rubble, dry	1000 - 3000
8	Limestone, gypsum	500 -3500
9	Sandstone	300- 3000
10	Salt beds and salt domes	>10000 high resistivity value
11	Granite	2000 - 10000 “
12	Gneiss	400- 6000 “

2.5.3.1. Electrical Profiling (Imaging)

using a Wenner array of cables that were obtained and electrodes with a Syscal Junior instrument to profile (image). The software Res2divn*64 is used to process the data collected by this instrument in order to perform profiling. As an alternative, extensive methods for subsurface characterization and knowledge of pertinent material qualities can be obtained using surface geophysical techniques (Marwa Mostafa, Amr Radwan, 2016). Geophysics is frequently a very cost-effective and efficient way to create contiguous 2D and 3D images of the subsurface and identify in-situ bulk properties, but it is not a replacement for geotechnical boring or testing (McColl, 2015).

2.5.3.2. Vertical Electrical Sounding

Using a Schulumberger array with electrodes spaced apart on either side of the cable, this vertical electrical resistance is conducted (Badr and Anwar, 2015). The electrical resistivity approach is applied using arrays with four electrodes; two current electrodes (A and B), and two potential electrodes (C and D). Ohm's law serves as the foundation for the link between electrical resistivity (R), current (I), and electrical potential (V). The geometric factor K, which varies depending on the kind of array, can be used to calculate the apparent resistivity (a) of subsurface soil (Patra and Devi, 2018). In order to produce a 1-D vertical apparent resistivity versus depth

model of the subsurface at a single observation location, vertical electric sounding (VES) uses collinear arrays. This method involves keeping a constant central reference point while collecting a series of potential differences at progressively wider electrode spacings.

At wider electrode spacings, the produced current penetrates increasingly deeper strata. The measurements of the potential difference are directly related to the changes in the deeper subsurface. The depth of the water table, the thickness and depth of the subsurface strata, and the overburden thickness can all be used to evaluate apparent resistivity values derived from measured potential differences. The Wenner and Schlumberger arrays are the two most popular arrays used for VES. When it comes to landslide investigation, ERT was used to find highly saturated and clay-rich zones that showed low resistivity (10–40 m) in the landslide (Perera et al., 2018).

2.6. Effect of Landslide

2.6.1. Landslide Related Costs

According to Msilimba (2012), the cost of landslide activity can be divided into three categories: personal loss, economic loss, and environmental harm. They could be short-term or long-term. Because landslides are connected to simultaneously occurring dangers, estimating the cost is challenging. The difficulty in obtaining data that is accurate or representative enough to show the true cost and trend of landslide hazards exacerbates this issue. (Abebe, Kumar Raghuvanshi, and Mulatu, 2009).

2.6.2. Environmental Costs

The slope and downstream implications may both be severe and long-lasting in extremely unstable situations that produce frequent or substantial volume slope shifts (McColl, 2015). Degradation of habitat, drainage system derangement, modification of drainage pathways, destruction of riparian vegetation, bank erosion within the stream channel, accelerated meander development, impediment to fish migration, and loss of the scenic beauty of mountainous environments are just a few of the environmental costs.

2.6.3. Economic Costs

The nature of society and the type of damaged area determine the direct economic effects of landslides. The direct costs of smaller-scale disasters are lower, yet they occur more frequently (Hulagabali, Gudissa, and Ararsa, 2008). Landslide-related indirect costs include mobilizing and supporting relief efforts; providing temporary housing or replacement housing; and supplying

food. Preventative costs, which are more difficult to quantify, include the price of conducting research and the price of putting preventative or control measures into place.

2.6.4. Personal Costs

Death, injury, and persistent issues with physical and mental health are all personal costs. These impacts can necessitate an expensive correction process. Long-term costs of injury include the potential reduction of a person's social and productive role as well as the potential for increased expenses for medical care and support (Fry et al., 2019).

2.7. Landslide Mechanics

The circumstance that results in slope movements is known as slope instability. The same author came to the conclusion that sliding occurs when the forces tending to cause movements are greater than those resisting them. On every slope, there are opposing forces (stresses) that tend to promote movement (shear stress) and opposing forces that tend to resist movement (shear strength). Under normal conditions, the shear stress and strength are equal, maintaining a state of equilibrium (Liu, Zheng, and Hu, 2013). However, increases in stress or a decrease in frictional force have the potential to upset this equilibrium.

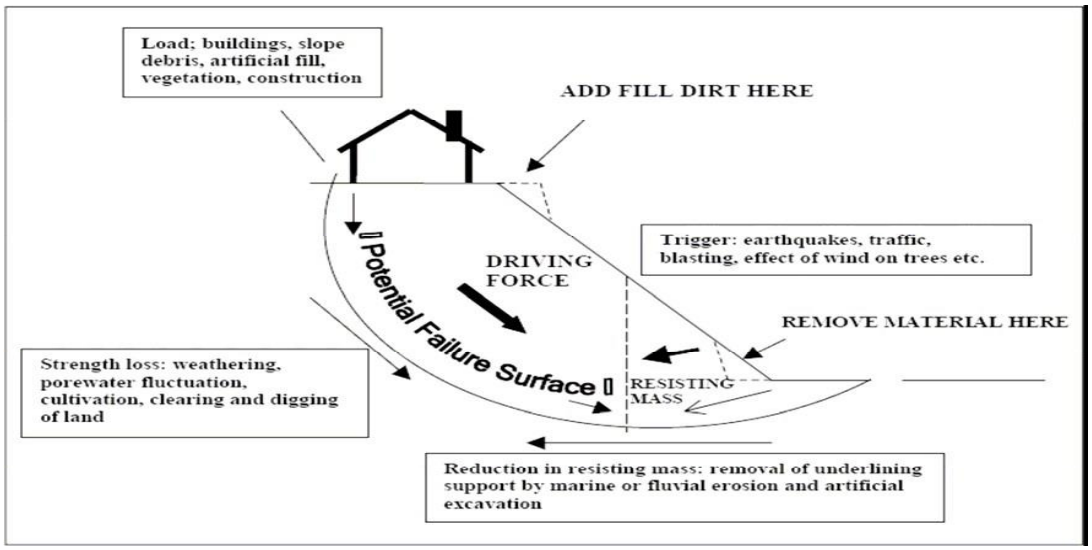

Figure 2-2: Landslide mechanics (Mersha and Meten, 2020)

2.7.1. Stress and Strain

Gravity acts on any mass on an inclined plane, and the magnitude of the gravitational force operating along the slope is precisely proportional to the slope's angle. Any more weight on the

slope increases the force of gravity, which puts the soil/rock mass under more stress (Mulatu, Kumar Raghuvanshi and Abebe, 2009). It should be emphasized that steeper slopes have higher slope angle values, higher gravitational force values, and a higher likelihood of material failure. "Strain" is the term for the impact of this shear stress on the soil or regolith (Patra and Devi, 2018). Although strain and stress are not directly related, it does provide a measurement of how much the stress has twisted the soil or regolith. It is determined by dividing the depth of the material by the displacement of the upper surface in relation to the bottom surface. The distribution of strain in the soil body may not be uniform; instead, it may be limited to the joints, which may finally fracture (Popescu, 2002).

2.7.2. Friction and Cohesion

The strength of the frictional force between the sliding mass and the bedrock has a role in the slope material's failure. The component of the weight of the sliding material perpendicular to the surface and the degree of surface roughness both affect this force. However, it is unaffected by the point at which the body of regolith and the underlying substrata come into contact (Tsige, Quezon and Woldearegay, 2017). Soil material can fail at the same angle in small and big areas. The weight component that is normal to the slope and the coefficient of friction are used to express the size of the frictional force. The "angle of plane sliding friction" is the essential angle at which sliding just starts. The critical frictional resistance and the critical applied force can then be used to express the balance of forces acting on the regolith. When the critical applied force is greater than the critical frictional resistance, failure begins. But for non-rigid objects, there is also an extra force known as cohesiveness that prevents down slope movement (Tsige, Quezon and Woldearegay, 2017).

2.7.3. Shear Strength of the Soil

The internal cohesion of the soil particles as well as the friction created between individual soil grains affect how the particles act collectively or as a mass (Walker and Shiels, 2013). Internal friction or shearing resistance is the name for the latter attribute.

2.7.4. Pore Water Pressure

According to experts, the primary initiating element for land sliding is a change in pore water pressure (Wang et al., 2021). When an external force, such as more water or overburden, is applied to a soil mass on a slope, the pore water pressure rises and water leaks out at weak points

(Tantri, Sari, and Lastiasih, 2014). The effective resistance of the soil body or regolith is decreased by the decrease in pore pressure in the Mohr-Coulomb equation. In this instance, the pore pressure lowers the effective normal stress and increases the soil's shear strength (Walle et al., 2020).

2.8. Slope Stability Analysis

Identifying the factor of safety (FS) of a certain slope, identifying when collapse is imminent, and evaluating corrective measures as needed are the main goals of a slope stability analysis. Therefore, a thorough understanding of geology, hydrology, and soil and rock qualities is required in order to apply slope stability concepts effectively. Engineering decisions must be supported by an evaluation of the findings of analyses that take into account acceptable risk or safety concerns (Hulagabali, Gudissa, and Ararsa, 2008).

2.8.1. Slope Stability Analysis Methods

There are numerous methods for determining if a slope is stable. Early slope stability analysis techniques typically relied on manual calculations that were subsequently sped up. With the widespread availability of sophisticated computers nowadays, specialists have created intricate yet accurate procedures. The following are some details of the slope stability analysis approach employed in this study:

2.8.1.1. Finite Element Method

The finite element method is a powerful calculating method in the engineering sciences. This method is by far the most used for analyzing geotechnical problems (Jacob et al., 2018). The finite element method considers linear and non-linear stress–strain behavior of the soil in calculating the safety factor for the analysis of a slope. In a finite element approach, the slope failure occurs through zones that cannot resist the shear stresses applied (Krahn, 2003). Finite element (FE) software has attracted increasing interest from both researchers and professionals. It is based on constitutive laws and appropriate soil models. A finite element code known as PLAXIS was created by PLAXIS-2D in collaboration with various universities, notably DUT in the Netherlands and NTNU in Norway, to analyze soil and rocks (PLAXIS 2004). (Liu, Zheng, and Hu, 2013).

2.8.2. The PLAXIS Software

In Plaxis, there are various material models to select from. The degree to which these models accurately depict the mechanical behavior of soils is where they diverge. Each model is created to explain the relationship between stress and strain in the material (Jacob et al., 2018).

I) Linear Elastic model (LE) model

The simplest stress-strain relationship available in PLAXIS is the linear isotropic elasticity. The Young's modulus, E, and the Poisson's ratio, v, are the only two input parameters for this model (Vinod et al., 2020). The complicated behavior of soil cannot be explained by a model like this, but it is appropriate for simulating large structural components and bedrock layers.

II) Mohr coulomb model (MC) model

A common first-order model for modeling soil action in general is the elastic-perfectly plastic Mohr-Coulomb model (Kabeta and Teshager, 2020). The Young's modulus, E, and Poisson's ratio, two defining factors from Hooke's law, determine how the model's stress strain responds in general stress states. The friction angle and cohesiveness are two parameters that characterize the failure criterion, while the dilation angle, which results from the use of a non-associated flow rule to mimic a genuine irreversible change in volume owing to shearing, is a parameter that describes the flow rule (Liu et al., 2017). The stability of dams, slopes, embankments, and shallow foundations can all be analyzed using this model. Although drained circumstances typically represent failure behavior adequately, the effective stress route taken by undrained materials may differ dramatically from observations. In an undrained analysis, it is desirable to utilize undrained shear parameters with a zero friction angle. It is difficult to accurately describe the stiffness (and thus deformation) behavior prior to the local shear. For complete plasticity, the model does not account for the strain-induced hardening or softening effects of soil (Krahn, 2003).

III) Drucker – Prager (DP) model

The Mohr-Coulomb model was simplified by the Drucker-Prager model, which altered the failure cone's hexagonal form to a simple cone. Even though it generally has the same advantages and disadvantages as the Mohr-Coulomb model, that model was chosen (Jacob et al., 2018). As a result, the modeling of failure might degrade dramatically. For issues where the primary stress channels involve either triaxial compression or triaxial extension, it is

straightforward to select the friction value in the DC model so that the failure behavior corresponds with that in the MC model.

IV) Cam-Clay (Modified) (Cc) model

The Modified Cam-clay is an elastic plastic strain hardening model in which hardening plasticity is used to simulate non-linear behavior (Nakamura et al., 2014). The void ratio, e, and the mean effective stress, ', have a logarithmic connection, according to the model's foundation in critical state theory. The most realistic compression and recompression lines for nearly typically cemented clays are linear in the e-log space. Before yielding, only linear elastic behavior is predicted, which may produce absurd numbers because of log-linear compression lines. This model, especially for typically cemented soft soils, is better suited to describe deformation than failure. Additionally, the model works well in applications involving loading circumstances like foundations or embankments. The isotropic logarithmic compression index, the swelling index, the Poisson's ratio for unloading and reloading, ur, the friction constant, M, the pre-consolidation stress, pc, and the initial void ratio, e are the four parameters that are involved. The only way to model shear strength is by using the effective friction constant. The model predicts more accurate undrained shear strength than the MC model for primary undrained deviatoric loading of soft soils (Mr. Digvijay P. Salunkhe et al., 2017). The widespread observation of a peak in the deviatoric stress before the critical state is attained in undrained experiments on loose sand and usually consolidated undisturbed clay is an essential element of behavior that this model is unable to anticipate. Due to its inability to foresee observed softening and dilatancy of dense sands and the undrained reaction of very loose sands, the critical state has been significantly less successful for modeling granular materials. Stiff overconsolidated clays did not appear to be typically modeled with critical state formulations, and the materials modeled by critical state models appeared to be largely limited to saturated clays and silts.

V) Duncan-Chang (Hyperbolic) (DC) Model

Soil exhibits extremely nonlinear behavior and prevents stiffness that is dependent on stress. The Duncan-Chang model, commonly known as the hyperbolic model, is an incremental nonlinear stress-dependent model in addition to the discussed elastic-plastic models (Liu et al., 2017). This model is based on a stress-strain curve that can be accurately approximated by a hyperbola in drained triaxial compression tests of both clay and sand. It is also predicated on the notion that soil stiffness can be expressed as a parameter that is stress-dependent using a power law

formulation. The two strength parameters proposed by Mohr and Coulomb serve as its failure criterion. The three key features of soil—namely, nonlinearity, stress dependence, and inelastic behavior of cohesive and cohesionless soil—are best described by this model (Serdarevic and Babic, 2019). Since the soil characteristics of the Duncan-Chang model can be easily derived from a typical triaxial test, it is commonly employed. It is a simple but noticeable improvement over the Mohr-Coulomb model. This model is preferred over the Mohr-Coulomb model in this regard. The Mohr-Coulomb failure criterion, which is used to define failure itself, is not correctly formulated in the plasticity framework. Dilatancy cannot therefore be described. This model is highly valued for practical modeling since it accurately describes soil behavior using only two stiffness parameters. A strictly hypo-elastic model cannot reliably discriminate between loading and unloading, in contrast to the elasto-plastic kind of model, which is one of this type of model's significant flaws. The model is also unsuitable for calculations of collapse loads in the entire plastic range. When shear failure is approaching, potential numerical stability could happen. When the model is used in three-dimensional stress space, an ad hoc solution must be used.

VI) Soft Soil model (SS) model

To calculate the primary compression of clay-type soils that are close to being naturally consolidated, the Soft Soil model, a Cam-Clay type model, is utilized. The Hardening Soil model outperforms the Soft Soil model, but Brinkgrere (2005) maintains that it is still used since it may be more familiar to older Plaxis users.

VII) Soft Soil Creep model (SSC) model

Since soft soils such as typically cemented clays, silts, and peat are where secondary compression occurs most frequently, a model specifically designed for this use has been created. According to Brinkgrere (2005), the Mohr-Coulomb model performs about as well as the Soft Soil Creep model for unloading issues like tunneling and excavation.

VIII) Plaxis Hardening Soil (HS) Model

For all types of applications, the Hardening Soil model is a real-second-order model for soils in general (including soft soils and harsher forms of soil) (Nakamura et al., 2014). Friction hardening and cap hardening are used in the model to represent the plastic volumetric strain in primary compression and the plastic shear strain under deviatoric loading, respectively.

There are two basic types of hardening that can be distinguished: compression hardening and shear hardening (Wu, 2019). Shear hardening: modeling of irreversible stresses resulting from

primary deviatoric loading Modeling of irreversible plastic stresses resulting from primary compression in isotropic loading and oedometer loading uses compression hardening. The current model includes both types of hardening. Using Mohr-Coulomb, failure is defined. The model is accurate for issues involving a decrease in mean effective stress and concurrent mobilization of shear strength due to the two types of hardening. Such circumstances can arise during excavation projects (retaining wall issues) and during tunnel construction. A power law formulation for stress-dependent stiffness, similar to that used in the Duncan-Chang model, is used in the model's stiffness behavior (Wu, 2019). In fact, while simulating a typical drained triaxial test, the model exhibits consistency with the Duncan-Chang model in terms of its hyperbolic stress-strain response. The Hardening Soil model solves the drawbacks and inconsistencies of the Duncan-Chang model with regard to dilatancy and neutral loading because it is based on hardening plasticity rather than non-linear elasticity. In addition, this model also takes yield cap and soil dilatancy into account. In a variety of geotechnical applications, this model can be used to precisely anticipate displacement and failure of common types of soil (Wu, 2019). The model excludes time-dependent behavior as well as anisotropic stiffness strength (creep). It only has a few dynamic application capabilities.

2.9. Landslide Hazard Mitigation Measures

Hazard mitigation is the term used to describe a sustainable action that lowers or eliminates the long-term danger that natural hazards and their impacts pose to people and property. Therefore, lowering vulnerability and exposure to landslides is the main objective. Both mild and harsh mitigations are offered. In this instance, the use of restrictions, zoning, and avoidance are the primary concerns addressed by soft measures (Kabeta and Teshager, 2020). Hard measures include building infrastructure to make slopes more stable. While hard methods have been promoted and put into practice for slope stabilization, research has demonstrated that soft solutions can successfully reduce hazards over the long run (Crozier, 1999). Improvement of stability through geometric methods; stabilization through drainage; rehabilitation through afforestation; slope reduction; engineering structures to mitigate damage; stabilization through vegetation; hardening of soils; and slip surface blasting are all terms that should be used in landslide mitigation.

2.9.1. Stabilization by Vegetation

Only for shallow sheet slides is afforestation a viable solution. Although vegetation can partially reduce surface water infiltration into the slope and hence indirectly aid in the stability of the slide, landslides with deep lying planes cannot be stopped by vegetation. Trees with high evaporation rates and high water usage are advised (Schuster, 1996).

It was found that land sliding was a result of deforestation everywhere. Large-scale tree planting and trench building may help stabilize slopes by reducing evaporative losses caused by tall, deeply-rooted plants (Sebastian Paul et al., 2018).

2.9.2. Hardening of Soils

The majority of techniques for hardening soil to stabilize slopes were adapted from engineering techniques. These techniques include electro-osmosis drainage. This technique works similarly to sub drainage, but it varies in that water is moved toward the drainage by the activity of an electric field and thermal treatment rather than by gravity (Popescu, 2002). The borehole is filled with exhaust gas that has a temperature of 10,000 oC, which seeps into the soil pores and bakes the soil into a hard substance. You can also carry out grouting, which entails removing water from cracks by filling them with cement mortar (Perera et al., 2018).

2.9.3. Engineering Structures to Mitigate Damage

Engineering structures can minimize damage in locations where mobility is unavoidable. One of these is the use of wire fences and cable nets to trap rock blocks before they cause damage. (I) a mass that can flow over without collapsing; (II) supporting structures such as rock sheds and tunnels; and (III) embankments whose size is determined by the gradient that generates a stable slope given the local hydraulic conditions (Popescu, 2002).

2.9.4. Engineering Methods to Resist Mass Movement

Some engineering techniques for preventing mass movement include building retaining walls, especially on slopes covered in silt or loosely consolidated rock, and sealing cracks with concrete and crushed rock to stop water from seeping into the rock and causing frost wedging (Serdarevic and Babic, 2019). However, it should be noted that building such structures requires a lot of manual labor and expertise, both of which are costly.

2.9.5. Slip Surface Blasting

Surface blasting is a component of slip surface blasting. This approach works better for landslides that occur along straight lines with firm rock under them (Symposium, 2018). The rock will be loosened by the explosion, which will also lessen groundwater uplift. The rock shards will mix with the clay particles underneath and raise the frictional resistance of the clay. However, when used to prevent deep landslides in fine-grained soils, this strategy is unreliable. Additionally, an explosion could have negative effects in the immediate region. Experts with experience are required for the calculations involving the number and placement of explosives (Tsige, Quezon, and Woldearegay, 2017). According to various academic studies, the distribution and characteristics of the soil in landslide-prone areas, slope steepness, geomorphic factors (slope), an increase in the groundwater table as a result of excessive rainfall, gravity, and a decrease in the permeability of the subsurface are the main causes and initiating factors for landslides.

2.9.6. Improving of Stability by Geometric Methods

Slope reduction is advised to create a softer slope since an increase in slope angle can alter the balance of forces. This might lessen the amount of gravitational force operating along the slope (Management, 2016). Construction of embankments, whose size can be defined by the gradient choice that will produce a stable slope given the local hydraulic circumstances, can provide stability in locations where slopes are falling on their own. The embankments may be made of wire mesh or stone (Msilimba, 2012).

2.9.7. Stabilization by Drainage

It has been discovered that drainage stabilization is a highly effective method of preventing unstable hill slopes from sliding. It was discovered that water had seeped through the aged and jointed beds, increasing both pore and cleft water pressures. The installation of concrete embankments could cause the slope to become more unstable due to a buildup of water. By installing curtains every five meters, the local ground level can be decreased. Stone embankments with wire mesh will greatly reduce the accumulation of water on the slope; these structures are more affordable and appropriate for developing nations (Tsige, Quezon and Woldearegay, 2017).

2.9.8. Slope Reduction

Weight across a potential shear plane may grow as the slope height rises (Vinod et al., 2020). The slope angle can be graded into mild ones to reduce the slope, as shown below. If there is not enough room for such extensive grading, terraces or benches may be excavated into the slope.

CHAPTER THREE

MATERIALS AND METHODS

3.1. Location of the Study Area

The Tullu Gola Peasant Association is situated in the Oromiya Region's Nansabo District's West Arsi zone in southern Ethiopia (Figure 3.1). The distance between Addis Abeba and Shashamane Town is about 415 kilometers. Its latitude and longitude were 729681N and 506629E, respectively, and its elevation at the inlet and outlet was 2503m and 2004m above sea level. In the western Arsi Zone, Nansabo is a woreda of Ethiopia's Oromiya Regional State. Its neighbors include the Guji Zone to the south; the Southern Nations, Nationalities, and Peoples Region to the west; Kokossa to the northwest; Dodola to the north; Adaba to the north-east; and the Guji Zone to the north. The region that the avalanche destroyed is the Tullu Gola Peasant Association..

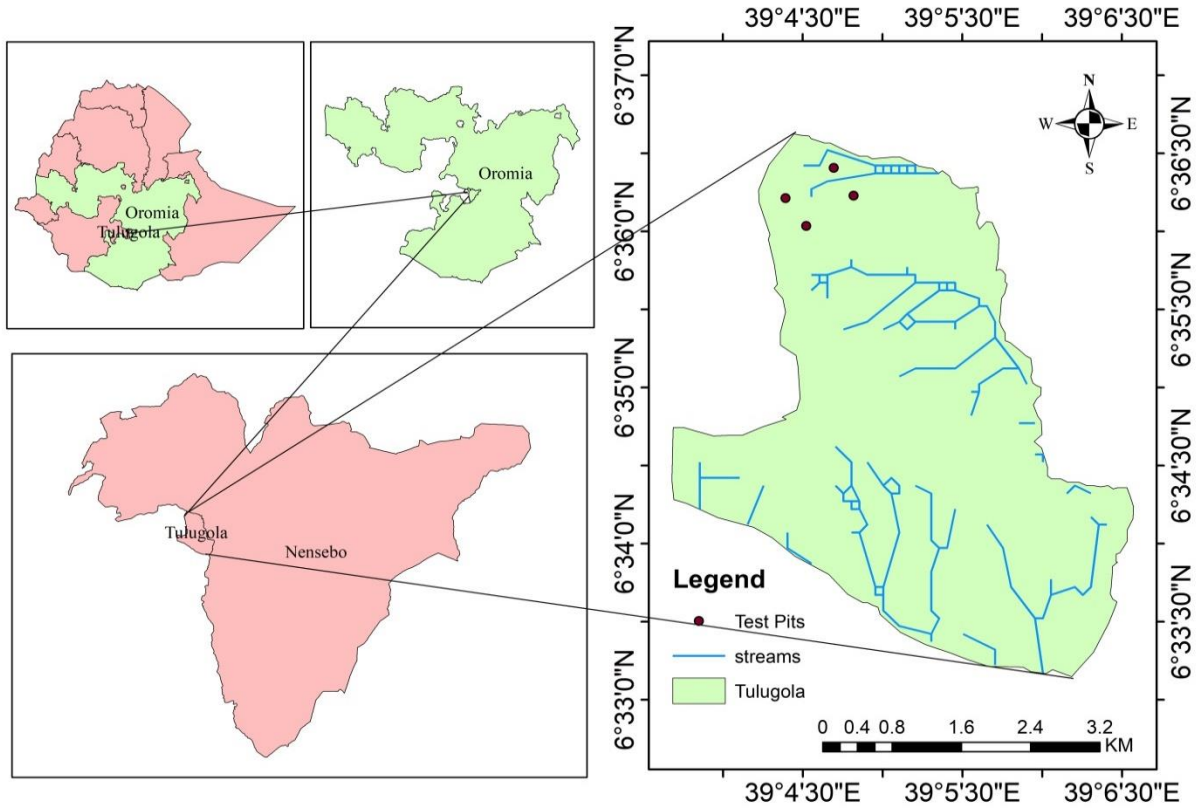

Figure 3-1: Study location map

3.2. Study Design

Both field surveys and laboratory tests were used in the investigation. It was applied research that also makes use of quantitative data types and primary data for experimental purposes. A field test was examined using the geophysical resistivity approach using both vertical electrical sounding and electrical profiling (imaging) (VES).

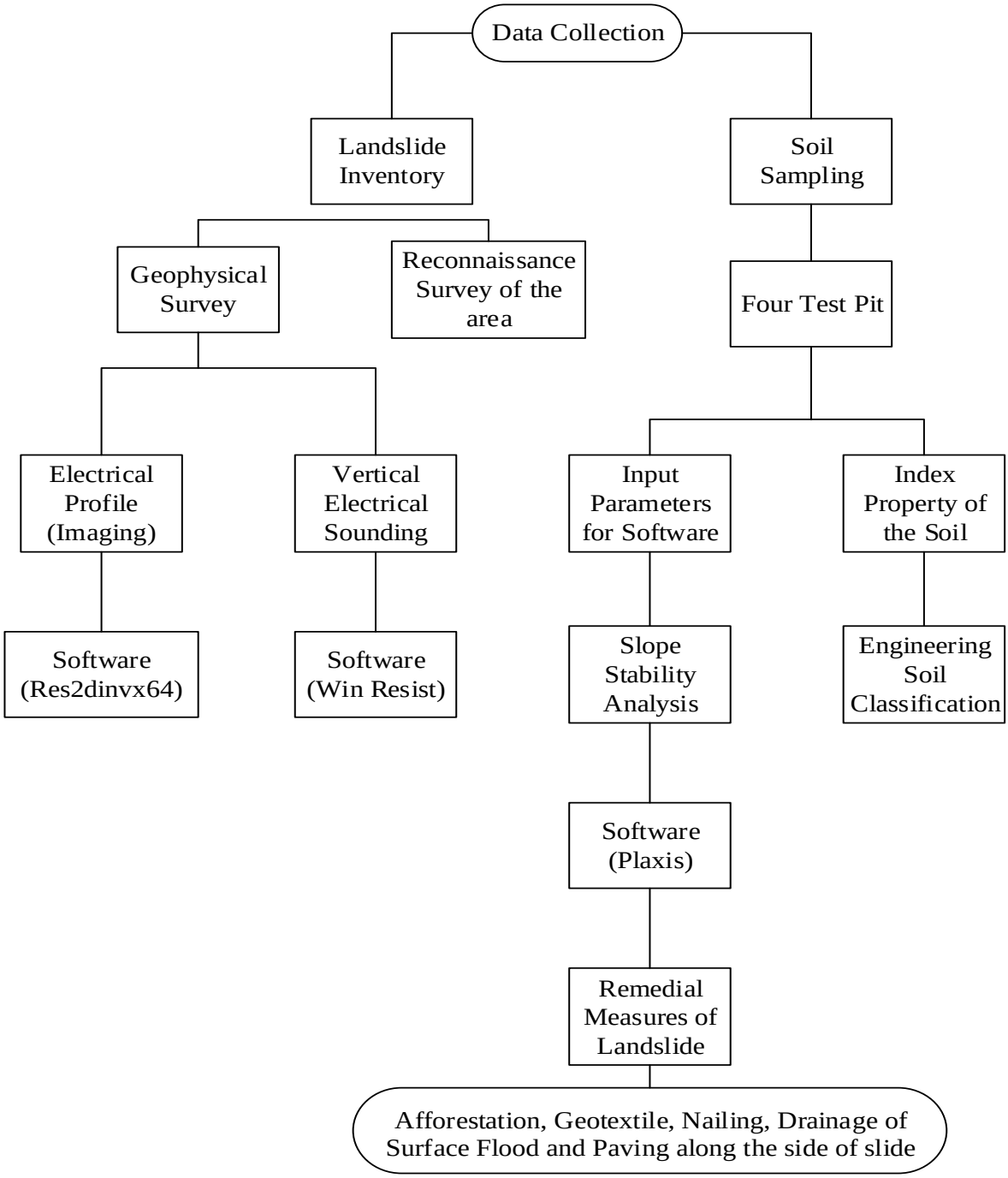

Figure 3-2: Showing the procedure used in this research

3.3. Parameters for Slope Stability Evaluation

Shear strength parameters (such as cohesion and angle of internal friction), unit weight of soil, Eref50, Erefur, and Erefoed, Angle of Dilation (), vur, Konc, grain size, specific gravity, permeability and thickness of sliding mass, and size of slide (length, depth, and width) were the parameters used for slope stability analysis.

3.4. Field Sampling and Laboratory Test

Soil samples were collected to ascertain the geotechnical properties of the soil in the research region. Using the protocols outlined in the ASTM Standard, simple samplings were conducted. Undisturbed and disturbed samples were received for each pit of samples. The sampling axes are provided in Table 3.1. In general, four samples from four trenches up to 3 m, both disturbed and undisturbed, were collected. Landslide-prone locations were chosen at random for the sampling pits (sites). The samples were taken from the slide side area's top, bottom, left, and right. Unaltered samples were collected using a shell tube, tied with plastic, and stored in bags to preserve their in-situ moisture content. To preserve the natural moisture content, the disrupted samples were placed in plastic bags and secured with ribbons. The samples were typically taken at their original moisture content using plastic bags. To stop moisture loss, the plastic bags were knotted. As soon as the samples were brought to the JU laboratory, the in-situ moisture levels were assessed using oven-dry equipment at 105 °C for each test sample. Each sample was dried in an oven to achieve a constant weight when weighing continuously. Every sample was dried for 24 hours in an oven set at 105 °C. Four test pits' worth of soil were sampled at different depths, and the samples were then analyzed to determine the soil's cohesion, angle of friction, unit weight, water content, liquid limit, plastic limit, plasticity index, Young's modulus, specific gravity, and grain size analysis (sieve and hydrometer) in the study area. The results of these tests were used to classify the soil and analyze the stability of the slope where the landslide occurred in the study region.

Figure 3-3: Open pit for taking sample soil test (15/10/2013)

Table 3-1: Types of sample and location

S/No	Test Pit Name	Sampling Depth(m)	Location			Samples type
			Easting	Northing	Elevation	
1	L.S.T.P-1	2	508319	729609	2068	Disturbed
		3				Undisturbed
2	B.S.T.P-2	2	508643	730297	2056	Disturbed
		3				Undisturbed
3	T.S.T.P-3	2	508862	729966	2115	Disturbed
		3				Undisturbed
4	R.S.T.P-4	2	508094	729940	2076	Disturbed
		3				undisturbed

3.5. Software and Instruments

The following hardware and software were utilized in the study: Arc GIS software is used to outline the study area and analyze spatial data. GPS tools to estimate landslide position and collecting pits location of slope profile data for slope stability analysis; Plaxis-2D software for slope stability analysis, Res2dinvx64 for looking at the horizontal profile of soil layers, Win Resist for looking at the vertical electrical resistivity of the soil profile, MS Word and Excel for looking at laboratory data and displaying research data, and a camera for documentation. Also employed in this study were all laboratory test equipment for Atterberg limits, water content,

direct shear, unit weight, specific gravity, and grain size tests, as well as field test equipment such as resistivity meters, electrodes, wires, and other cables.

3.6. Data collection procedures

The study's methodology included: (a) a review of related studies and literature; (b) a geotechnical examination of the soils and rocks; (c) measurement of landslide features, such as length, area, and depth; and (d) the choice of suitable slope stability analysis techniques.

3.7. Field work

Fieldwork included traveling the landslide area's map, identifying the types of landslides that occurred there, measuring the size of the landslides (length, area), looking at the direction in which they fell there, separating the geological strata, determining whether there was a river at the landslide's base, whether there were springs or ponds of water, determining whether any infrastructure had been built in the landslide area, and observing. It was decided to sample soils in order to find out their physical features. Core sampling was done according to ASTM's established standards.

3.8. Landslide Inventory

During the site inspection, there were various markers that helped to identify the occurrence of a landslide at the research location. These include uneven slopes, rock exposure, the presence of an unlined river, the pounding of water at the side of the area, rolling or sliding of the rock from the hill, cracking and sliding of the road along Worka to Dodola Town, circular back scars and surface cracks, destruction of natural features of the area, affecting coffee, maize, wheat, and Teff farm and other farmland areas, damage and tilting of plants, and investigation of the types of layering strata.

3.9. Laboratory Soil Testing Procedures

3.9.1. Water Content Determination

The four (4) test samples from the research region were dried in an oven at 105 °C temperatures in order to assess their natural moisture content in the laboratory, in accordance with ASTM D2216 testing methods. In order to prevent mistakes, three sets of samples were created for each test sample. A suitable sample size was taken for the purpose of determining the moisture content. The three sets of sample natural moisture contents were then determined.

3.9.2. Specific Gravity Determination

According to ASTM D854 testing procedures, the laboratory estimated the specific gravity of soil from four test pits. Three trial samples were gathered from each of the four test pits. Oven-dried specific representative samples have been collected. The provided sample has been prepared for testing by being separated over a No. 10 sieve with a 10 gm sample. The sample was then put through the test procedures. In order to determine the specific gravity, the findings from the three trial samples' average were finally calculated to two decimal places in accordance (see Appendix A).

3.9.3 Determination of Unit Weight of Soil

By inserting a cone cutter into the soil, this test can be used to estimate the in-place density of undisturbed soil. The bulk density is the product of the volume of the soil sample divided by the mass of the moist soil, and the dry density is the product of the volume divided by the mass of the dry soil. The unit weight is determined using the subsequent techniques. A mass of the empty cone cutter was measured, B a soil sample was collected with a cone cutter, and C a mass of the sample with the cone cutter was measured (d). From the recorded data (e), the soil specimen's length (L), diameter (D), and mass (Mt) were estimated. The soil's moisture content was then determined. I decided to compute (w).

3.9.4 Determination of Grain Size Analysis

According to ASTM D422 testing protocols, the laboratory determines the soil grain size analyses for four test pits. For coarse-and fine-grain soils, respectively, the two most frequent tests utilized were sieve size analysis and hydrometer analysis. In this investigation, four samples that were taken from four test pits within the study region were subjected to both particle size determination methods. Due to the high concentration of fine-grained soils in the samples, the silt and clay content in the samples were removed using the wet sieve method, which involved washing the oven-dry sample through a 0.075 mm sieve size. The sticky particles in the fine cohesive soils were dispersed using sodium hexametaphosphate dispersing agent during the hydrometer test. Both assessments were conducted on disturbed soil samples using the ASTM standards D1140-97 and D422-63, respectively. On semi-logarithmic graph paper, the grain size for each sieve and the corresponding particle diameter from the hydrometer analysis against the percentage finer are shown. The graph was utilized to categorize the soil.

3.9.5 Atterberg Limit

To express the plastic and liquid limitations of a fine-grained soil, the Atterberg limit test was carried out. The ASTM standards and ASTM standards of plasticity charts were used to express the soil type name (Figure 4.2). The purpose of this test was to determine the soils' structural strength throughout the entire research area.

3.9.5.1 Determination of Liquid Limit

The (LL) experiments were carried out to find out how much water the soils needed to lose their cohesion and flow as a liquid. The liquid limit is the moisture content at which the strength of the soil suspension changes from zero to very little. The adjustment plate was fastened by tightening its screws after the adjustment was finished. A paste was created in the evaporation dish by combining distilled water with about 125 g of dirt that had been put through a 425 micron screen. Water was allowed to infiltrate the soil. There was a 24-hour mature period. The paste was separated along the cup's diameter with the aid of a grooving tool, designated "a." As a result, a V-shaped gap emerged that was 8mm deep, 2mm wide at the top, and 11mm wide at the bottom. The number of revolutions needed to make the groove close was noted for a groove with a length of about 10 mm. The remaining dirt was taken from the cup and combined with the dirt that had previously been spread out on the marble plate.

Depending on the soil's moisture level, more water was added to the mixture or the soil was allowed to dry to vary the consistency. The number of rotations required to seal the groove was counted, and the liquid limit was established in accordance with ASTM D4318.

3.9.5.2 Determination of Plastic Limit

The percentage of water at which a soil can no longer be distorted by rolling into 3.2 mm diameter threads without disintegrating is known as the (PL) value. Using the Casagrande method and air-dried soil that had been put through a 425 micron screen, the plastic limit was estimated. To make the sample pliable enough to form into a ball, it was combined with distilled water. At least 24 hours were given for the plastic substance to develop and become permeable to water. A ball made of around 8g of the plastic soil was taken and rolled over glass or marble. The ball was rolled into a thread with a constant diameter throughout its length, using just enough pressure to roll it into a ball. The specimen was kneaded together and rolled out once

more when the thread's diameter dropped to 3.2mm. The procedure was carried out until the thread's 3.2mm diameter point of collapse. The readings were taken in order to assess the soil's flexibility.

3.9.5.3 Determination of Plasticity Index

To determine the range over which the soils in the study areas stay plastic before deformation, the PI was computed using liquid and plastic limits. The liquid limit, plastic limit, and plasticity index comparative tests are provided in (Appendix A, Table 3).

3.9.6. Shear strength Parameter Determination

The shear strength of the soils can be determined using a variety of techniques. Both the triaxial compression test and the unconfined compression test were carried out for this investigation.

3.9.6.1 Unconfined Compression Strength Determination

This test's main goal is to ascertain the cohesive soils' unconfined compressive strength on an undisturbed sample, which is then used to calculate the material's undrained shear strength.In order to determine the modulus of deformation of the soils from the stress-strain curve of the test result, techniques were used to conduct the test on undisturbed samples from a three-trial test pit for the unconfined compressive strength of ASTM D2166. In Appendix G, the complete test results are provided.

3.9.6.2. Triaxial Compression Determination (UU Test)

This test method, ASTM D4767, includes determining the strength and stress-strain correlations of a cylindrical specimen of cohesive soil that has either been undisturbed or remolded. In a trial chamber, the specimens are placed under a restricted fluid pressure. During the test, no drainage of the specimen is allowed. The specimen undergoes a constant rate of axial deformation while being sheared in compression without drainage (strain controlled). This test method offers information on the undrained strength characteristics of soils as well as the relationship between stress and strain.

3.9.7. Falling Head Permeability Determination

At a depth of 3 meters from the four test pits, undisturbed samples were used to measure the coefficient of permeability using ASTM D5856 protocols. A permeability or hydraulic conductivity test was conducted to evaluate whether water could pass through soil particles.

Different soil particles have varying hydraulic conductivities based on the size, shape, and water viscosity of the soil particles. The void ratio of soil particles and permeability are directly proportional to one another. Four soil samples were tested using this method since fine-grained soils were the most prevalent soil type in the study area and the Falling Head Approach was appropriate for these soils.

3.9.8. Free Swelling Determination

By dividing the volume difference between the volume of kerosene and the volume of water, free swell—which reflected soil expansion—was calculated. It was completed using a pot and 10g of dry soil that passed through sieve no. 40. It serves as a gauge for the soil property, indicating whether it is compact, somewhat expansive, or expansive in relation to other index qualities. Four samples were used in the free swell test for this study.

3.9.9. Consolidation of Soil Determination

The test is carried out in accordance with ASTM D2435 test method guidelines. A decline in the void volume and soil settling result from water tending to extrude from the void as a result of increased soil load. Consolidation is the term for the phenomena of this compression brought on by the very slow extrusion of water from the void in a fine-grained soil as a result of increased loading. When estimating the amount of settlement, the one-dimensional consolidation test is utilized to acquire compression parameters, and consolidation parameters like CV are used to forecast the rate of soil settlement. This test can also be used to determine the pre-consolidation pressure and the OCR. The soil is confined laterally in a metal ring during a conventional consolidation test, allowing only vertical movement for drainage and settlement. For the majority of loading scenarios, these circumstances are fairly representative of what really happens.

3.10. Geophysical Resistivity survey

In order to ascertain the thickness, nature, and lateral variations of the geological formations, which were used to obtain a complete geological picture of the study area, both Electrical Profiling (EP) and Vertical Electrical Sounding (VES) were conducted along a single line of profile in the study area close to the side of a landslide. Profile lines were arranged from northeast to southeast.

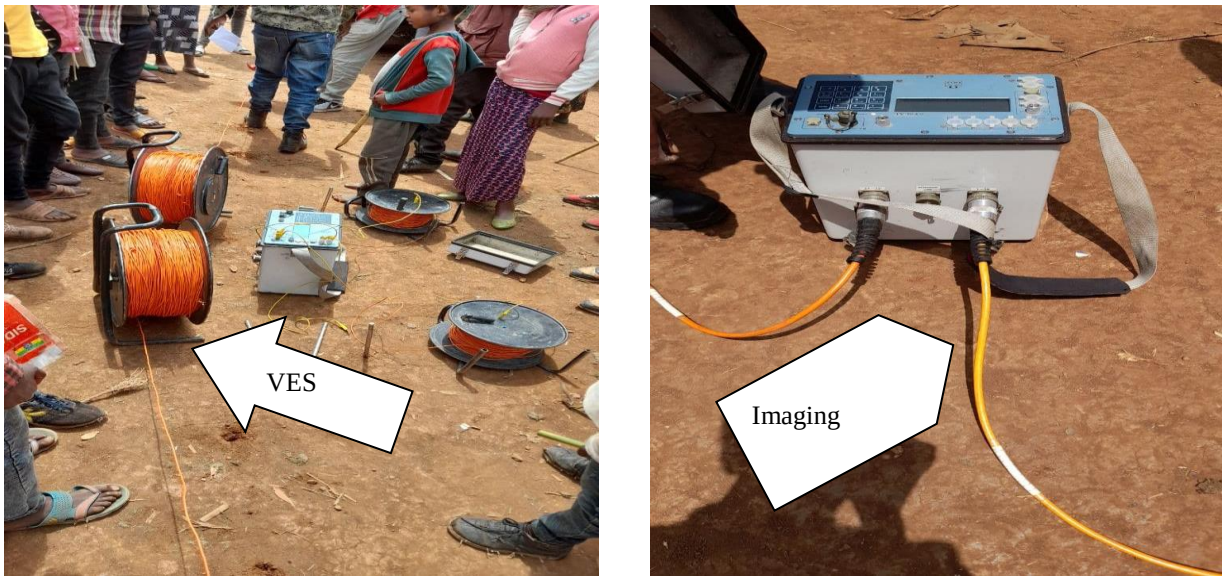

Figure 3-4: VES and Imaging Geophysical Resistivity survey

Four electrodes, in a Schlumberger Array configuration, with maximum current electrodes AB/2 varied between 1.5 and 330 meters and potential electrodes MN/2 separated between 0.5 and 45 meters, were used to conduct VES measurements in the Tullu Gola area. Resistance meters from the SYSCAL Pro line were used to take the measurements. Using the RESIST program's curve matching technique, the initial and final interpretation of the VES were created (Vander Velpen, 1988). Using the program Win Resist, the Tullu Gola Peasant Association produced an electrical resistivity sounding (VES) inversion result along a North to South axis at (507353, 729480) coordinate and 2271 meters above sea level with a VES length of 330 meters. The cable initially gathers subsurface data from NE to SE for imaging. Second, the subsurface data supplied is analyzed using the software program Res2dinvx64. Thirdly, after displaying the "x" data point, this modeling image was enlarged horizontally and then returned to being vertical under the surface. Fourthly, it was translated into a picture with varying depth and resistivity. Finally, the reasons for the landslide were determined based on the resistivity value.

3.11. Slope Stability Analysis using FEM

3.11.1. Soil Elements

In Plaxis-2D, 15-node triangular components that can simulate soil deformation and tension were used to model the soil layers. The best soil modeling and analysis for displacements is provided by the 15-node triangle, which also features twelve stress points and a fourth-order interpolation (Brinkgreve, 2005).

3.11.2. Calculation Types

The three types of computations that are offered in Plaxis are plastic calculation, consolidation analysis, and phi-c reduction. The user can select the plastic computation to do an elasto-plastic deformation investigation without accounting for the evolution of surplus pore pressures. A plastic computation does not account for time effects. Soft soils allow for the use of plastic calculations, which provide an accurate approximation of the end condition rather than allowing for tracking of loading history and consolidation. The consolidation analysis should be utilized when it's crucial to monitor how surplus pore pressure in soft soils changes over time. When the circumstances of the problem call for the estimation of the safety factor, the phi-c reduction in Plaxis is a safety analysis that is helpful. It is possible to do a safety study after each individual calculation phase, but it is best to wait until all calculation phases have been established. It is especially foolish to begin the computation with a safety analogue (Brinkgreve, 2005). The phi-c reduction approach was selected for this study; as a result, the analysis focused on the safety factor.

3.11.3. Material Modeling

Numerous constitutive models have been used to examine soil behavior, and depending on how many and how they were chosen as parameters, these models could be simple or complex. More complicated models typically involve the addition of more parameters, whose determination is frequently attainable through the execution of challenging soil mechanics experiments. On the other hand, although using fewer parameters, simplistic models have lower modeling accuracy. However, the classification of soil in this study as silt soils was made on the basis of results for unconfined compressive strength. In their numerical modeling, the hardening soil model (HS) is the most effective soil model for stiff and hard soil. As a result, the HS model overcomes the limitations of dilatancy and neutral loading and takes into consideration the soil's stress-

dependent stiffness. Due to the densification of soil particles after loading, which results in a decreased volume of voids, a soil's stiffness may rise. It is noted that this phenomenon occurs as plastic deformation begins. The HS model incorporates a volumetric cap yield surface that causes soil stiffness to decrease in response to large amplitude strain, as well as the expansion and contraction of the shear yield surface (Verghese, Nguyen and Bui, 2013).

And the modulus in the hardening soil model is described more accurately by adding three moduli; Eur, which refers to reloading/unloading modulus E_{50} and E_{oed}. E_{50}. Refers to secant modulus from tri-axial test and E_{oed}refers to tangent modulus that corresponds to a modulus for stresses higher than the pre-consolidation pressure evaluated from the CRS test.

In the above-mentioned formulas, the $E_{ref}$is the reference Young`s modulus and P_{ref} is reference stress for the stiffness and is set to 100kPa, as a default value in Plaxis. Plastic soil stiffness parameters E_{50}^{ref} and E_{ur}^{ref} selected confining pressure determined from triaxial compression test results. E_{50}^{ref}calculated as the ratio of 50% deviatoric stress to 50% strain (Wu, 2019) E_{ur}^{ref} =3 E_{50}^{ref}. Considering confining pressures the average values of model parameters at σ_3 = 100 kPa, 200kPa, and 300kPa were calculated and the average values was presented. E_{50}^{ref} and E_{ur}^{ref} and used as input parameters for software analysis. v_{ur} is pure elastic parameter and its value used as 0.2 default setting and Ko^{NC} is an independent input parameters and Plaxis uses as a default setting k_o^{NC} =1 – sinϕ. It is assumed that Plaxis used an average value of the failure ratio as R_f = 0.9 default value. The Values of input parameters were illustrated in Table 3:8. In Hardening soil model (HS) the model consider the dilatancy angle. Dilatancy angle be observed in laboratory tests for cohesive soils, it can be assumed that dilatancy depends on the preconsolidation state. Hence, dilatancy angle can be taken as (Obrzud and Truty, 2018):

ψ = 0 for normally and lightly over consolidated soil

$\psi = \frac{\phi}{6}$ for over consolidated soil and

$\psi = \frac{\phi}{3}$ for heavily over consolidated soil

3.11.4. Geometrical Model of the Slope

The initial layer in this investigation was 15 meters of silty soil, followed by five somewhat fragmented rocks, 45 meters of very massive rocks, and 10 meters of highly massive volcanic and basement bed rocks. These layers were referred to as the upper, middle, lower, and bedrock layers. Two pieces of the model were created based on the sides of test pits that were seen. Given

that the first section was found on the slope's right side, this side had a slope failure. The upper side of the slope, where the slope collapse also occurred, was the segment that came next. Both sides' test pits were visible. The quality of the ground water was overlooked in this instance, and the findings of the geophysical survey showed that GWT was discovered at a significant depth. The input parameters have been listed in Table 3:2 for each section.

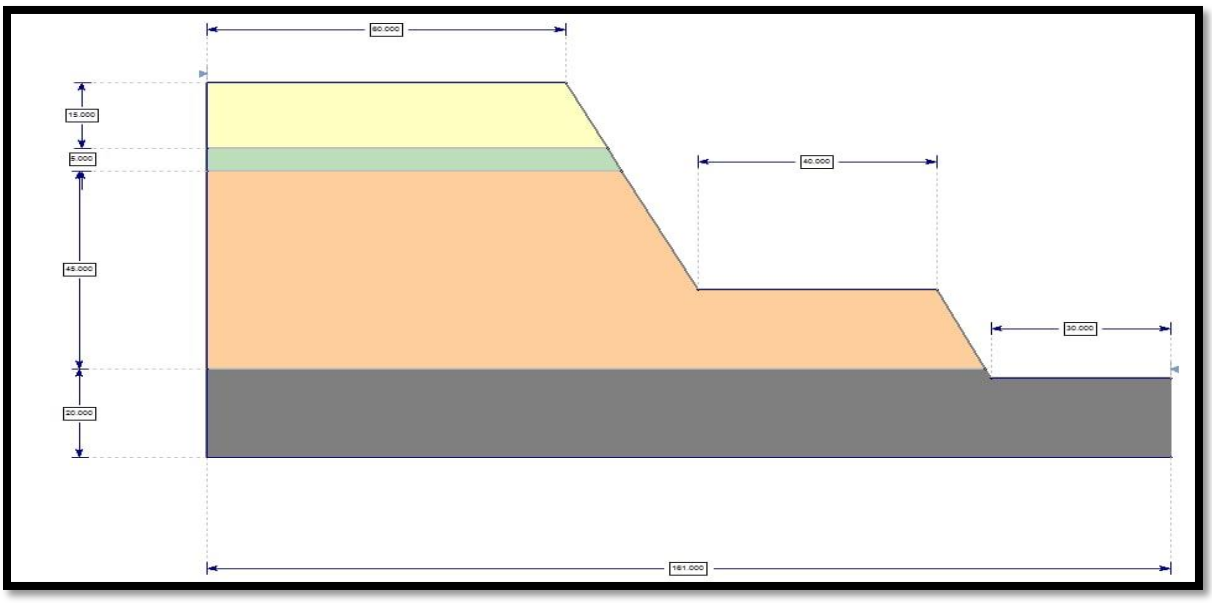

Figure 3-5: Geometrical model

3.11.5. Boundary Condition of the Slope

The slope's base was fixed in both the X and Y directions. It was open at the top of the slope to permit dirt to deform downward and open on either side of the movement of soil mass. Only the soil's vertical mobility was permitted because the right side of this model had an X-axis fixed in place. Figure 3:6 illustrates the slope failure's boundary condition.

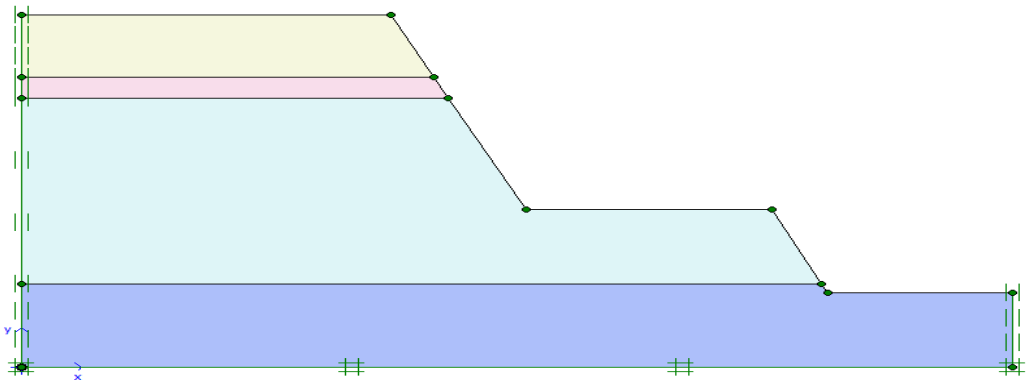

Figure 3-6: The boundary condition of the slope

3.11.6 Input Parameters for Slope Stability

Table 3:2 for both sections lists the input materials for the hardening soil model. Section I identified the slope's right side, and Section II identified the slope's top side failure. The landslide occurred only on the right and top side. Because of this, the test result that was obtained from the two sides was used as input parameters for slope stability.

Table 3-2: input parameters for software analysis

Determination No:-	Section I	Section II
Un saturated Unit weight, ($y_{unsat.}$), kN/m^3	16.93	17.06
Saturated unit weight, ($y_{sat.}$), kN/m^3	20.09	20.25
Cohesion Pressure, C, kN/m^2	18.95	26.77
Angle of friction, ø (˚)	11.30	32.95
Dilatancy angle ψ (˚)	3.77	10.98
$E^{ref}_{oed,}$ Mpa	93.339	35.44
$E^{ref}_{50,}$ Mpa	60.09	35.44
$E^{ref}_{ur,}$ Mpa	180.27	106.32
Kx,m/day	$1.33*10^{-4}$	$1.33*10^{-4}$
Ky,m/day	$1.41*10^{-4}$	$1.41*10^{-4}$
Power (m)	1	1
Cc	0.32	0.32
Cs	0.18	0.18
$e_{init.}$	1.31	1.31
R_{inter}	0.9	0.9
V_{ur}	0.2	0.2
P_{ref}	100	100
Ko^{nc}	0.804	0.456
C_{incr}	50.0	50.0
R_{ref}	1.0	1.0

These input parameters were got from labratory test result like triaxial, consolidation, permeability and unit weight test result calculated by using formula.

CHAPTER FOUR

RESULTS AND DISCUSSIONS

4.1. Laboratory Test Results

4.1.1. Water Contents of the Soil

According to the Tullu Gola Peasant Association, Table 4.1's description of the landslide study area's natural moisture is accurate. These results for natural moisture content varied because of the various topographies. This indicates that the terrain characteristics in the research area were both up and down. The soils' water content ranged from 28.82 to 29.03 percent. According to this finding, the soil was a hard silty clay and the amount of water increased from high to low land. The amount of water present increases with increased rainfall, contact with weak zones, and the relationship between soil particle releases and collapses. Increased natural water content may have an impact on the soil's ability to withstand shear, and as water content rises, the friction angle will also decrease, which could contribute to landslides in the research area.

Table 4-1: Natural Moisture content Result

Test Pit	Depth of sample taken (m)	Water content in %
L.S.T.P-1	2.5-3	28.82
B.S.T.P-2	2.5-3	28.9
T.S.T.P-3	2.5-3	28.85
R.S.T.P-4	2.5-3	29.03

4.1.2. Specific Gravity of Soil

The soil has a specific gravity ranging from 2.65 to 2.74. According to this range of specific gravity values, the soil is silty (Table 4.2). This test therefore shows that the soil type of the research region was silty soils, which are weaker and generally have multiple weak points, which caused the Tullu Gola landslide to occur. The aforementioned findings indicate that the soils were inorganic because the specific gravity (GS) values were greater than 2.5. It is possible to draw the conclusion that the study area's soils are light and permeable, which promotes the permeability of the region. However, as the time it takes for water to seep into the earth's mass increases, the weight of the soils rises and pore pressure develops, which, along with other triggering factors, contributes to the development of landslides in the study area. The variation

that was found in table 4.2 was due to geological formation, chemical composition, pressure, and temperature.

Table 4-2: Specific Gravity

Test Pit	Sample depth (m)	The Average specific gravity
L.S.T.P-1	2-3	2.66
B.S.T.P-2	2-3	2.65
T.S.T.P-3	2-3	2.74
R.S.T.P-4	2-3	2.72

4.1.3. Unit weights of the Soils

The soils from the Tullu Gola Peasant Association were reported as unit weights in Table 4.3. The soil samples for the research region were taken at a depth of 3 meters and given a unit weight. The soils ranged in unit weight from 19.995 to 20.482 kN/m3, with the lower figure being a result of the soils' high moisture content. At low land, the moisture content is high, and at high land, it is low. Because of this, such a variation was obtained.

Table 4-3: Unit weights of the soils samples

Pit No	L.S.T.P-1	B.S.T.P-2	T.S.T.P-3	R.S.T.P-4
Diameter of cone cater, mm	116.0	116.0	116.0	116.0
Height of sample in cone cutter, mm	120.0	120.0	120.0	120.0
Volume of samples, mm^3	1267555.2	1267555.2	1267555.2	1267555.2
mass of cone cutter+sample, g	2833.5	2825.8	2887.6	2857.3
mass of cone cutter, g	243.8	242.2	241.1	243.5
Mass of samples, g	2589.8	2583.6	2646.5	2613.7
density of soil, kg/m^3	2.043	2.038	2.088	2.062
unit weight, kN/m^3	20.043	19.995	20.482	20.228

4.1.4. Grain Size Analysis of the Soils

The curves for the combined grain size analyses and the results of the sieve analysis were shown in Table 4.4 and Appendix D, Figures D1 through D4. The grain size ranged from 0.0 to 0.95 percent for gravel, 3.92 to 13.67 percent for sands, and 85.11 to 96.73 percent for fines, according to Table 4.4. The majority of the soil in the study region was made up of fine (silty) soil. According to the universal soil classification (USCS) method, soil is categorized as having

finer grains if more than 50% of the sample fits through sieve No. 200 (0.075 mm). As a result, the soil test revealed that the Tullu Gola Peasant Association has fine (silty) soils, which are listed in appendix D.

Table 4-4: Grain size

Test Pit	Sample depth (m)	Percentage of Gravel	Percentage of Sandy Soil	Percentage of silt soil	Percentage of clay soil
L.S.T.P-1	2.5	0.95	13.67	64.39	20.72
B.S.T.P-2	2.5	0.0532	12.801	67.62	19.52
T.S.T.P-3	2.5	0	3.9254	60.28	28.64
R.S.T.P-4	2.5	0.0532	5.9174	65.88	28.15

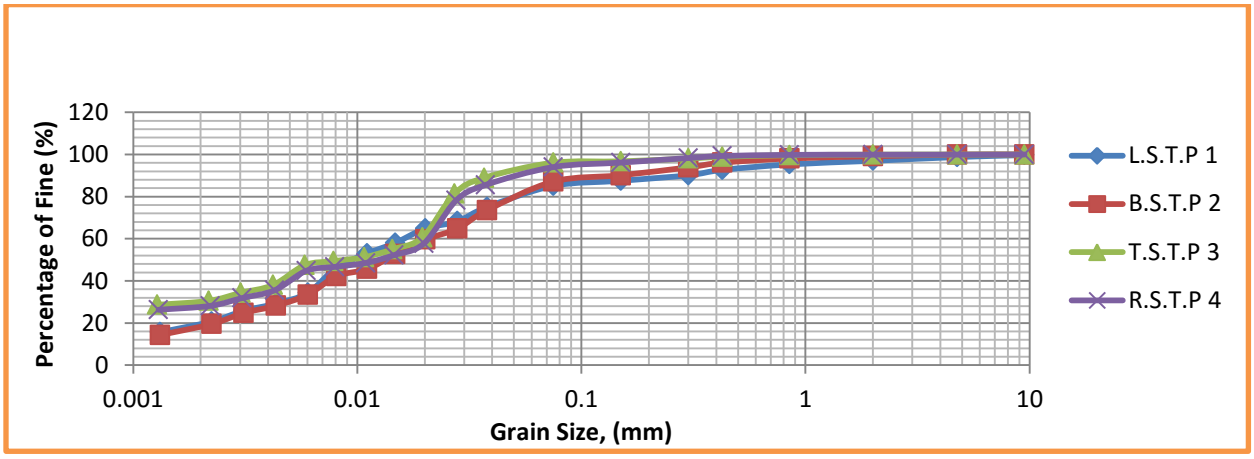

Figure 4-1: Grain size of the soil

4.1.5. Atterberg Limit

According to Table 3.8's findings, the soil masses' liquid limit (LL), plastic limit (PL), and plastic index (PI) ranged from 49.20 to 61.00 percent, 30.52 to 38.49 percent, and 18.68 to 31.11 percent, respectively. The liquid limit value in these tests was greater than 50% for all slope profiles, and the liquid limit to plastic index exists below the A-line, indicating that the soil was an inorganic silty soil with high plasticity. According to MH (from Figure 4.2), more than 80% of the sample passed through sieve No. 200. Sand predominates on average, while gravel makes up less than 15% of the total. This variation was due to different mineral compositions found in silt soil at table 4.5.

Table 4-5: Summary of Atterberg Limits

Test Pit	sample depth (m)	LL (%)	PL (%)	PI (%)
L.S.T.P-1	2	49.2	30.52	18.68
B.S.T.P-2	2.5	69.6	38.49	31.11
T.S.T.P-3	2.5	56.55	36.85	19.7
R.S.T.P-4	2.5	61	31.84	29.16

The soil classification using the USCS classification method is depicted in Figure 4.2, which is provided below. The Plasticity Index and liquid limitations served as its foundation. As a result, the USCS results show that fine-grained soils predominate in the research area's soil. The soil is classified as silt soil in every test pit, according to the results. Three of the four test samples were classified as very silty soils and placed in the MH group, while the fourth sample, which was taken at a depth of roughly 2 meters, was placed in the ML silt soils category. This silt soil's poor permeability coefficient can cause a landslide to occur.

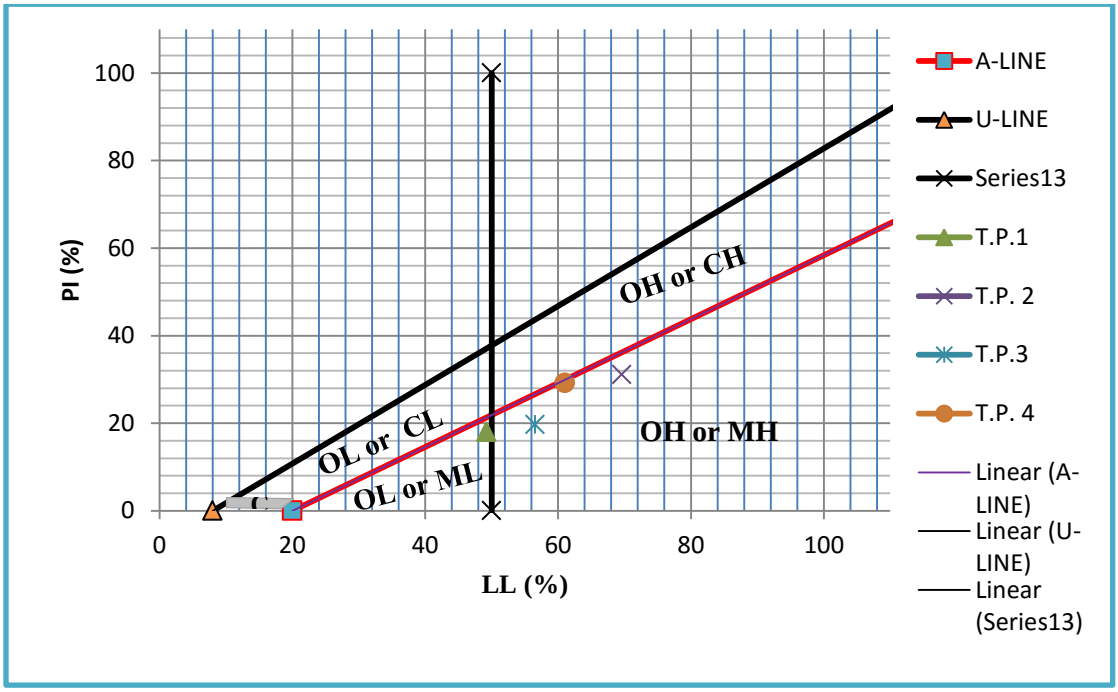

Figure 4-2: Soil classification using USCS

4.1.6. Free Swell

The volume difference between the volume of kerosene and water was divided into the volume of kerosene to produce a free swell, which indicated soil expansion.

According to the test results, the soil under study has a free swell that ranges from 25 to 33.33 percent. A low degree of expansion is defined as soils with a free swell of less than 50%. As a result, none of the soil samples under study were expansive soils. High-weathered minerals are found in silt soils that are swelling rapidly. Those who have not been heavily weathered, on the other hand, swell slightly.

Table 4-6: Free Swell Test Result

Test Pit	Sample depth (m)	Free Swell (%)	Remark
L.S.T.P-1	2	25	Not expansive soil
B.S.T.P-2	2.5	25	Not expansive soil
T.S.T.P-3	2	33.33	Not expansive soil
R.S.T.P-4	2	30.77	Not expansive soil

4.1.7. Coefficients of the Permeability

The engineering qualities of soil are greatly impacted by its permeability. Different soil particles have varied hydraulic conductivity depending on their particle size, shape, void ratio, water characteristics, soil structure, and specific surface area. In terms of soil permeability, coarse-grained soils fall under the highly permeable category, whereas fine-grained soils fall under the poor to impervious category. The vacancy ratio of soil particles affects permeability significantly, and their relationship is inversely proportional. Four soil samples were tested using the falling head method since fine-grained soils predominate in the study area and the falling head method is appropriate for this type of soil. Because the results ranged between 1.33*10-4 and 2.7*10-4 cm/s, the coefficient of permeability obtained from this test result suggests that the soil of the research region was classified as silt soil. Because silt is the most common soil type in the study area, the findings demonstrate that the soil under investigation contains essentially semi-impervious elements. An important factor in the occurrence of mass movements in this study region is the presence of bedrock beneath the slope that is impervious and the property of silt soils that were identified at the top section of the slope. When moisture reaches the bedrock, it stops moving and begins to accumulate. The moisture was penetrated during the rainy season.

The soil at the weak layer is easily destroyed and turns into a slick surface when soil moisture levels rise and reach that layer. The soil that was discovered above this crucial line might thus easily be shifted from an unstable position to a stable position and result in a landslide. As a result, one of the initiating variables for the occurrence of a landslide was the permeability of the materials in the research region. The sample test was taken at T.S.T.P-3, which is found on high land, and there was highly decomposed material that was filled with stiff to hard fine soil. Because of this, the permeability was low relative to the other one.

Table 4-7 : Coefficients of the Permeability

Test Pit	Sample depth (m)	Coefficients of permeability in (cm/s)
L.S.T.P-1	3	$1.66*10^{-4}$
B.S.T.P-2	3	$2.7*10^{-4}$
T.S.T.P-3	3	$1.33*10^{-4}$
R.S.T.P-4	3	$1.41*10^{-4}$

4.1.8. Classification of Tullu Gola Peasant Association Soil

4.1.8.1. Unified Soil Classification (USC) System

One can see from the grain size distribution curves in Figure 4.1 that for all samples, more than 50% of the soils pass sieve No. 200 (0.075mm), allowing for broad classification as fine-grained soils. The soil was categorized as MH, which stands for silty soil, in the Tullu Gola Peasant Association according to table 4.8.

Table 4-8: Unified Soil Classification (USC) System of the Tullu Gola Peasant Association

Test Pit designation	Depth (m)	LL (%)	PL (%)	PI (%)	USCS
L.S.T.P-1	2	49.20	30.52	18.68	ML
B.S.T.P-2	2.5	69.60	38.49	31.11	MH
T.S.T.P-3	2.5	56.55	36.85	19.70	MH
R.S.T.P-4	2.5	61.00	31.84	29.16	MH

4.1.9. Unconfined Compression Strength

Based on the findings of an unconfined compressive strength test, the soil in this study was consistently categorized as stiff to hard soil. In Plaxis, the Hardening Soil model, an elasto-plastic second-order hyperbolic isotropic hardening model, has been used in finite element analysis for stiff soils. It allows for the modeling of complex nonlinear soil behavior as well as a

number of interface conditions with various interface geometries and soil properties. The sample that was taken at T.S.T.P-3 on the top side of the landslide was the stiff to hard soil obtained here. Because the lava flow made contact with the basement during magma eruption, and very hard minerals were formed during that time. Even when highly weathered, the fineness of these minerals' particles is stiff to hard.

Table 4-9: Unconfined Compression test results

Soil	qu (kpa)
T.S.T.P-3	381.04
R.S.T.P-4	122.86

Based on consistency and unconfined compression strength of silt, Table 4.9's findings indicate that the soil in Pit 3 is hard silt soil and the soil in Pit 4 is stiff silt soil.

4.1.10. Consolidation Test

The void ratio that was determined from the odometer test results was 1.31. The Compression Index (Cc) and swelling index (Cs) have respective percent values of 0.32 and 0.18. Preconsolidation pressure, which is the highest pressure, is 400 kPa, whereas overburden pressure is 55.26 kPa. Preconsolidation pressure divided by overburden pressure equals the overconsolidation ratio, which is 7.24, which is more than 1. The soil is over-consolidated since its OCR value is greater than 1. This demonstrates that the soils have previously undergone higher effective vertical pressure and/or that the soil may be pre-consolidated. 344.74 is the overconsolidation margin.

4.1.11. Triaxial Test (UU Test)

High silt associated with R.S.T.P-4 was suggested by the sample under T.S.T.P-3. This variation may be the result of topographical and geological formation disruption, weathering, and load pressure.

Table 4-10: Triaxial test result of σ3

Triaxial test result of σ3	Sample Name	
	T.S.T.P-3	R.S.T.P-4
Chamber pressure,σ3, (kN/m^2)	Deviator stress,(kN/m^2)	Deviator stress, (kN/m^2)
100	186.07	132.26
200	292.12	182.10
300	395.17	232.10

The sample's angle of internal friction and cohesion pressure were determined to be less than T.S.T.P-3 and were found to be below R.S.T.P-4. This might be as a result of the silt soil's mineral composition. When these particles come into contact with water, their link breaks and the research area fails.

Table 4-11: The Triaxial Test For c and ø

Pit No:-	T.S.T.P-3	R.S.T.P-4
Cohesion Pressure, c (kN/m^2)	26.77	18.95
Angle of Friction, ø (˚)	32.95	11.33

Table 4-12: General summary of the properties of soils from landslide affected area

Soil properties/sample type	L.S.T.P-1	B.S.T.P-2	T.S.T.P-3	R.S.T.P-4
Water content (%)	28.82	28.90	28.85	29.03
Wet Unit weight (kN/m^3)	16.74	17.55	17.774	16.26
Gs (G_s)	2.66	2.65	2.74	2.72
LL (%)	49.20	69.60	56.55	61
PL (%)	30.52	38.49	36.85	31.84
PI (%)	18.68	31.11	19.70	29.16
Percent of fines (silt & clay)	85.11	87.15	96.07	94.03
Sand (%)	13.67	12.80	3.925	5.917
Gravel (%)	0.95	0.0532	0	0.053
Class of soil	ML to MH	MH	MH	MH
Angle of internal friction $(\phi)^o$	-	-	32.96	11.30
Cohesion (c) (Kpa)	-	-	26.77	18.95
qu(Kpa)	-	-	381.04	122.86

4.2. Causes and Triggering Factors for Landslide at Tullu Gola Peasant Association

4.2.1. Geology

4.2.1.1. Regional Geology

Three sections make up the Ethiopian rift system. The East African Rift System includes it. The Main Ethiopian Rift (MER), the South Western Rift Zone, and Afar are the three. The Ethiopian highlands are divided into two plateaus by the main Ethiopian Rift: the northwestern plateau and the south-eastern plateau. The distance between the south-western rift zone and the horizon is roughly 650 km. Extensional faults connected to a number of volcanic activities define it. The Northern, Central, and Southern regions make up the three geographic divisions of the MER (Woldegebrielet al. 1990). At the southernmost edge of the central sector of the MER, which is almost 175 km long and 75 km wide, is where the current study site is situated. stretching to the northeast and getting smaller to the south (Mohr. 1967).

The primary formations of the Southeastern highlands, which date back to between 38 and 7 million years ago during the Oligocene and Miocene geological eras, are where the Nansabo district is situated. The studied region included aphyric and porphyritic basal, less vesicular basalt and ignimbrite rock, quartzo-feldsphatic, shist, fels, gneiss, trachytic tuffs, and small basalt and trachyte flows and sediments, as well as aphyric and porphyritic basal (Figure 4.3).

4.2.1.2. Local Geology

4.2.1.2.1. Geology of the Study Area

At the base of the research area, there is a river called Belechu, which is the primary river. During the magma flow in this region, several geographical features were created. These many terrain elements include rivers, various topographies, weathering rocks, ground water flow directions, unstable structural geology, sediment, base material, and volcanic rocks. Intercalation of silt with weathering volcanic and basement rocks is how the geology of the study region was formed at the top. Massive volcanic rock intercalated with basement makes up the centre of the stratum identified in the research region. Due to its high resistivity, this basement kept water from percolating through it. So, during the rainy season, water seeped through the top layer and ended up in the basement. High pressure formed at this moment between the water and the soft top layer. Low shear resistance caused the top layer to fail. The geological formation present in the studied area was often one of the causes of landslides. The local geology that was discovered in the research region is described as follows in Figure 4:2.

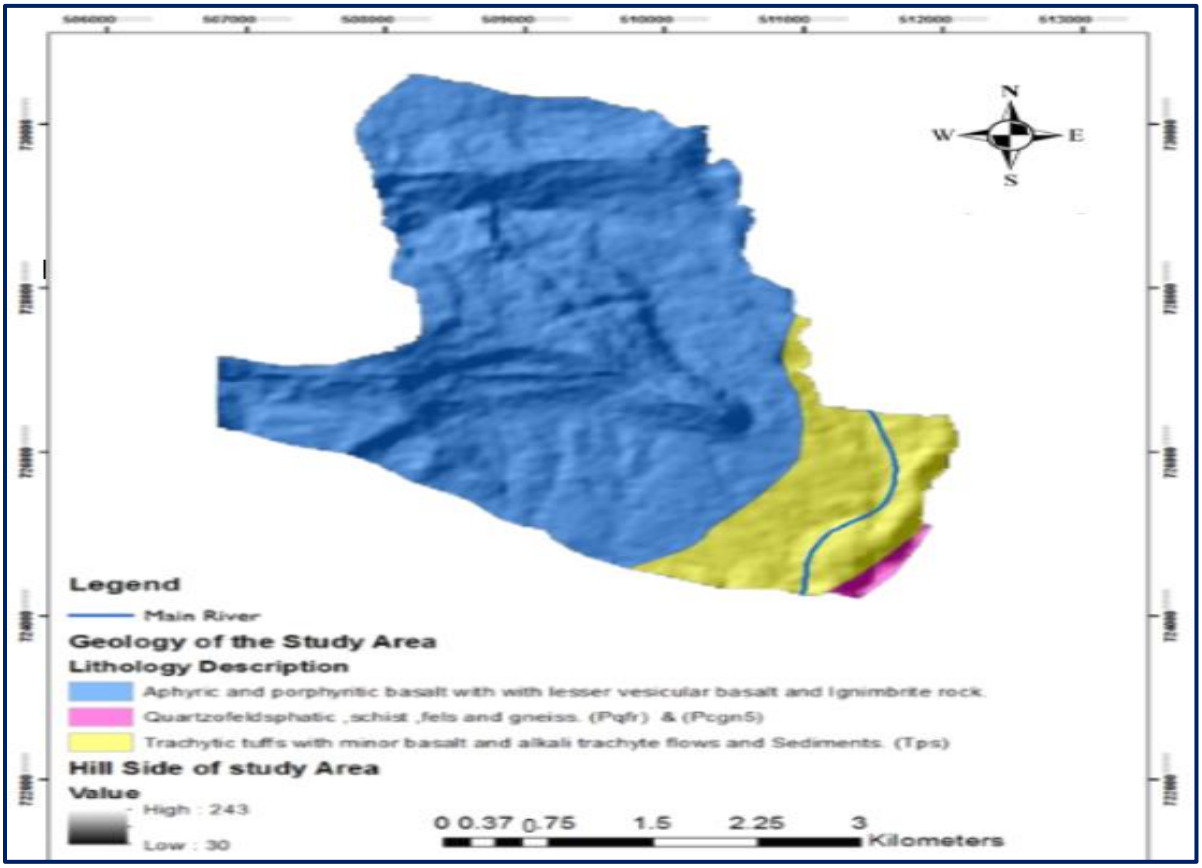

Figure 4-1: Geology of the study Area

4.2.1.2.2. Land Use and Settlement

The study region was primarily made up of cultivated land, and the primary land use in the study area is agricultural cropping, with perennial crops like coffee, enset, and chat, as well as wheat, Teff, barley, sorghum, and maize. A diversity of ecosystems and land uses, including forests, grazing land, and shrub/woodland, are supported in the study region, which benefits the national economy. The main vegetation types in the research region include several varieties of acacia trees; woodlands; bamboo; forests; shrubs; and grasslands. The study area's rapidly growing population has resulted in a significant demand for agricultural land. Deforestation of vegetation as a result can weaken the soil's shear strength. By strengthening the soil slope or by minimizing the quantity of water that has already seeped through during the rainy season, vegetation can maintain the stability of the slope. Therefore, the lack of this vegetation may adversely affect the research area's mass movement.

4.2.1.2.3. Topography

The topography of Nansabo woreda is varied, with undulating terrain, mountains, hills, plains, plateaus, and valleys. Its elevation varies from 1600 to 3500 meters above mean sea level. Hills and mountain ranges make up 70% of the landform in the region, with the most well-known being Rusa Mountain, Gubo, Ladamo, Guticho, Barleda, Mire, and Tunse Mountain (CSA, 2007). The study area includes Mire Mountain. This mountain has a long, steep slope. The reddish to brownish silty clay soil of the hills of this mire mountain is interspersed with somewhat weathered basalt, ignimbrite rock, metamorphic rock including gneiss, and schist (Figure 4.3). The terrain of the Tullu Gola Peasant Association is between 1663 and 2246 meters above sea level, according to the Digital Elevation Model (DEM-30m resolution). In the research region, the hill slopes are steep enough to approach the limit equilibrium state, and external factors like rainfall infiltration and/or excavations (man-made or natural) could cause slope collapses. The majority of landslides happened at elevations between 1828 and 2072 meters, which is a little higher than the research region. This is because the area's geological strata and soil type both play a significant role in the occurrence of landslides at this level. The elevation of the research region shows that one of the factors that causes the Tulu Gola landslide to occur is the slope's geometry. Elevation variation is another important component in the incidence of large-scale migration in the research area.

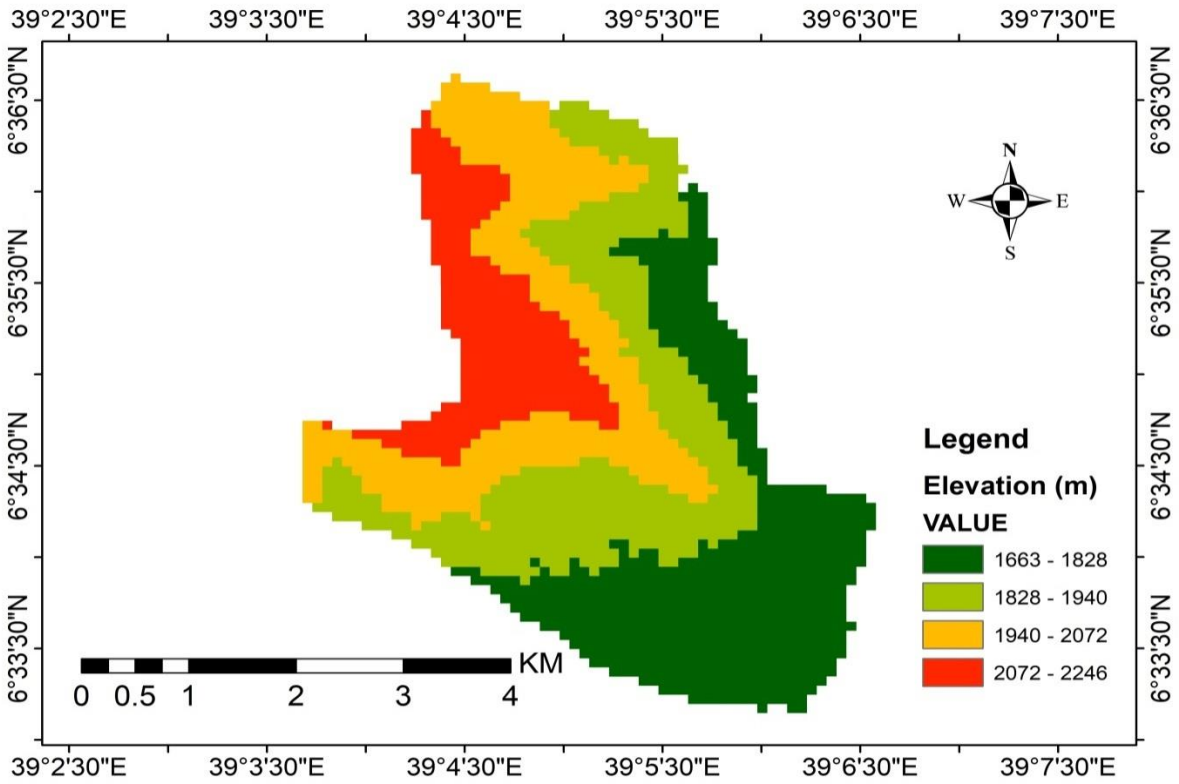

Figure 4-2: Elevation map of the study area showing various classes of topography

4.2.1.2.4. Slope Gradient of the Study Area

If only the slope factor is considered, steeper slopes generally have a larger probability of landslides, yet they can also happen on softer slopes depending on other environmental factors. According to Dai et al. (2001), slope angle is commonly used in landslide susceptibility studies since land sliding is closely related to it slopes depending on other environmental factors. According to Dai et al. (2001), slope angle is commonly used in landslide susceptibility studies since land sliding is closely related to it. As the slope becomes steeper, the tangential component of a mass's weight and shear stress increase, while the perpendicular component of its weight decreases. An object will tend to slide down a slope if the sliding stress is greater than the total of the opposing forces keeping it there. As a result, when assessing landslides, it's crucial to take the slope of the ground into account. According to the classification, there is 15, 25, 45, and more than 45 percent flat terrain, rolling terrain, mountainous terrain, and cliff terrain. Less than 45% of the study area's landslides were actual events.

This demonstrates that one of the causes of the study area's landslides is the gradient of the slope.

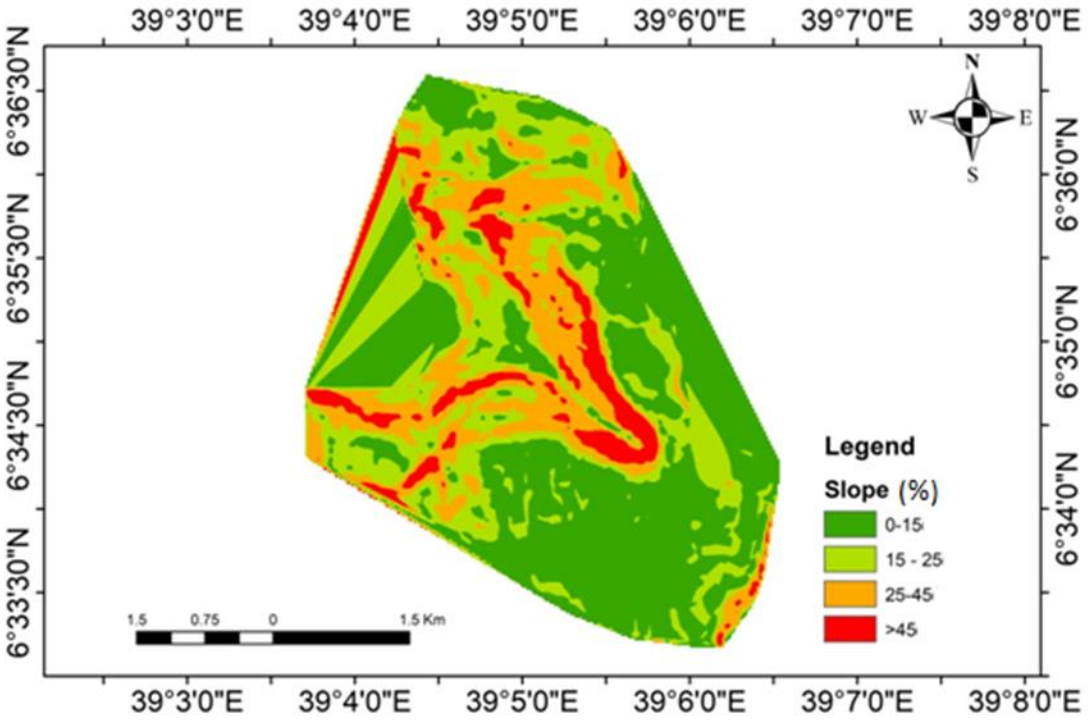

Figure 4-3: Slope map of the study area

4.2.1.2.5. Drainage

The Hodem, Bedesa, Belacho, Sida, Bohera, and Hamile rivers, which are tributaries of the Ghenale River, have emptied the Nansabo woreda. One of the rivers that may be located at the base of the landslide research area and flows to the Ghenale River is the Belacho. The Ghenale catchment, where the landslides were researched, is where the Tullu Gola Peasant Association is situated. Along with rainfall, streams' erosive activity exacerbates slope instability. Streams erode the valley walls, which makes the adjacent slope region unstable (Bathrellos et al., 2009). This is a result of streams undercutting one another. The slope is more likely to receive water and generate pore pressure as it gets closer to a stream. By eroding slopes or saturating the lowest portion of the material, streams can negatively impair stability and raise the ground water table. Therefore, one of the pieces of information needed for most landslide susceptibility zonation is the distance to the stream.

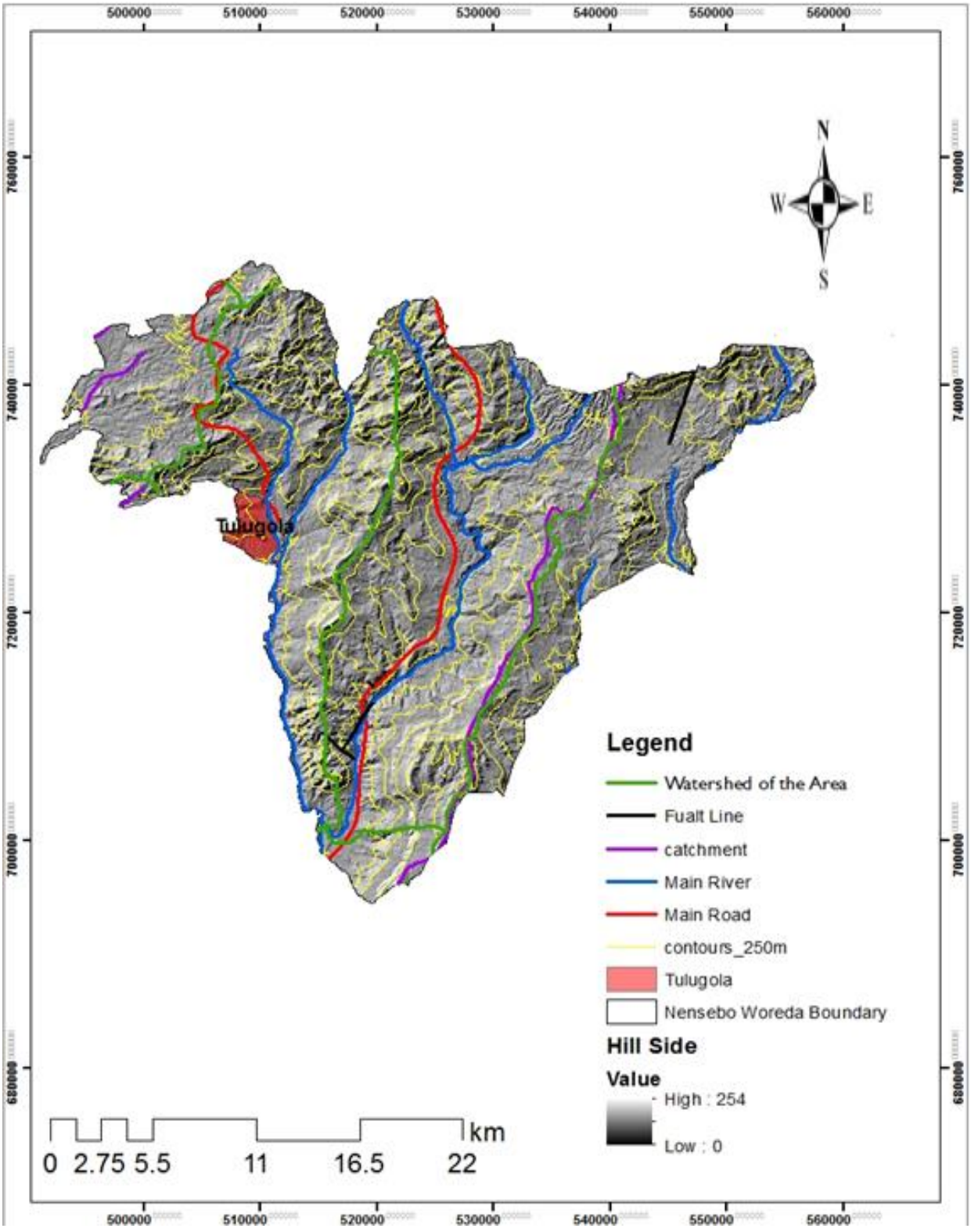

Figure 4-4: Map of physiography and drainage of the study area

4.2.1.2.6. Rainfall Analysis

The high yearly precipitation and the concentrated amount of rain that falls during one rainy season (from June to September) cause the soil to get saturated and create positive pore pressure, which may function as a catalyst to help the other causation variables trigger a landslide more quickly. The area has had more rain since 2006, with the largest annual rainfall record occurring in 2012, as shown in Figure 4.6 from the annual analysis of Tullu Gola rainfall. According to information gathered from locals during a site inspection, the landslide happened following the area's severe rainfall in 2018. Due to the great intensity of the rainfall, soil shear strength decreases, which causes a landslide to occur in Tullu Gola. The Tullu Gola Peasant Association recorded 1,407.16mm of mean annual precipitation, with maximum and lowest values of 2451.2 and 946 mm, respectively. This demonstrates that recent rainfall records in the past may have contributed to landslide activity.

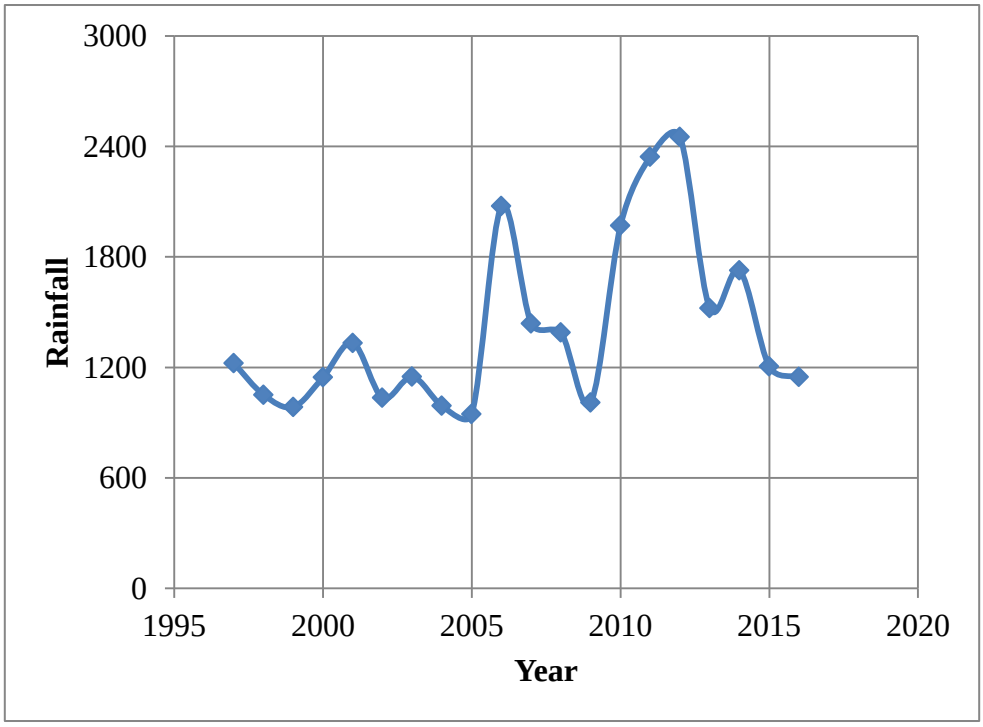

Figure 4-5: Rainfall analysis of the study area

4.2.1.2.7. Influence of Soil Permeability

Permeability refers to a soil's capacity to allow water to pass through it. The permeability of a soil is influenced by a number of things (or rock material). It is therefore important to examine the grain size and plasticity of soil samples before being classified. One can determine the range of soil permeability from the classification of the soil. The permeability of the studied region ranged from 1.33*10-4 to 2.7*10-4 cm/sec. The soil type of the Tullu Gola Peasant Association landslide was defined as silty soil since this overburden soil type was classed as fine-grained soil. The bulk movement of overburden material is caused by the differential in permeability between the layers. The formation of springs and seepages at the interface between the covering soil and the weathered volcanic rock indicates the presence of a pervious zone at the soil-rock interface and a general decrease in permeability of the underlying rock with depth.

4.2.1.2.8. Unstable Geological Structure

According to Ethiopia's geological map (Alemayehu Gudaya, 1991), the local geology of the Tullu Gola Peasant Association is characterized by Precambrian basement, Mesozoic sedimentary rocks, and Cenozoic volcanic rocks. The Precambrian rocks are deposited on top of the unconformable sedimentary and volcanic rocks. This consists of porphyritic basalt with less vesicular basalt and ignimbrite rock, tiny basalt and trachyte flows and deposits, and quartzo-feldsphatic, shist, fels, gneiss, and trachytic tuffs. Regional geology is one of the factors that contributed to the landslide in the study area.

4.2.1.2.9. River, Stream and Spring

In several instances, failure was caused by the river undercutting the slope, particularly during a flood. This undercutting serves to reduce stability, raise the slope gradient, and remove toe weight. Additionally, a river may be located at the area's toe in the Tullu Gola Peasant Association. One of the causes of the landslide in the study region was the presence of streams. These streams were filled with water that was stopped by a large foundation or wall.

4.3. Depth of the Groundwater Table (GWT)

Both vertical electrical sound and electrical resistivity profiling revealed the presence of worn and fractured horizons, which together make up the aquifer zones. Imaging and VES data show that the ground water table is located at a depth of 113 meters..

4.3.1. Electrical Profiling (Imaging)

Figure 4.7, the results of geophysical resistivity profiling (imaging) in the Tullu Gola Peasant Association's landslide-affected area using the software Res2dinvx64, shows the observed apparent resistivity, estimated apparent resistivity, and inverse model resistivity section.

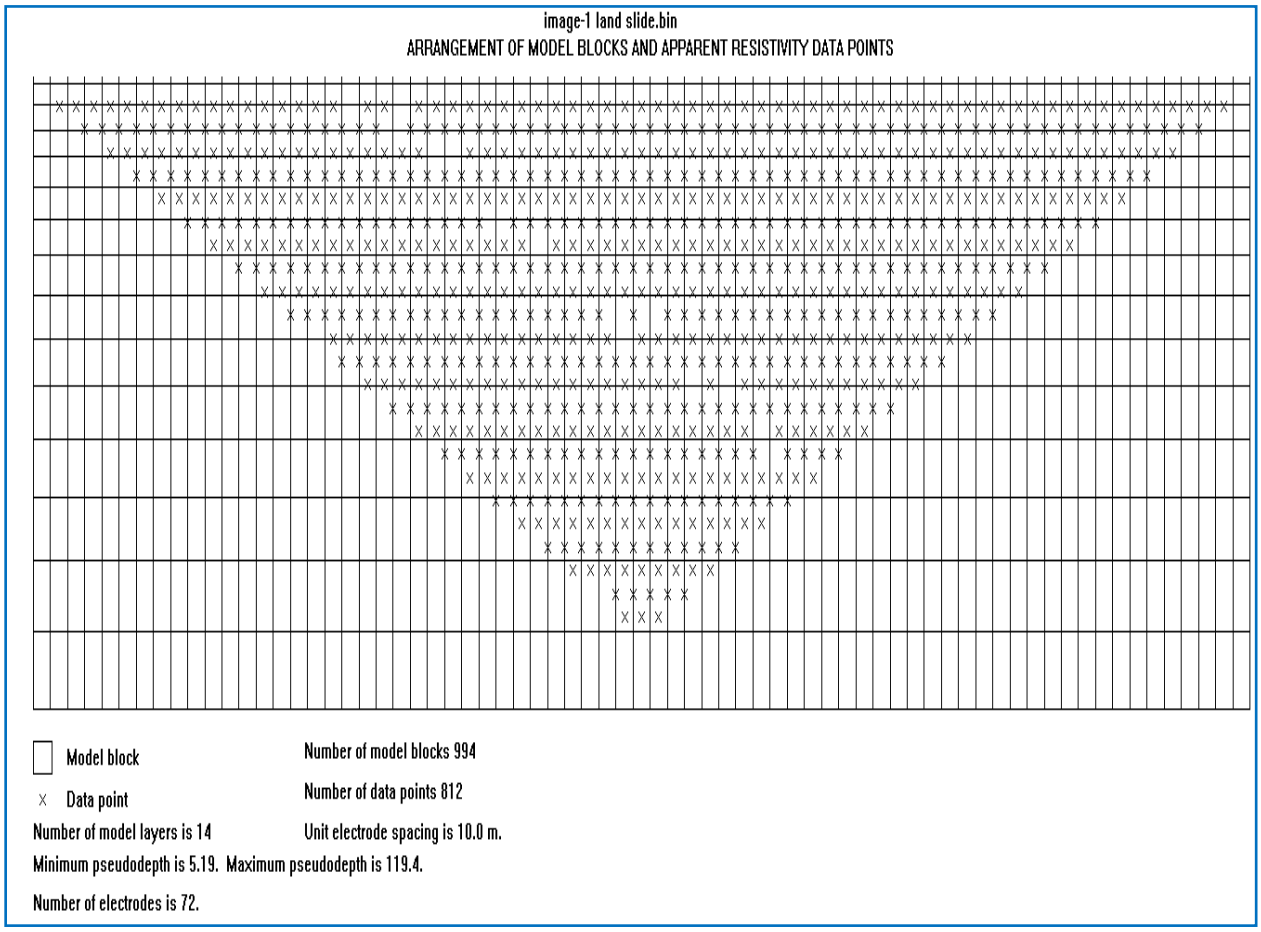

Figure 4-6: Arrangement of model blocks and apparent data point

The formation of the subsurface is shown in Figure 4.8 to have been gathered from horizontal to vertical by the imaging apparatus, saved, and then shown as "data points" when the instrument is connected to a computer. This data point was transformed using the Res2dinvx64 software tool into imagery that depicts the subsurface by each stratum's hue and resistivity.

. **Notice**: **the blue color** represented silt, clay, and moisture content.

The reddish color represented a very hard strata or basement.

The yellowish color represents fractured rocks.

The greenish color represented contacts of the boundary.

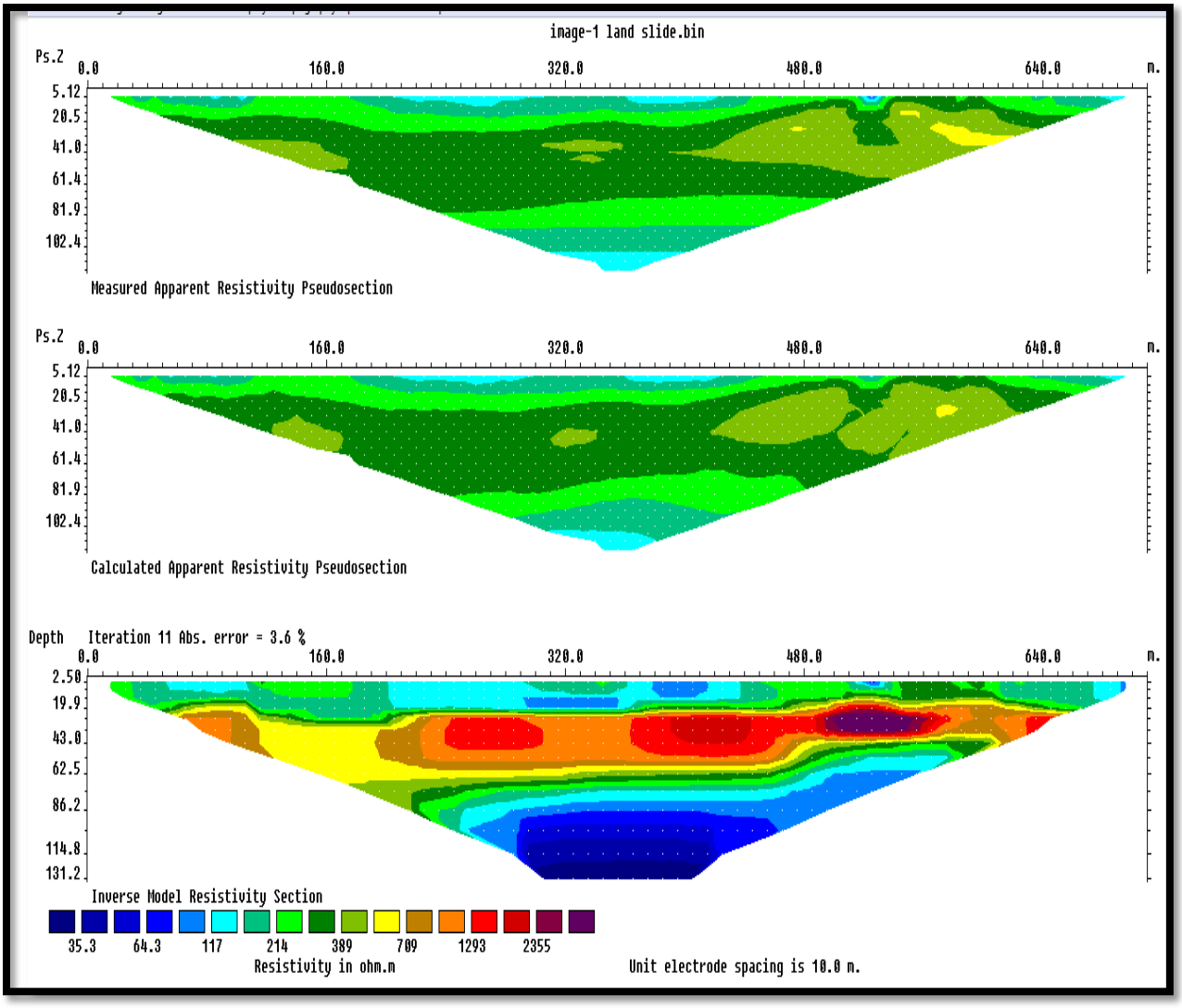

Figure 4-7: Calculated apparent resistivity pseudo section.

The subsurface of the research region is depicted in these figures from the beginning to the final interpretation. According to the colors and resistivity seen in Fig. 4.8, the landslide area's moisture content, weak zone, basement formation, huge igneous rock, sediment, structural geology, and ground water table Due to rocky strata below this layer that did not allow rainwater from Tullu Gola Peasant Association to permeate, the top layer of soil, which is between 0 and 15 meters deep, is silty and readily collapses during the rainy season.

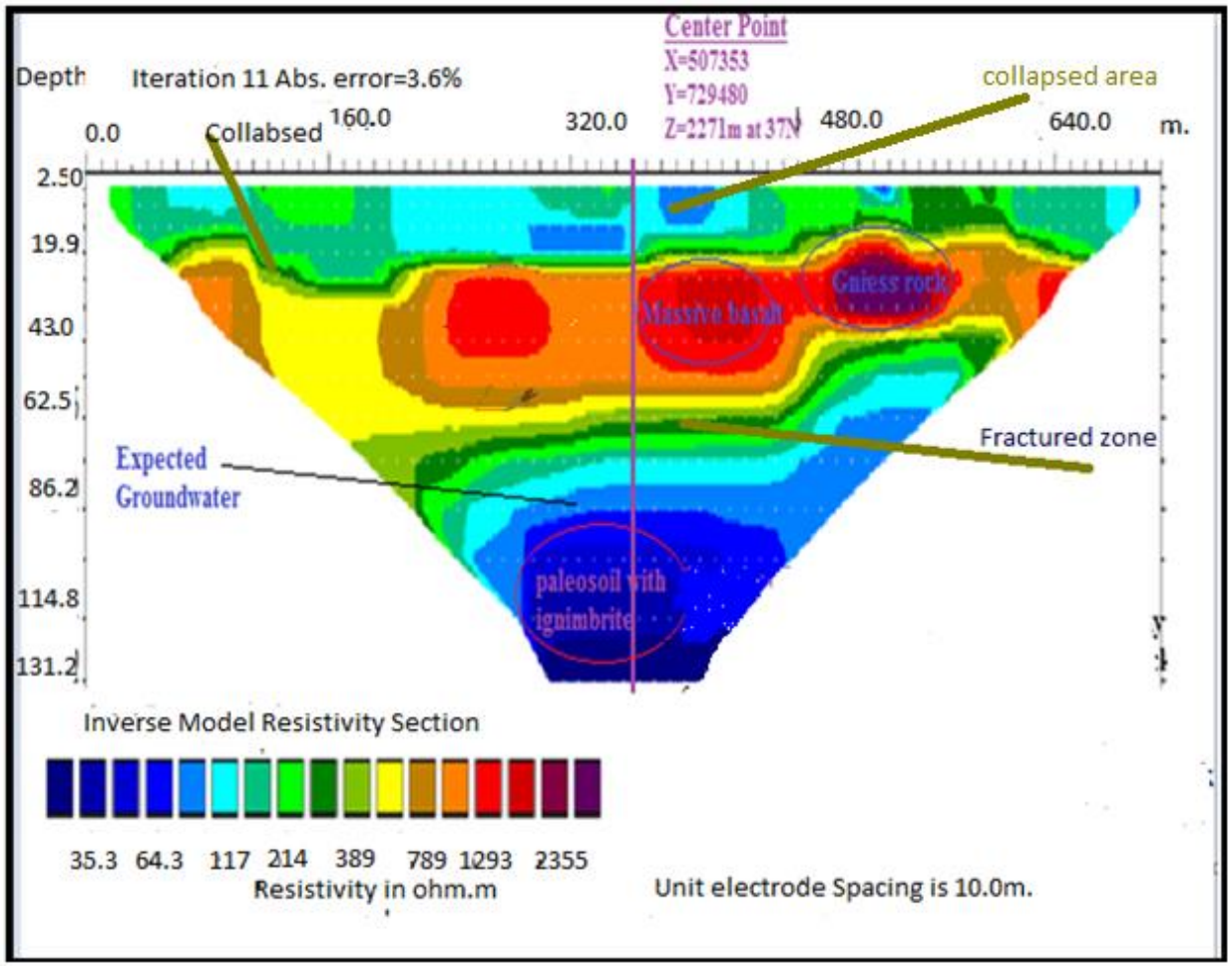

Figure 4-8: The image of profile and geology formation of the study area

As shown Figure 4.9 the geology of the study area were estimated:

0-2.5m silt and clay

2.5-15m highly decomposed Ignimbrite with silt soil

15-20m slightly fractured rock

20-65m highly massive rocks

65-85m massive rocks

65-85m moderately massive basaltic rock

85-100m highly weathered & fractured ignimbrite rock and

100-131m paleosoil intercalated with highly weathered ignimbrite rock

The final inverse model resistivity section, which is depicted in Figure 4.9, was obtained from a profiling image of several electrical resistivity layers and indicates the likelihood of an aquifer

between the fractures. As shown in Figure 4.9, the results of resistivity profiling revealed that basaltic rock that was slightly fractured and weathered in the upper soil had a resistivity of about 214 ohm-m. This was overlaid by a middle resistivity value of 35–117 ohm-m, which represents the soft to stiff soil material that was discovered during field investigation and could be the cause of a landslide due to an unstable geological structure and rain. Between the top layer and the bottom layer, there is a basement and a large basalt formation that was intruded by volcanic rock during a magma eruption. These formations show a resistivity value of 1293–2355 ohm–m. During the rainy season, these layers are impermeable, and the weak zone collapses as the soil becomes saturated. Groundwater with a high potential exists at a depth of 113 meters, and its resistivity ranges from 35 to 64 ohms per meter. Since this deep groundwater has tremendous potential, the investigation is unaffected by its location. At the heterogeneous contact boundary, ground water may flow from one direction to another. The inverse model resistivity and landslide correlations show nearly identical characteristics.

4.3.2. Vertical Electrical Resistivity Sounding Methods

As the depth increased, there were varying resistivity values from this VES, as shown in the table below. The change in these resistivities shows the degree of weathering and disturbance of the subsurface geological formation. One of the landslide triggers in the research location was this circumstantial change.

Table 4-13: Vertical Electrical Resistivity Sounding

AB/2	MN/2	Rho	AB/2	MN/2	Rho
1.5	0.5	55	30	6	389.3
2.1	0.5	62.5	45	6	750.5
3	0.5	70.5	66	6	1200.5
4.2	0.5	85.5	100	6	125
6	0.5	117	150	45	100.5
9	0.5	135.5	150	6	50.25
13.5	0.5	145.3	220	45	650
20	0.5	180.4	220	45	1250.6
20	6	190.06	330	45	2650.5
30	0.5	300.5			

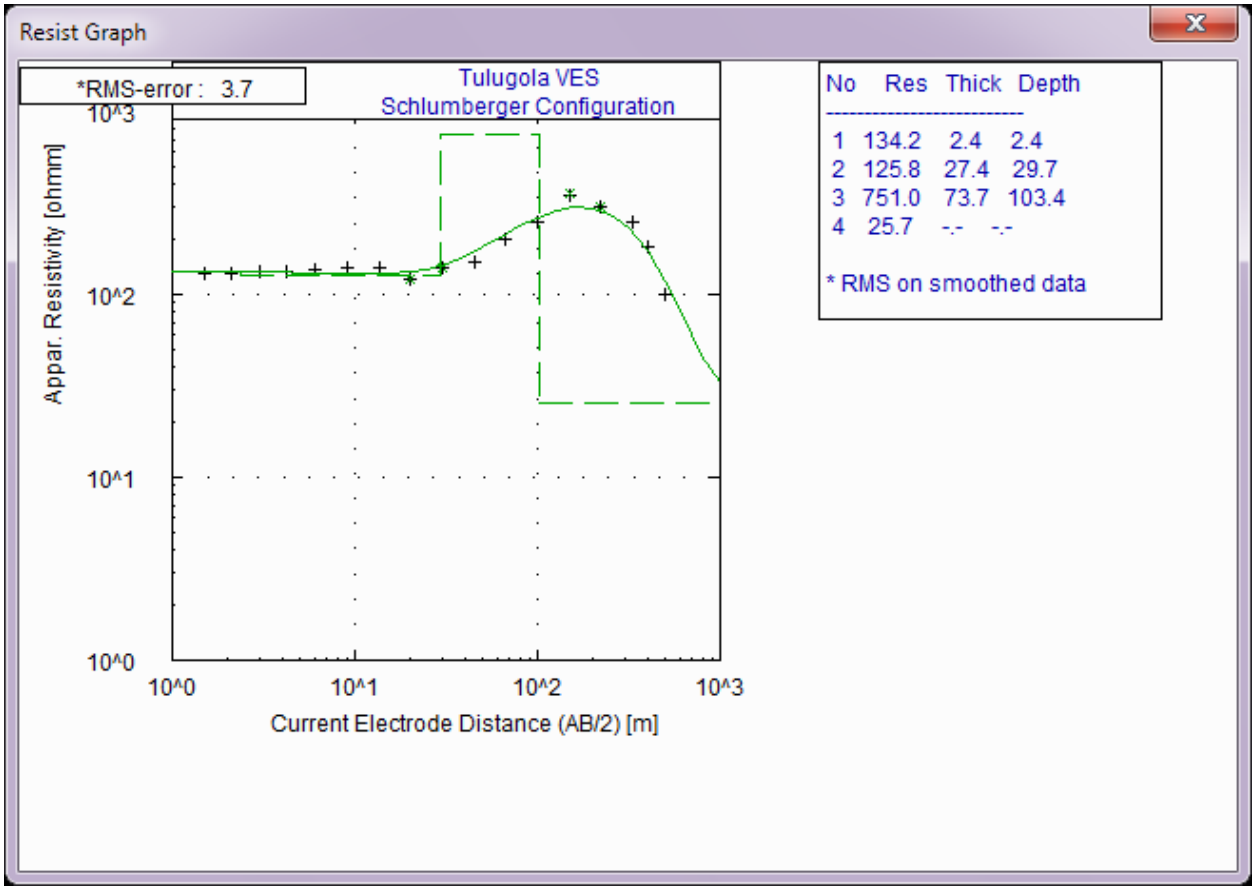

Figure 4-9: Resistivity inversion model-VES 1 along NE –SE Tullu Gola Peasant Association

The subsurface region was generated by the formation of various layers; the geophysical resistivity survey (i.e., VES) results indicate that there are four distinct layers that were discovered in various value ranges. The first layer (0–15 m) is silty soil. This layer was operational until it failed. The second layer (15–29.7 m), which is found between the top massive basalt and an impermeable layer, is somewhat fractured ignimbrite. The highly massive basalt is found in the third stratum (29.7–103.4 m). There is highly prospective ground water up to the basement's fourth stratum, 113.4 meters. Accordingly, the first layer, which has a resistivity of 134.2 ohms per meter, is 2.4 meters thick; the second layer, which has a resistivity of 125.8 ohms per meter, is 27.4 meters thick; the third layer, which has a resistivity value of 751.0 ohms per meter, is 73.7 meters thick; and the fourth layer, which has a resistivity of 25.7 ohms per meter, has a resistivity of 25.7 ohms per meter.

4.4. Slope Stability Analysis Using Plaxis 2D Software

The Plaxis-2D software package was used to conduct the study's slope stability, and the output result was discussed below. Stable slopes are assumed to have safety factors larger than 1, while unstable slopes are assumed to have safety factors less than 1. But the safety factor of greater than or equal to 1.5 is best suited to determining whether the slope is stable or unstable because it takes into account the amount of uncertainty that can occur during laboratory experiments. Therefore, the factor of safety greater than 1.5 is regarded as a stable slope in this study while taking into account the amount of uncertainty that may arise over the entire procedure.

4.4.1Analysis of the Top Side Slope (T.S.T.P-3)

The affected slope, which is present at the upper section of the slope, is the top side slope. The software analysis's finding for the factor of safety for this slope is 0.62. In accordance with the site's actual condition and the criteria described above, FS = 0.62 indicates an unstable slope. This slope is particularly degraded and steep in the study area.

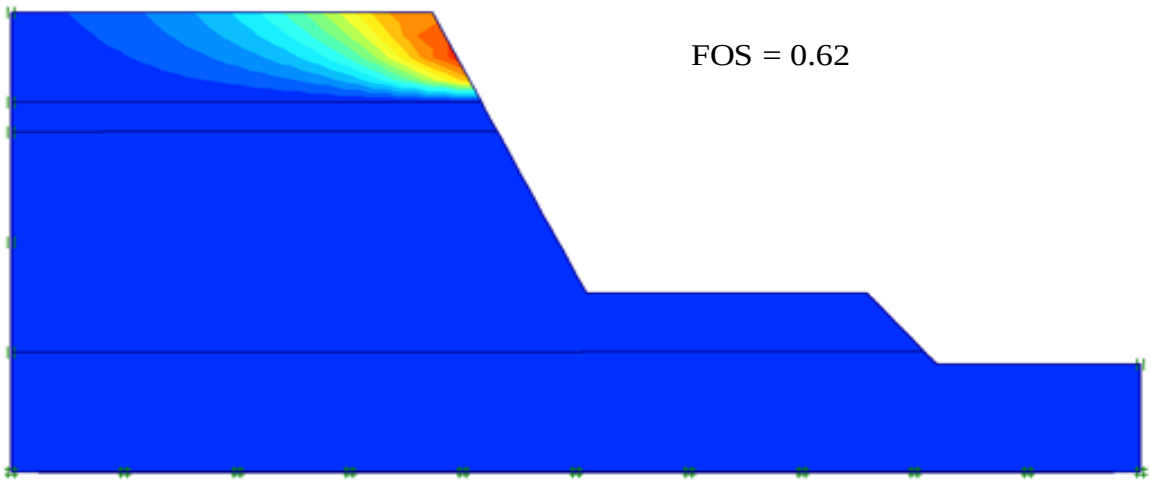

Figure 4-10: Factor of Safety output from software analysis

The soil that was discovered on the steep slope was movable and had already moved from its original position to the right side of the hill, as indicated in Figure 4.12 below. All of the soils that were shifted from this slope's upper portion were moved to the slope downstream. All of the domestic animals, plants, and human life were harmed by the movement of this slope. As a result, the software's output closely matches the real state of the site as it was seen.

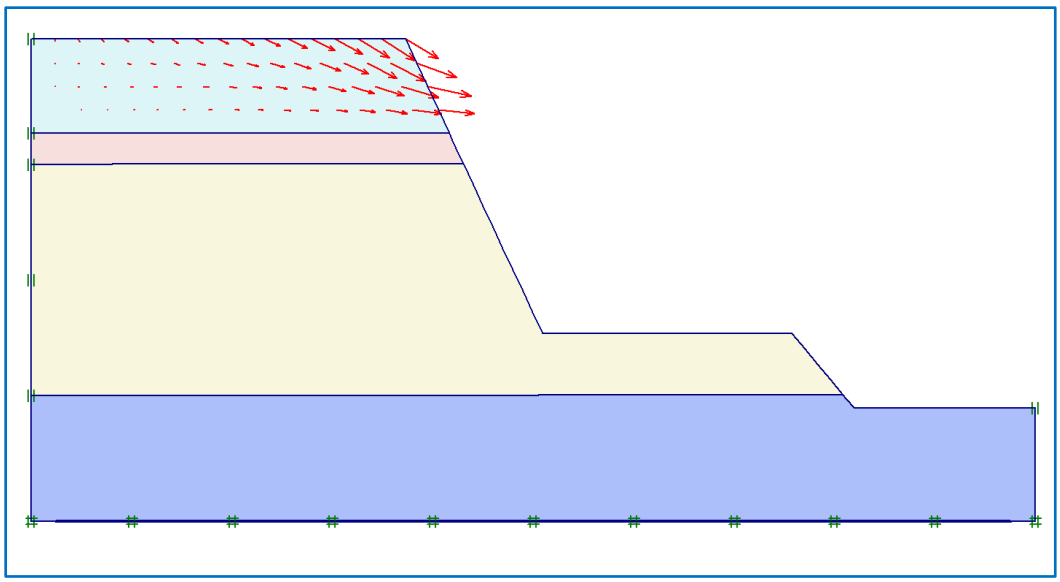

Figure 4-11: Direction of soil movement

The groundwater table is not taken into account during the stability study because the projected groundwater level is quite deep. In addition to the software analysis, the data collected from locals allows us to draw the conclusion that the stability of the slope is significantly impacted during the rainy season.

4.4.2. Analysis of the Right Side Slope (R.S.T.P-4)

The material that was transported down the right side slope's face is side slope soil that comes from higher up. This slope has an unstable factor of safety of 1.00, according to the software analysis. Numerous academic works refer to FS = 1 as a steady slope. Accepting FS = 1 as the table slope is not a wise choice, nevertheless, because some uncontrollable mistakes occurred during laboratory tests and software analysis. As a result, this study's right-side slope's stability condition is an unstable slope. Additionally, this outcome is in excellent agreement with the slope's real state as seen during field observation. Figure 4.13 shown below reveals that the soil is displaced at the middle of the third layer in the right direction along the surface of the slope. This is basically due to the fact that the soil that was found along this direction was originally the collapsed soil that was displaced from the upper part of the slope a long time ago.

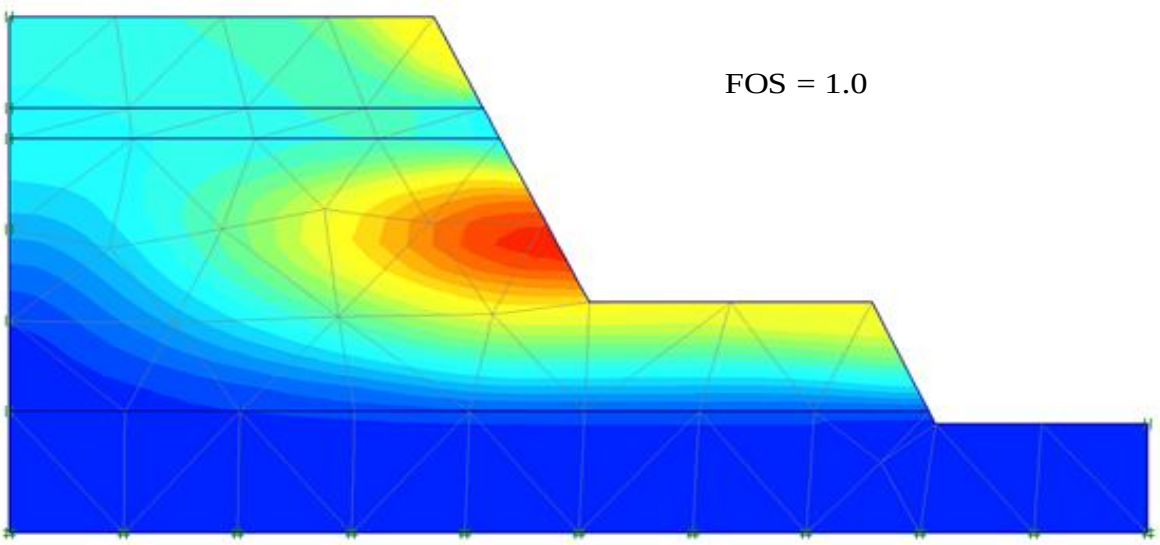

Figure 4-12: Factor of Safety output from software analysis

4.5. Consequence of Tulu Gola Landside

4.5.1. Disturbance of Environmental Features

Tullu Gola's environmental features were destroyed when a landslide occurred. Due to unfavorable conditions for obtaining food, some trees fell and mixed with sludge soil that was fragmented; nevertheless, other trees were released from their original growing region and sloughed by standing before drying. The region's land mass began to lose its original traits and collapse. The stream was diverted away from its native bank and dispersed unevenly, with some of it being stored off to the side and the remainder flowing outside.

Figure 4-13: Surface damage due to landslide of Tulu Gola landslide

4.5.2. Socio- Economic Problems

Due to earth subsidence in the study region, coffee plants and various fruits were killed. After a landslide devastated the area, the area where animals were utilized for grazing was destroyed because it was believed that the cattle might fall into the hole that had been created. Ponds that were kept at the edge of the slide area were flowing toward and distorting people's homes.

Figure 4-14: Died of cattle due to landslide of Tulu Gola Landslide

4.5.3 Loss of Human Life’s

Due to this destructive phenomenon, the lives of human beings are lost in this study area. According to the information obtained from local people, a lot of human beings passed away, including pregnant women, children, and the elderly.

Figure 4-15: Lose of Human Lives Due to Tulu Gola Landslide

4.6. Remedial Measures

The following methods were suggested for remedial measures after the landslide that happened at Tullu Gola Peasant Association..

4.6.1. Providing Surface Drainage

The geomorphology of the research area had a steep slope and was unstable. The mountain's summit had no effective drainage system diverting water toward the exit. Because of them, runoff erodes and scars the earth, creating openings and maybe interfering with weak points. By creating unlined surface drainage along the North to South side of the slide zone and controlling the runoff from the upper course, the continuity of the landslide at Tullu Gola will be lessened.

4.6.2. Rehabilitation by Afforestation

Increased evaporative losses caused by tall, deeply-rooted vegetation may help to stabilize the slopes if the slide region is forested with numerous trees and trenches are built.

4.6.3. Mitigate Damaged Area by Engineering Structures

The landslide-damaged area of Tullu Gola Peasant Association will be minimized by using engineering structures. To direct the entry of weathered debris into the stream, such structures are built by building geomembrane, geotextile, nailing and by removing loose material along the streamside. constructing embankments along areas that have slid, the size of which is defined by the gradient that, given the regional hydraulic conditions, generates a stable slope.

CHAPTER FIVE

CONCLUSIONS AND RECOMMENDATIONS

5.1. Conclusions

The study's location was the Tullu Gola Peasant Association in southeastern Ethiopia's Tullu region. During the site inspection, it was discovered that a sizable portion of Tullu Gola was affected by a landslide, which resulted in significant harm to the infrastructure, human lives, domestic animals, and the environment. As a result, the main goal of this study was to identify the soil type, contributing variables, and stability situation and suggest corrective actions for the landslides that occurred in the study region. The following findings of this study were advanced based on the site visiting, field study, laboratory test findings, and stability analysis. The results of soil laboratory tests conducted on both disturbed and undisturbed soil samples collected from four boreholes (i.e. grain size, Atterberg limits, water content, unit weight of soil, specific gravity, triaxial, UCS, swelling, consolidation, and permeability) in general show that the geotechnical characterization of soils at Tullu Gola was stiff to hard silt soil. All of the soil's attributes were found to be consistent with those of fine-grained soils based on the findings of laboratory tests (silt). According to the findings of a test on grain size, approximately 85.11 percent of soil types were made up mostly of fine-grained soils, which have a high degree of flexibility and are easily impacted during the saturation state. Four test pits' worth of soil were found to be highly silty (MH) soils, according to the plasticity chart produced by Atterberg limits testing. The semi-impervious nature of the soil collected for this study defined its type. As a result, the study area's landslides were caused by the disparity in permeability between the overburdened materials and the large rock at the interface. According to this study, weaker soils that typically have several weak points, have high compressibility and high flow potential, and deform like plastic were predominant in the study area. These soils can easily cause a landslide to occur when they become saturated and lose their shear strength. The impacted area's (the top side of the slope's) factor of safety was obtained using Plaxis software 2D at 0.62, while the right side's factor of safety was at or near 1, indicating an unstable slope for both slopes. The study area's triggering elements, including topography, drainage, elevation, slope gradient, and soil type, were identified using Arc GIS 10.3. According to the results of the geophysical resistivity survey profiling (imaging), the subsurface region was produced from the intercalation of

degraded ignimbrite rocks with silt and clay soil in the top geological layer. This layer was followed by a large rock and gneiss formation. Due to the heavily fragmented zone at the third layer, there is significant potential groundwater. The basement-like last layer prevented water from percolating. The subsurface region was created by the construction of various layers; four distinct layers were identified in different value ranges by the geophysical resistivity survey (i.e., VES) results. The first layer is a 0-2.4 m thick layer of silt interspersed with broken ignimbrite rocks. The second layer, which is found atop massive basalt, is 2.4–29.7 meters of silt with heavily weathered ignimbrite. The highly massive basalt is found in the third layer, which is 29.7-103.4 meters thick. There is highly prospective ground water in the fourth layer, 103.4 meters up to the basement. The results of the soil laboratory revealed silt soil and steep to gentle terrain; these results demonstrate the primary causes and precipitating variables for landslide occurrence in the research region. The main remedy to this issue is to provide enough surface drainage, engineering structures, and afforestation.

5.2. Recommendation

Engineers pay attention to researching this troublesome scenario all around the world because landslides are a destructive phenomenon that can happen anywhere. The results of this study are also provided for the study area's landslide. Additionally, based on the results of this study, the following advice was given to other researchers:

- Detail Investigation on the effect of climate change and landslide hazard on Tulu Gola landslide.
- Landslide hazard zonation in the West Arsi zone and border of Nansabo District like Guji zone and Sidama region, Ethiopia
- Detail investigation of the effect of rainfall during summer reason in the study area

REFERENCES

[1] Abebe, B., Dramis, F., Fubelli, G., Mohhammed, U., Asrat, A., (2010a) 'Landslides in the Ethiopian highlands and the Rift margins', *Journal of African Earth Sciences*, 56(4–5), pp. 131–138. doi: 10.1016/j.jafrearsci.2009.06.006.

[2] Abebe, B., Dramis, F., Fubelli, G., Mohhammed, U., Asrat, A., (2010b) 'Landslides in the Ethiopian highlands and the Rift margins', *Journal of African Earth Sciences*, 56(4–5), pp. 131–138. doi: 10.1016/j.jafrearsci.2009.06.006.

[3] Ali, S., Tiruneh, A. and Safara, T. (2017) 'April); Causes & reasons of land sliding in laga gaba highland area, Gimbi town, West wollega zone', *Advance Research Journal of Multidisciplinary Discoveries*, 12(0), pp. 23–31.

[4] Azeze, A. W. (2020) 'Assessments of Geotechnical Condition of Landslide Sites and Slope Stability Analysis Using Limit Equilibrium Method around Gundwin Town Area, Northwestern Ethiopia'. doi: 10.21203/rs.3.rs-20574/v1.

[5] Badr, M. and Anwar, E.-D. (2015) 'Application of Electrical Resistivity in Site Investigation', (March). Available at: https://www.researchgate.net/publication/299452589.

[6] Brinkgreve, R. B. J. (2005) 'Copyright ASCE 2005 69 Soil Constitutive Models Evaluation, Selection, and Calibration', *Geo-Frontiers Congress 2005*, pp. 69–98. doi: 10.1158/1538-7445.AM2013-1522.

[7] Broothaerts, N., Kissi, E., Poesen, J., Van Rompae, A., Getahun, K., Van Ranst, E., Diels, J., (2012) 'Spatial patterns, causes and consequences of landslides in the Gilgel Gibe catchment, SW Ethiopia', *Catena*, 97, pp. 127–136. doi: 10.1016/j.catena.2012.05.011.

[8] Choi, K. Y. and Cheung, R. W. M. (2013) 'Landslide disaster prevention and mitigation through works in Hong Kong', *Journal of Rock Mechanics and Geotechnical Engineering*, 5(5), pp. 354–365. doi: 10.1016/j.jrmge.2013.07.007.

[9] Coutinho, R. Q. and Da Silva, M. M. (2013) 'Geotechnical Characterization, Stability

Analysis, and the Stabilization Process for a Landslide in a area of Barreiras Formation and Granite Residual Soils, Pernambuco', *18th International Conference on Soil Mechanics and Geotechnical Engineering: Challenges and Innovations in Geotechnics, ICSMGE 2013*, 3(2007), pp. 2173–2176.

[10] Cruden, D. M. (2003) 'The first classification of landslides?', *Environmental and Engineering Geoscience*, 9(3), pp. 197–200. doi: 10.2113/9.3.197.

[11] Cruden, D. M. and Varnes, D. J. (1996) 'Chapter 3 LANDSLIDE TYPES AND PROCESSES', *Landslides: Investigation and Mitigation, Transportation Research Board Special Report 247, Washington D.C.*, (Bell 1992), pp. 36–75.

[12] Duan, G., Chen, D. and Niu, R. (2019) 'Forecasting groundwater level for soil landslide based on a dynamic model and landslide evolution pattern', *Water (Switzerland)*, 11(10). doi: 10.3390/w11102163.

[13] F. Mahler, C., Varanda, E. and C. D. de Oliveira, L. (2012) 'Analytical Model of Landslide Risk Using GIS', *Open Journal of Geology*, 02(03), pp. 182–188. doi: 10.4236/ojg.2012.23018.

[14] Fisseha, S. and Mewa, G. (2016) 'Road failure caused by landslide in north Ethiopia: A case study from Dedebit - Adi-Remets road segment', *Journal of African Earth Sciences*, 118, pp. 65–74. doi: 10.1016/j.jafrearsci.2016.02.022.

[15] Fry, M. J. (2019) *Copyright 2019 Cengage Learning. All Rights Reserved. May not be copied, scanned, or duplicated, in whole or in part. WCN 02-200-203*.

[16] Gaurina-Medjimurec, N. (2014) *Handbook of research on advancements in environmental engineering*, *Handbook of Research on Advancements in Environmental Engineering*. doi: 10.4018/978-1-4666-7336-6.

[17] Geertsema, M., Highland, L. and Vaugeouis, L. (2009) 'Environmental impact of landslides', *Landslides - Disaster Risk Reduction*, (1), pp. 589–607. doi: 10.1007/978-3-540-69970-5_31.

[18] Girma, F., Raghuvanshi, T. K., Ayenew, T., Hailamariam, T., (2015) 'Landslide hazard zonation in Ada Berga District, Central Ethiopia – A GIS based statistical Approach',

J.ournal of Geomatics, 90(1), pp. 25–38.GUERRA, A. J. T. *et al.* (2017) 'Slope Processes, Mass Movement and Soil Erosion: A Review', *Pedosphere*, 27(1), pp. 27–41. doi: 10.1016/S1002-0160(17)60294-7.

[19] Hamza, T. and Raghuvanshi, T. K. (2017) 'GIS based landslide hazard evaluation and zonation – A case from Jeldu District, Central Ethiopia, GIS based landslide hazard evaluation and zonation', *Journal of King Saud University - Science*, 29(2), pp. 151–165. doi: 10.1016/j.jksus.2016.05.002.

[20] Highland, L. M. and Bobrowsky, P. (2008) 'The landslide Handbook - A guide to understanding landslides', *US Geological Survey Circular*, (1325), pp. 1–147. doi: 10.3133/cir1325.

[21] Hulagabali, A., Gudissa, D. and Ararsa, W. (2008) 'Analysis of Landslide near Ambo City, Ethiopia, East Africa', *International Research Journal of Engineering and Technology*, 513, pp. 513–517. Available at: www.irjet.net.

[22] J.Crozier, T. G. and M. (2004) 'Part 1 Conceptual Models in Approaching', in.

[23] Jacob, A., Thomas, A. A., G Nath, A., MP, A., (2018) 'Slope Stability Analysis Using Plaxis 2D', *International Research Journal of Engineering and Technology*, pp. 3666–3668.

[24] Kabeta, W. F. and Teshager, D. K. (2020) 'Assessments of Geotechnical Conditions and Slope Stability Analysis : Case Study in Gedo town , Ethiopia', 6(3), pp. 1250–1258.

[25] Krahn, J. (2003) 'The 2001 R.M. Hardy Lecture: The limits of limit equilibrium analyses', *Canadian Geotechnical Journal*, 40(3), pp. 643–660. doi: 10.1139/t03-024.

[26] Liu, J. (2017) 'Stability Analysis of Road Embankment Slope Subjected to Rainfall Considering Runoff-Unsaturated Seepage and Unsaturated Fluid–Solid Coupling', *International Journal of Civil Engineering*, 15(6), pp. 865–876. doi: 10.1007/s40999-017-0194-7.

[27] Management, W. (2016) 'Guideline on Landslide Treatment and Mitigation', 2016(June).

[28] Marwa Mostafa, Amr Radwan, and M. B. (2016) 'Application of electrical resistivity in site investigation', (December 2015).

[29] McColl, S. T. (2015) *Landslide Causes and Triggers, Landslide Hazards, Risks, and Disasters*. Elsevier Inc. doi: 10.1016/B978-0-12-396452-6.00002-1.

[30] Mengistu, M. and Senamaw, A. (2020) 'Remote Sensing and GIS Based Potential Landslide Hazard Zonation in Ambo Woreda: Central Ethiopia', *Journal of Environment and Earth Science*, 10(2), pp. 19–27. doi: 10.7176/jees/10-2-03.

[31] Mersha, T. and Meten, M. (2020) 'GIS-based landslide susceptibility mapping and assessment using bivariate statistical methods in Simada area, northwestern Ethiopia', *Geoenvironmental Disasters*, 7(1). doi: 10.1186/s40677-020-00155-x.

[32] Mia, M., Sultana, N. and Paul, A. (2016) 'Studies on the Causes, Impacts and Mitigation Strategies of Landslide in Chittagong city, Bangladesh', *Journal of Environmental Science and Natural Resources*, 8(2), pp. 1–5. doi: 10.3329/jesnr.v8i2.26854.

[33] Mr. Digvijay P. Salunkhe *et al.* (2017) 'An Overview on Methods for Slope Stability Analysis', *International Journal of Engineering Research and*, V6(03), pp. 528–535. doi: 10.17577/ijertv6is030496.

[34] Msilimba, G. (2012) 'Landslide Inventory and Susceptibility Assessment for the Ntchenachena Area, Northern Malawi (East Africa)', *Approaches to Managing Disaster - Assessing Hazards, Emergencies and Disaster Impacts*, (1995). doi: 10.5772/28091.

[35] Mulatu, E., Kumar Raghuvanshi, T. and Abebe, B. (2009) 'LANDSLIDE HAZARD ZONATION AROUND GILGEL GIBE-II HYDROELECTRIC PROJECT, SOUTHWESTERN ETHIOPIA', *SINET: Ethiop. J. Sci*, 32(1), pp. 9–20.

[36] Nakamura, S. (2014) 'Earthquake-induced landslides: Distribution, motion and mechanisms', *Soils and Foundations*, 54(4), pp. 544–559. doi: 10.1016/ j.sandf.2014.06.001.

[37] Nelson, S. A. (2013) 'Slope Stability, Triggering Events, Mass Movement Hazards', *EENS 3050 Natural Disasters Tulane University*, pp. 1–17.

[38] Ortigao, J. A. R., Sayao, Alberto S. F. J. and Sayao, A. S. F. J. (2004) 'Soil Slope Stability', *Handbook of Slope Stabilisation*, pp. 89–108. doi: 10.1007/978-3-662-07680-4_5.

[39] Patra, P. and Devi, R. (2018) ‘Assessment, prevention and mitigation of landslide hazard in the Lesser Himalaya of Himachal Pradesh’, *Environmental & Socio-economic Studies*, 3(3), pp. 1–11. doi: 10.1515/environ-2015-0062.

[40] Patra, P. and Devi, R. (2018) ‘Assessment, prevention and mitigation of landslide hazard in the Lesser Himalaya of Himachal Pradesh’, *Environmental & Socio-economic Studies*, 3(3), pp. 1–11. doi: 10.1515/environ-2015-0062.

[41] Popescu, M. E. (2002) ‘Landslide causal factors and landslide remediatial options’, *3rd International Conference on Landslides, Slope Stability and Safety of Infra-Structures*, pp. 1–21.

[42] Radbruch-Hall, D. H. and Varnes, D. J. (1976) ‘Landslides - Cause and effect’, *Bulletin of the International Association of Engineering Geology*, 13(1), pp. 205–216. doi: 10.1007/BF02634797.

[43] Reichenbach, P. (2014) ‘The Influence of Land Use Change on Landslide Susceptibility Zonation: The Briga Catchment Test Site (Messina, Italy)’, *Environmental Management*, 54(6), pp. 1372–1384. doi: 10.1007/s00267-014-0357-0.

[44] Schuster, R. L. (1996) ‘Socioeconomic significance of landslides’, *Special Report - National Research Council, Transportation Research Board*, 247, pp. 12–35.

[45] Serdarevic, A. and Babic, F. (2019) ‘Landslide Causes and Corrective Measures – Case Study of the Sarajevo Canton’, 9(2), pp. 51–57. doi: 10.5923/j.jce.20190902.02.

[46] Symposium, R. (2018) *Advances in Landslide Research*, *Advances in Landslide Research*. doi: 10.5474/9789616498593.

[47] Tantri, P., Sari, K. and Lastiasih, Y. (2014) *Slope Stability of Road Embankment on Soft Soil*. Available at: http://www.uho.ac.id/cices2014.

[48] Tsige, D., Quezon, P. E. T. and Woldearegay, K. (2017) ‘Geotechnical Conditions and Stability Analysis of Landslide Prone Area: A Case Study in Bonga Town, South-Western Ethiopia’, 8(4).

[49] Verghese, S. J., Nguyen, C. T. and Bui, H. H. (2013) ‘Evaluation of plasticity-based soil constitutive models in simulation of braced excavation’, *International Journal of*

GEOMATE, 5(2), pp. 672–677. doi: 10.21660/2013.10.3328.

[50] Vinod, B. R., (2020) 'Slopes Stability Analysis Using the Plaxis 2D Program and Taylor 's Stability Equation', (2907), pp. 2907–2910.

[51] Walker, L. R. and Shiels, A. B. (2013) 'Chapter 4 Biological consequences for Landslide Ecology', *Landslide Ecology*, pp. 46–82.

[52] Walle, F. M., (2020) 'Landslide hazard zone mapping using Information Value model : the case of Gidole Landslide , Southern Ethiopia', (May).

[53] Wang, G. and Sassa, K. (2003) 'Pore-pressure generation and movement of rainfall-induced landslides: Effects of grain size and fine-particle content', *Engineering Geology*, 69(1–2), pp. 109–125. doi: 10.1016/S0013-7952(02)00268-5.

[54] Wang, G. and Sassa, K. (2003) 'Pore-pressure generation and movement of rainfall-induced landslides: Effects of grain size and fine-particle content', *Engineering Geology*, 69(1–2), pp. 109–125. doi: 10.1016/S0013-7952(02)00268-5.

[55] Woldearegay, K. *et al.* (2004) 'Controlling parameters and failure mechanisms of a large-scale landslide in Ethiopia', *Felsbau*, 22(3), pp. 46–55.

[56] Woldearegay, K. (2013) 'Review of the occurrences and influencing factors of landslides in the highlands of Ethiopia: With implications for infrastructural development', *Momona Ethiopian Journal of Science*, 5(1), p. 3. doi: 10.4314/mejs.v5i1.85329.

[57] Wu, J. T. H. (2019) 'Determination of Model Parameters for the Hardening Soil Model'.

[58] Yifru, B. A. and Ayehu, F. M. (2017) 'Prediction of Groundwater Level Fluctuation towards Rainfall Induced Landslide: Case of Blue Nile Gorge, Central Ethiopia', *Open Journal of Modern Hydrology*, 07(04), pp. 274–297. doi: 10.4236/ojmh.2017.74016.

APPENDIX A

A. LABORATORY RESULT ANALYSIS

Moisture Content

Table A.1 Soil sample at the left side: -- Moisture Content Data Sheet

Sample depth = 2.5m

Project Name: Nansabo District, Tullu Gola Peasant Association

Sample Number: L.S.T.P-1

Sample Description: Gray to brownish- silt soil

Depth of Sample(m)	2.5	2.5	2.5
Moisture can code	D	R-30	D-3
MC= Mass of empty, clean can + lid (grams)	21.41	21.14	21.26
MCMS= Mass of can,lid,and moist soil (grams)	86.53	80.39	83.77
MCDS= Mass of can, lid, and dry soil (grams)	71.96	67.15	69.77
MS= Mass of soil solids (grams)	50.55	46.01	48.51
MW= Mass of pore water (grams)	14.57	13.24	14
w = Water content, w%	28.82	28.78	28.86
Average Water content, w%	28.82		

Table A.2 Soil sample at the Bottom side: -Moisture Content Data Sheet

Sample depth = 3m

Project Name: Nansabo District, Tullu Gola Peasant Association

Sample Number: B.S.T.P-2

Sample Description: Gray to brownish- silt soil

Depth of Sample(m)	2.5	2.5	2.5
Moisture can code	A-3	A-6	A-2
MC= Mass of empty, clean can + lid (grams)	21.44	21.25	21.40
MCMS= Mass of can,lid,and moist soil (grams)	87.47	89.73	83.73
MCDS= Mass of can, lid, and dry soil (grams)	72.74	74.38	69.68
MS= Mass of soil solids (grams)	51.30	53.13	48.28
MW= Mass of pore water (grams)	14.73	15.35	14.05
w = Water content, w%	28.71	28.89	29.10
Average Water content, w%	28.90		

Table A.3 Soil sample at the Top side: -Moisture Content Data Sheet
Sample depth = 2.5m

Project Name: Nansabo District, Tullu Gola Peasant Association

Sample Number: T.S.T.P-3

Sample Description: Gray to brownish- silt soil

Depth of Sample(m)	2.5	2.5	2.5
Moisture can code	C-3	D-7	D-2
MC= Mass of empty, clean can + lid (grams)	21.25	21.45	21.28
MCMS= Mass of can,lid,and moist soil (grams)	84.97	81.52	82.23
MCDS= Mass of can, lid, and dry soil (grams)	70.69	68.69	68.60
MS= Mass of soil solids (grams)	49.44	46.61	47.32
MW= Mass of pore water (grams)	14.28	13.46	13.63
w = Water content, w%	28.88	28.88	28.80
Average Water content, w%	28.85		

Table A.4 Soil sample at the Right side: -Moisture Content Data Sheet

Sample depth = 2.5m

Project Name: Nansabo District, Tullu Gola Peasant Association

Sample Number: R.S.T.P-4

Sample Description: Gray to brownish- silt soil

Depth of Sample(m)	2.5	2.5	2.5
Moisture can code	A-10	A-1	D-5
MC= Mass of empty, clean can + lid (grams)	21.31	21.14	21.19
MCMS= Mass of can,lid,and moist soil (grams)	73.82	83.36	79.03
MCDS= Mass of can, lid, and dry soil (grams)	62.00	69.37	66.02
MS= Mass of soil solids (grams)	40.69	48.23	44.83
MW= Mass of pore water (grams)	11.82	13.99	13.01
w = Water content, w%	29.05	29.01	29.02
Average Water content, w%	29.03		

APPENDIX B

Specific Gravity Lab Test Result Data Sheet

Table B. 1 Soil sample at the left side: - Specific Gravity Data Sheet

Sample depth =2m

Project Name: Nansabo District, Tullu Gola Peasant Association

Sample Number: L.S.T.P-1

Sample Description: Gray to brownish- silt soil

Test Pit-1	Depth=2m		
Pycnometer No	B	C	D
Mass of calibrated Pycnometer (clean and dry)(Mp) in gm.	15.038	16.114	17.56
Mass of Pycnometer +Water (Mpw) in gm. at Ti=21c	43.494	44.127	44.53
Mass of Dry soil (Ms) in gm.	10	10	10
Mass of specimen +Pycnometer (Mps) in gm.	25.038	26.114	27.56
Mass of Pycnometer + soil + Water (Mpsw) in gm.	49.78	50.367	50.73
Temp Of Contents of Pycnometer when Mpsw was taken, TX in Cº	22	22	22
Mass of Pycnometer + Water at tempertureTx(Mpw) in gm.	43.488	44.121	44.525
K for TX	0.9996	0.9996	0.9996
Specific gravity at TX	2.70	2.66	2.64
Specific gravity at 20Cº	2.70	2.66	2.63
Average specific gravity at 20Cº	2.66		

Table B. 2 Soil sample at the Bottom side:-Specific Gravity Data Sheet

Sample depth = 2m

Project Name: Nansabo District, Tullu Gola Peasant Association

Sample Number: B.S.T.P-2

Sample Description: Gray to brownish- silt soil

Test Pit Two	Depth=2m		
Pycnometer No	B	4	C1
Mass of calibrated Pycnometer (clean and dry)(Mp) in gm.	17.82	24.2	25.11
Mass of Pycnometer +Water (Mpw) in gm. at Ti=21c	76.463	74.533	76.62
Mass of Dry soil (Ms) in gm.	11.467	11.345	11.04
Mass of specimen +Pycnometer (Mps) in gm.	29.287	35.545	36.15
Mass of Pycnometer + soil + Water (Mpsw) in gm.	82.67	81.271	83.05
Temp Of Contents of Pycnometer when Mpsw was taken, TX in Cº	22	22	22
Mass of Pycnometer + Water at tempertureTx(Mpw) in gm.	75.498	74.223	76.21
K for TX	0.9996	0.9996	0.9996
Specific gravity at TX	2.67	2.64	2.63
Specific gravity at 20Cº	2.67	2.64	2.63
Average specific gravity at 20Cº	2.65		

Table B-3 Soil sample at the Top side:-Specific Gravity Data Sheet

Sample depth = 2m

Project Name: Nansabo District, Tullu Gola Peasant Association

Sample Number: T.S.T.P-3

Sample Description: Gray to brownish- silt soil

Test Pit Three	Depth=2m		
Pycnometer No	2	6	C1
Mass of calibrated Pycnometer (clean and dry)(Mp) in gm.	15.57	12.67	14.09
Mass of Pycnometer +Water (Mpw) in gm. at Ti=21c	42.576	38.957	42.63
Mass of Dry soil (Ms) in gm.	10.381	10.245	10.05
Mass of specimen +Pycnometer (Mps) in gm.	25.951	22.915	24.14
Mass of Pycnometer + soil + Water (Mpsw) in gm.	48.998	45.522	49.09
Temp Of Contents of Pycnometer when Mpsw was taken, TX in Cº	22	22	22
Mass of Pycnometer + Water at tempertureTx(Mpw) in gm.	42.571	38.952	42.624
K for TX	0.9996	0.9996	0.9996
Specific gravity at TX	2.63	2.79	2.80
Specific gravity at 20Cº	2.62	2.79	2.80
Average specific gravity at 20Cº	2.74		

Table B. 4 Soil sample at the Right side:-Specific Gravity Data Sheet

Sample depth = 2m

Project Name: Nansabo District, Tullu Gola Peasant Association

Sample Number: R.S.T.P-4

Sample Description: Gray to brownish-silt soil

Test Pit Four	Depth=2m		
Pycnometer No	3	1	C1
Mass of calibrated Pycnometer (clean and dry)(Mp) in gm.	14.825	12.9	14.59
Mass of Pycnometer +Water (Mpw) in gm. at Ti=21c	42.252	40.268	41.63
Mass of Dry soil (Ms) in gm.	10.089	10.364	10.66
Mass of specimen +Pycnometer (Mps) in gm.	24.914	23.264	25.25
Mass of Pycnometer + soil + Water (Mpsw) in gm.	48.607	46.85	48.37
Temp Of Contents of Pycnometer when Mpsw was taken, TX in Cº	22	22	22
Mass of Pycnometer + Water at tempertureTx(Mpw) in gm.	42.247	40.263	41.625
K for TX	0.9996	0.9996	0.9996
Specific gravity at TX	2.71	2.74	2.72
Specific gravity at 20Cº	2.70	2.74	2.72
Average specific gravity at 20Cº	2.72		

APPENDIX C

Atterberg Limit Lab Test Result Data Sheet

Table C. 1 Soil sample at the left side: - Atterberg Limit Data sheet

Sample depth = 2m

Project Name: Nansabo District, Tullu Gola Peasant Association

Sample Number: L.S.T.P-1

Sample Description: Gray to brownish- silt soil

TEST Pit-1			PLASTIC LIMIT		LIQUID LIMIT		
Variable	NO		1	2	1	2	3
	Var.	Units					
Number of Blows	N	blows	---	---	30	23	17
Can Number	---	---	PT10	2	P3	ZE	3
Mass of Empty Can	M_C	(g)	17.797	18.362	36.082	32.203	18.2
Mass Can & Soil (Wet)	M_{CMS}	(g)	27.968	29.898	60.388	56.659	36.255
Mass Can & Soil (Dry)	M_{CDS}	(g)	25.564	27.23	52.424	48.569	30.183
Mass of Soil	M_S	(g)	7.767	8.868	16.342	16.366	11.983
Mass of Water	M_W	(g)	2.404	2.668	7.964	8.09	6.072
Water Content	*w*	(%)	30.95	30.09	48.73	49.43	50.67
Liquid Limit	PL	%	49.20				
Plastic Limit	PL	%	30.52				
Plastic Index	PI	%	18.68				

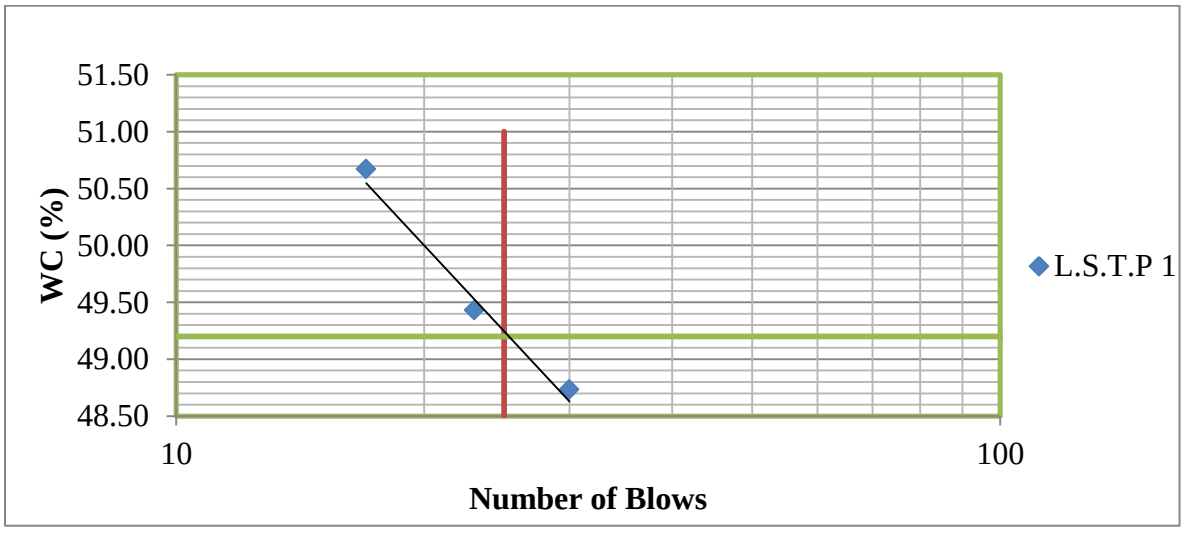

Figure C-1 Liquid limit sample water content (%) and Number of blows for test pit-1

Table C. 2 Soil sample at the Bottom side: - Atterberg Limit Data sheet

Sample depth = 2m

Project Name: Nansabo District, Tullu Gola Peasant Association

Sample Number: B.S.T.P-2

Sample Description: Gray to brownish- silt soil

TEST Pit-2			PLASTIC LIMIT		LIQUID LIMIT		
Variable	NO		1	2	1	2	3
	Var.	Units					
Number of Blows	N	blows	---	---	27	23	17
Can Number	---	---	A-1	B-2	HD	SB	A
Mass of Empty Can	M_C	(g)	17.71	17.151	17.411	18.395	37.164
Mass Can & Soil (Wet)	M_{CMS}	(g)	24.686	22.362	35.941	38.977	56.903
Mass Can & Soil (Dry)	M_{CDS}	(g)	22.744	20.916	28.398	30.436	48.48
Mass of Soil	M_S	(g)	5.034	3.765	10.987	12.041	11.316
Mass of Water	M_W	(g)	1.942	1.446	7.543	8.541	8.423
Water Content	*w*	(%)	38.58	38.41	68.65	70.93	74.43
Liquid Limit	LL	%	69.60				
Plastic Limit	PL	%	38.49				
Plastic Index	PI	%	31.11				

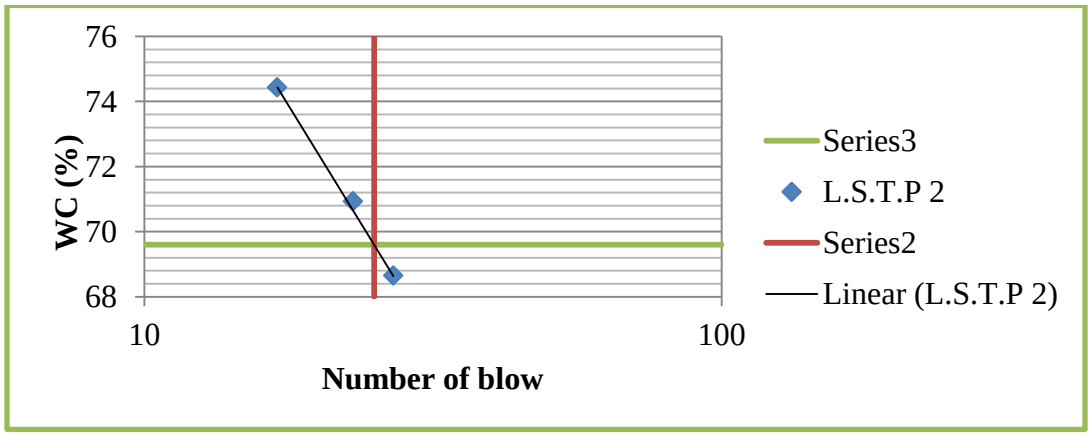

Figure C-2 Liquid limit sample water content (%) and Number of blows for test pit-2

Table C. 3 Soil sample at the Top side: - Atterberg Limit Data sheet

Sample depth = 2m

Project Name: Nansabo District, Tullu Gola Peasant Association

Sample Number: T.S.T.P-3

Sample Description: Gray to brownish- silt soil

TEST Pit-3			PLASTIC LIMIT		LIQUID LIMIT		
Variable	NO		1	2	1	2	3
	Var.	Units					
Number of Blows	N	blows	---	---	28	21	16
Can Number	---	---	P1	F1	SSB1	3	ZE
Mass of Empty Can	M_C	(g)	17.497	18.368	17.175	17.523	33.161
Mass Can & Soil (Wet)	M_{CMS}	(g)	26.357	28.648	43.049	40.975	55.325
Mass Can & Soil (Dry)	M_{CDS}	(g)	23.98	25.87	33.74	32.44	47.16
Mass of Soil	M_S	(g)	6.483	7.502	16.565	14.917	13.999
Mass of Water	M_W	(g)	2.377	2.778	9.309	8.535	8.165
Water Content	*w*	(%)	36.67	37.03	56.20	57.22	58.33
Liquid Limit	LL	%	56.55				
Plastic Limit	PL	%	36.85				
Plastic Index	PI	%	19.70				

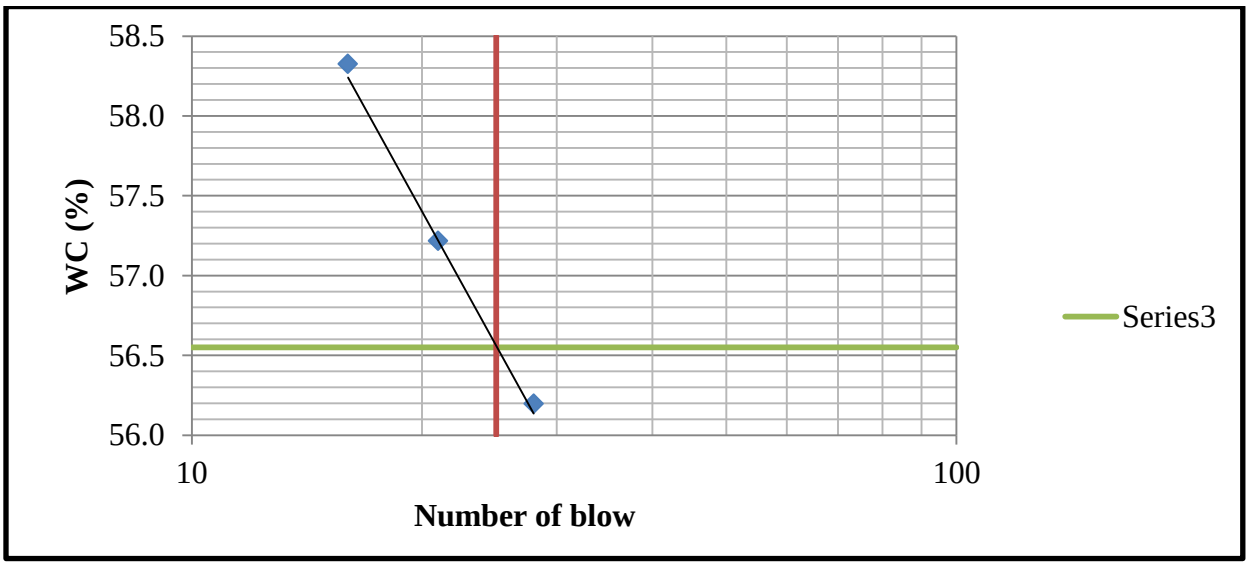

Figure C-3 Liquid limit sample water content (%) and Number of blows for test pit-3

Table C. 4 Soil sample at the Right side: - Atterberg Limit Data sheet

Sample depth = 2m

Project Name: Nansabo District, Tullu Gola Peasant Association

Sample Number: R.S.T.P-4

Sample Description: Gray to brownish- silt soil

TEST Pit-4			PLASTIC LIMIT		LIQUID LIMIT		
Variable	NO		1	2	1	2	3
	Var.	Units					
Number of Blows	N	blows	---	---	32	21	19
Can Number	---	---	A1	H2	1S1	B3	S3
Mass of Empty Can	M_C	(g)	17.724	17.601	36.568	18.206	18.385
Mass Can & Soil (Wet)	M_{CMS}	(g)	27.898	26.75	55.428	38.886	40.915
Mass Can & Soil (Dry)	M_{CDS}	(g)	25.43	24.55	48.37	30.998	32.24
Mass of Soil	M_S	(g)	7.706	6.949	11.802	12.792	13.855
Mass of Water	M_W	(g)	2.468	2.2	7.058	7.888	8.675
Water Content	*w*	(%)	32.03	31.66	59.80	61.66	62.61
Liquid Limit	LL	%	61.00				
Plastic Limit	PL	%	31.84				
Plastic Index	PI	%	29.16				

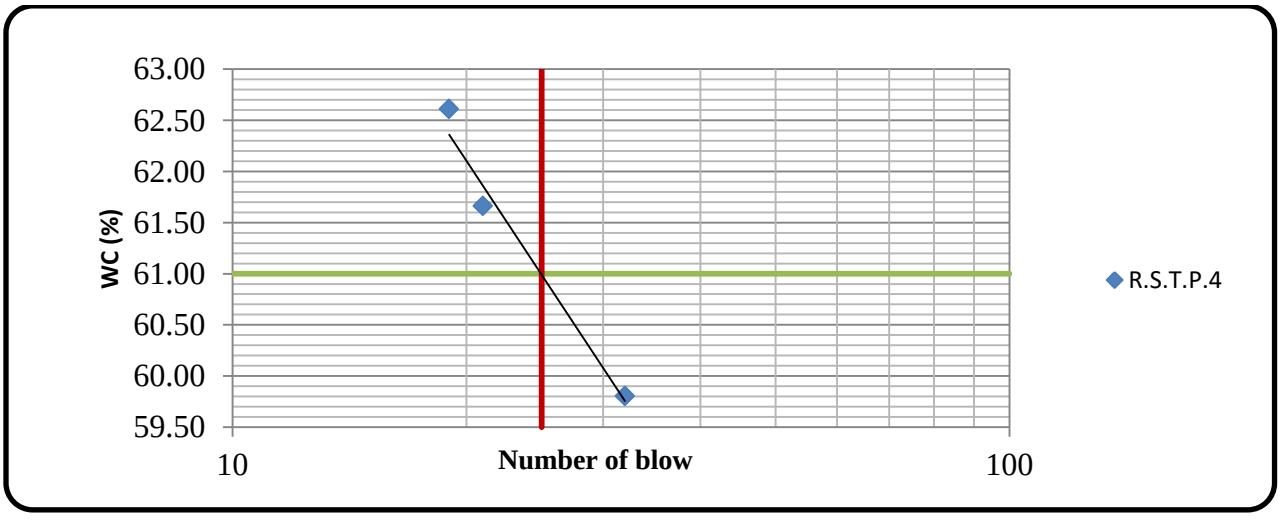

Figure C-4 Liquid limit sample water content (%) and Number of blows for test pit-4

APPENDIX D

Grain size Lab Test Result

Table D. 1 Soil sample at the left side: - Grain size Data Sheet

Sample depth = 2m

Project Name: Nansabo District, Tullu Gola Peasant Association

Sample Number: L.S.T.P-1

Sample Description: Gray to brownish- silt sandy with soil

Test Pit 1				
Total mass		500mg		
Sieve Size, mm	Mass.Ret.	% Ret.	% Cum. Ret.	% P
9.5	1.392	0.2784	0.2784	99.7216
4.75	4.74	0.947	1.23	98.7746
2	9	1.774	3.00	97.0006
0.85	8.49	1.6982	4.70	95.3024
0.425	13.109	2.6218	7.32	92.6806
0.300	12.807	2.5614	9.88	90.1192
0.150	12.946	2.5892	12.47	87.53
0.075	12.115	2.423	14.89	85.11
Pass	425.535	85.107	100.00	0.00

Sieve Analysis Result					
Determination of (PI)	LL (%)	91	Percentage of Course Soil	0.95	Soil group symbol
(LL - PL)	PL (%)	39.82	Percentage of Sandy Soil	13.67	ML to MH
	PI (%)	51.18	Percentage of Fine Soil	85.11	

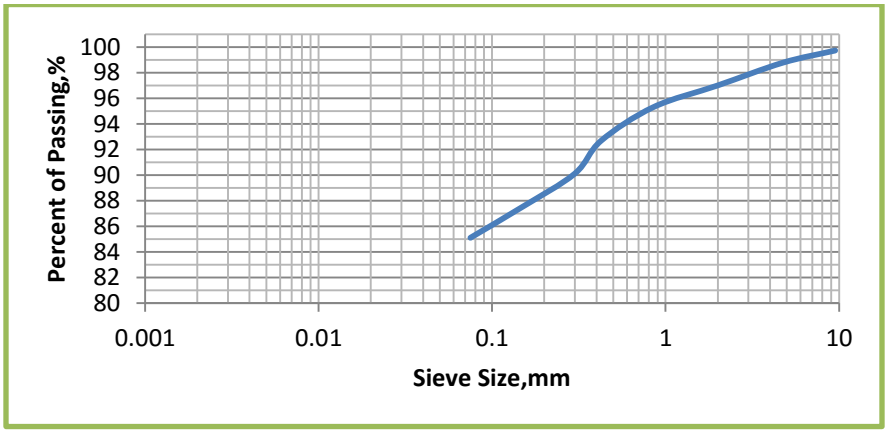

Figure D-1 Grain sieve analysis sample percent of passing (%) and Grain size for test pit-1

HYDROMETER ANANYSIS

Elapsed time, Min	Temp. ^{0}C	Actual Hydr. Reading,Rh	Hydr. reading corr. for meniscus(R')	Effective Depth, L (mm)	Particle Diameter (mm)	Corr. Hydr. Reading.	a, ASTM152 forGs =2.66	% Finer (P)	% Adjusted Finer (PA)
1	21	50	51	7.9	2.810693865	44.2	0.997726756	88.20	75.07
2	21	46	47	8.6	2.073644135	40.2	0.997726756	80.22	68.27
4	21	44	45	8.9	1.491643389	38.2	0.997726756	76.23	64.88
8	21	40	41	9.6	1.095445115	34.2	0.997726756	68.24	58.08
15	21	37	38	10.1	0.820568908	31.2	0.997726756	62.26	52.99
30	21	33	34	10.7	0.597215762	27.2	0.997726756	54.28	46.19
60	21	26	27	11.9	0.445346307	20.2	0.997726756	40.31	34.31
120	21	23	24	12.4	0.321455025	17.2	0.997726756	34.32	29.21
240	21	21	22	12.7	0.230036229	15.2	0.997726756	30.33	25.81
480	21	18	19	13.2	0.16583124	12.2	0.997726756	24.34	20.72
1440	21	15	16	13.7	0.097539166	9.2	0.997726756	18.36	15.62

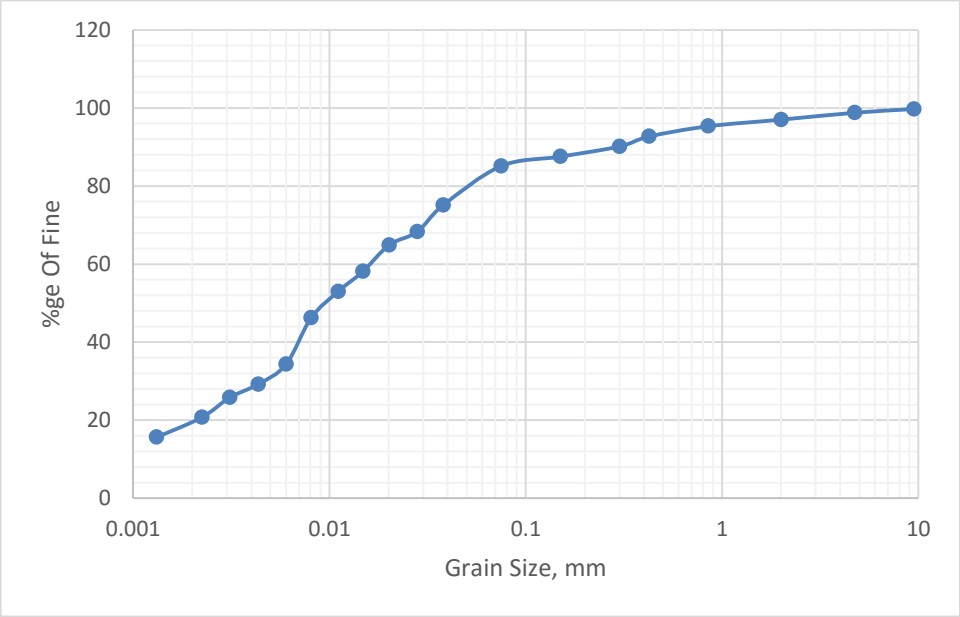

Combined Hydrometer and Sieve Analysis

WET SIEVE ANALYSIS

Table D-2 Soil sample at the Bottom side: - Grain size Data Sheet

Sample depth = 2m

Project Name: Nansabo District, Tullu Gola Peasant Association

Sample Number: B.S.T.P-2

Sample Description: Gray to brownish- silt soil

Test Pit- 2				
Total mass		500		
Sieve Size, mm	Mass.Ret.	% Ret.	% Cum. Ret.	% P
9.5	0	0	0	100
4.75	0.266	0.0532	0.0532	99.9468
2	4.005	0.801	0.8542	99.1458
0.85	5.162	1.0324	1.8866	98.1134
0.425	9.994	1.9988	3.8854	96.1146
0.300	11.132	2.2264	6.1118	93.8882
0.150	18.764	3.7528	9.8646	90.1354
0.075	14.948	2.9896	12.8542	87.15
Pass	435.729	87.1458	100.00	0.00

Sieve Analysis Result					
Determination of (PI)	LL (%)	91	Percentage of Course Soil	0.0532	Soil group symbol
(LL - PL)	PL (%)	39.82	Percentage of Sandy Soil	12.8010	MH
	PI (%)	51.18	Percentage of Fine Soil	87.15	

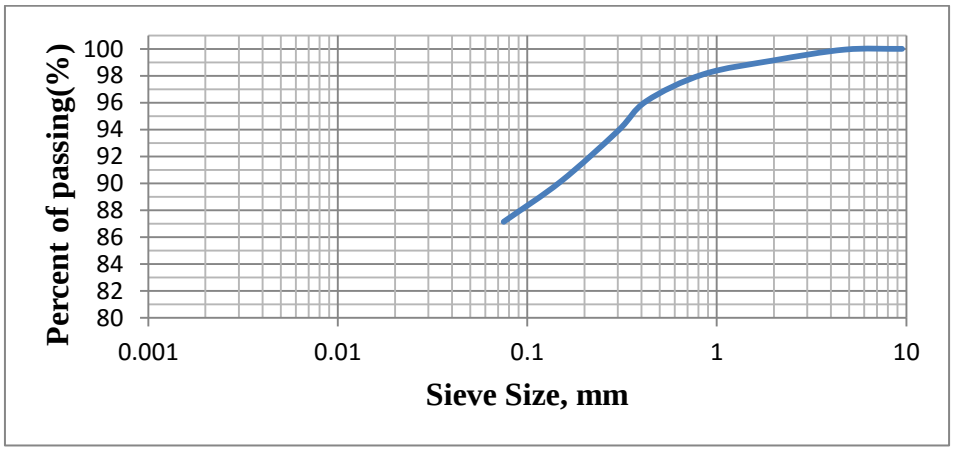

Figure D-2 Grain sieve analysis sample percent of passing (%) and Grain size for test pit-2

HYDROMETER ANANYSIS

Elapsed time, Min	Temp. ^{0}c	Actual Hydr. Reading,Rh	Hydr. reading corr.	Effective Depth, L (cm)	Particle Diameter (mm)	Corr. Hydr. Reading. (R'')	% Finer (P)	% Adjusted Finer (PA)
1	21	48	49	7.9	2.810693865	42.2	84.40	73.55
2	21	43	44	8.6	2.073644135	37.2	74.40	64.84
4	21	40	41	8.9	1.491643389	34.2	68.40	59.61
8	21	36	37	9.6	1.095445115	30.2	60.40	52.64
15	21	32	33	10.1	0.820568908	26.2	52.40	45.67
30	21	30	31	10.7	0.597215762	24.2	48.40	42.18
60	21	25	26	11.9	0.445346307	19.2	38.40	33.47
120	21	22	23	12.4	0.321455025	16.2	32.40	28.24
240	21	20	21	12.7	0.230036229	14.2	28.40	24.75
480	21	17	18	13.2	0.16583124	11.2	22.40	19.52
1440	21	14	15	13.7	0.097539166	8.2	16.40	14.29

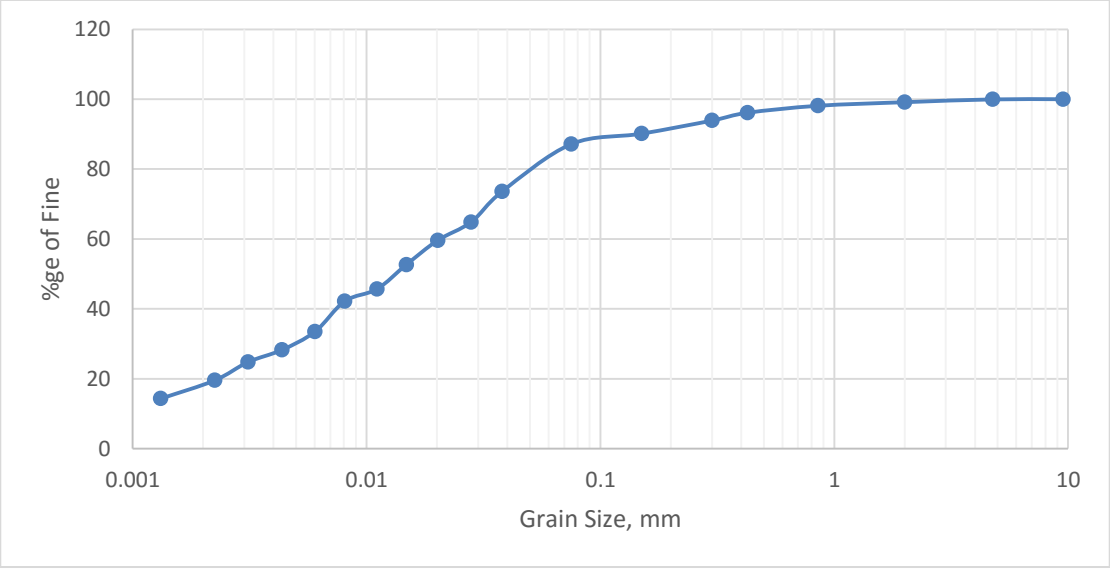

Combined wet sieve analysis and hydrometer analysis graph

Table D-3 Soil sample at the Top side: - Grain size Data Sheet

Sample depth = 2m

Project Name: Nansabo District, Tullu Gola Peasant Association

Sample Number: T.S.T.P-3

Sample Description: Gray to brownish-silt soil

Test Pit- 3				
Total mass		500mg		
Sieve Size, mm	Mass.Ret.	% Ret.	% Cum. Ret.	% P
9.5	0	0	0	100
4.75	0.000	0	0.0000	100
2	0.375	0.075	0.0750	99.925
0.85	1.335	0.267	0.3420	99.658
0.425	3.843	0.7686	1.1106	98.8894
0.300	4.197	0.8394	1.9500	98.0500
0.150	6.543	1.3086	3.2586	96.7414
0.075	3.334	0.6668	3.9254	96.07
Pass	480.373	96.0746	100.00	0.00

Sieve Analysis Result					
Determination of (PI)	LL (%)	91	Percentage of Course Soil	0.0000	Soil group symbol
(LL - PL)	PL (%)	39.82	Percentage of Sandy Soil	3.9254	
	PI (%)	51.18	Percentage of Fine Soil	96.07	MH

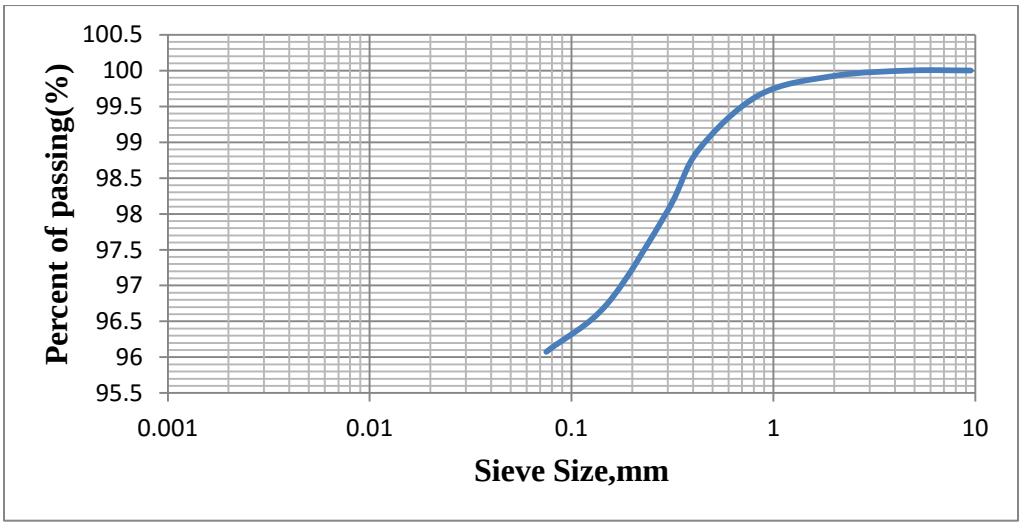

Figure D-3 Grain sieve analysis sample percent of passing (%) and Grain size for test pit-3

HYDROMETER ANANYSIS

Elapsed time, Min	Temp. ^{0}c	Actual Hydr. Reading,Rh	Hydr. reading corr. for meniscus(R')	Effective Depth, L (cm)	Particle Diameter (mm)	Corr. Hydr. Reading. (R'')	a, ASTM152 forGs =2.74	% Finer (P)	% Adjusted Finer (PA)
1	21	53	54	7.9	0.03682009	47.2	0.980481457	92.56	88.92
2	21	49	50	8.6	0.027164738	43.2	0.980481457	84.71	81.38
4	21	38	39	8.9	0.019540528	32.2	0.980481457	63.14	60.66
8	21	35	36	9.6	0.014350331	29.2	0.980481457	57.26	55.01
15	21	33	34	10.1	0.010749453	27.2	0.980481457	53.34	51.24
30	21	32	33	10.7	0.007823526	26.2	0.980481457	51.38	49.36
60	21	31	32	11.9	0.005834037	25.2	0.980481457	49.42	47.47
120	21	26	27	12.4	0.004211061	20.2	0.980481457	39.61	38.05
240	21	24	25	12.7	0.003013475	18.2	0.980481457	35.69	34.29
480	21	22	23	13.2	0.002172389	16.2	0.980481457	31.77	30.52
1440	21	21	22	13.7	0.001277763	15.2	0.980481457	29.81	28.64

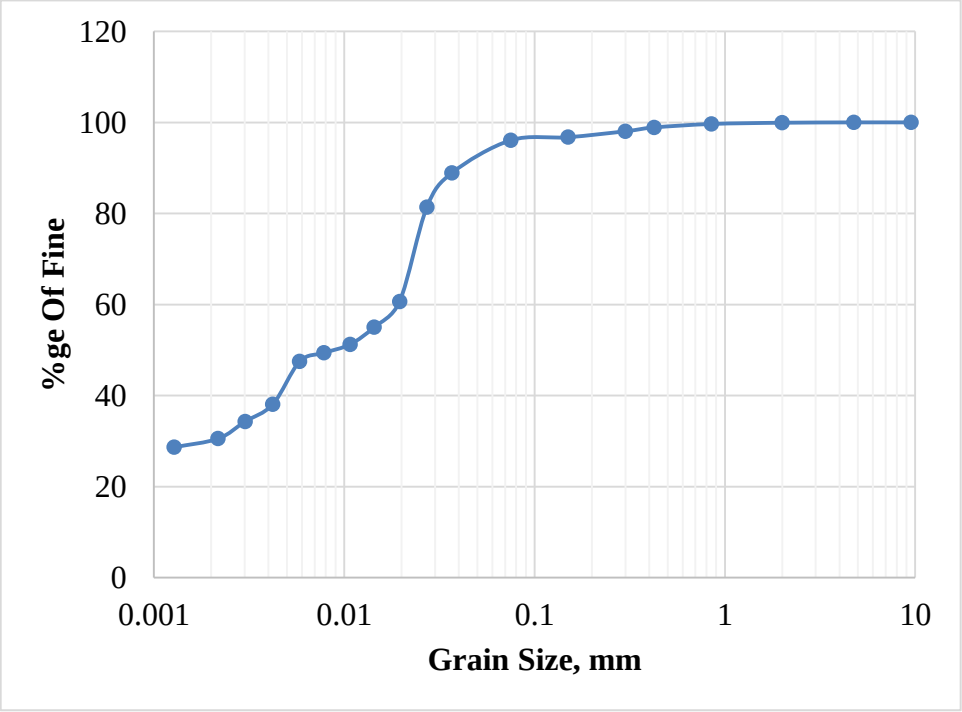

Combined Hydrometer and Sieve Analysis

Table D-4 Soil sample at the Right side: - Grain size Data Sheet

Sample depth = 2m

Project Name: Nansabo District, Tullu Gola Peasant Association

Sample Number: R.S.T.P-4

Sample Description: Gray to brownish-silt soil

Test pit 4				
Total mass		500mg		
Sieve Size, mm	Mass.Ret.	% Ret.	% Cum. Ret.	% P
9.5	0	0	0	100
4.75	0.266	0.0532	0.0532	99.9468
2	0.133	0.0266	0.0798	99.9202
0.85	0.493	0.0986	0.1784	99.8216
0.425	2.688	0.5376	0.7160	99.2840
0.300	4.847	0.9694	1.6854	98.3146
0.150	10.811	2.1622	3.8476	96.1524
0.075	10.615	2.123	5.9706	94.03
Pass	470.147	94.0294	100.00	0.00

Sieve Analysis Result

Determination of (PI)	LL (%)	91	Percentage of Course Soil	0.0532	Soil group symbol
(LL - PL)	PL (%)	39.82	Percentage of Sandy Soil	5.9174	
	PI (%)	51.18	Percentage of Fine Soil	94.03	MH

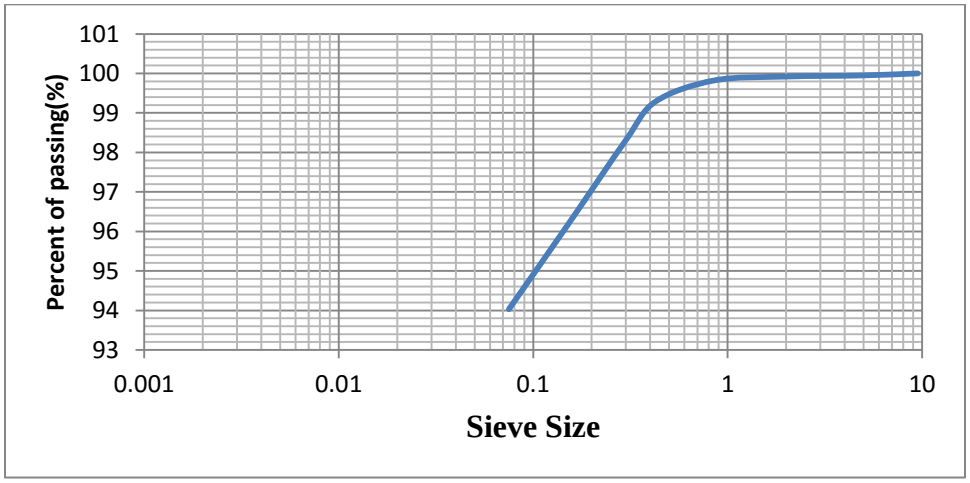

Figure D-4 Grain sieve analysis sample percent of passing (%) and Grain size for test pit-4

HYDROMETER ANANYS

Elapsed time, Min	Temp. ^{0}C	Actual Hydr. Reading,Rh	Hydr. reading corr. for meniscus(R')	Effective Depth, L (cm)	Particle Diameter (mm)	Corr. Hydr. Reading. (R'')	a, ASTM152 forGs =2.72	% Finer (P)	% Adjusted Finer (PA)
1	21	52	53	7.9	0.037382228	46.2	0.984642387	90.98	85.55
2	21	48	49	8.6	0.027579467	42.2	0.984642387	83.10	78.14
4	21	37	38	8.9	0.019838857	31.2	0.984642387	61.44	57.77
8	21	34	35	9.6	0.01456942	28.2	0.984642387	55.53	52.22
15	21	32	33	10.1	0.010913566	26.2	0.984642387	51.60	48.52
30	21	31	32	10.7	0.00794297	25.2	0.984642387	49.63	46.66
60	21	30	31	11.9	0.005923106	24.2	0.984642387	47.66	44.81
120	21	25	26	12.4	0.004275352	19.2	0.984642387	37.81	35.55
240	21	23	24	12.7	0.003059482	17.2	0.984642387	33.87	31.85
480	21	21	22	13.2	0.002205555	15.2	0.984642387	29.93	28.15
1440	21	20	21	13.7	0.001297271	14.2	0.984642387	27.96	26.29

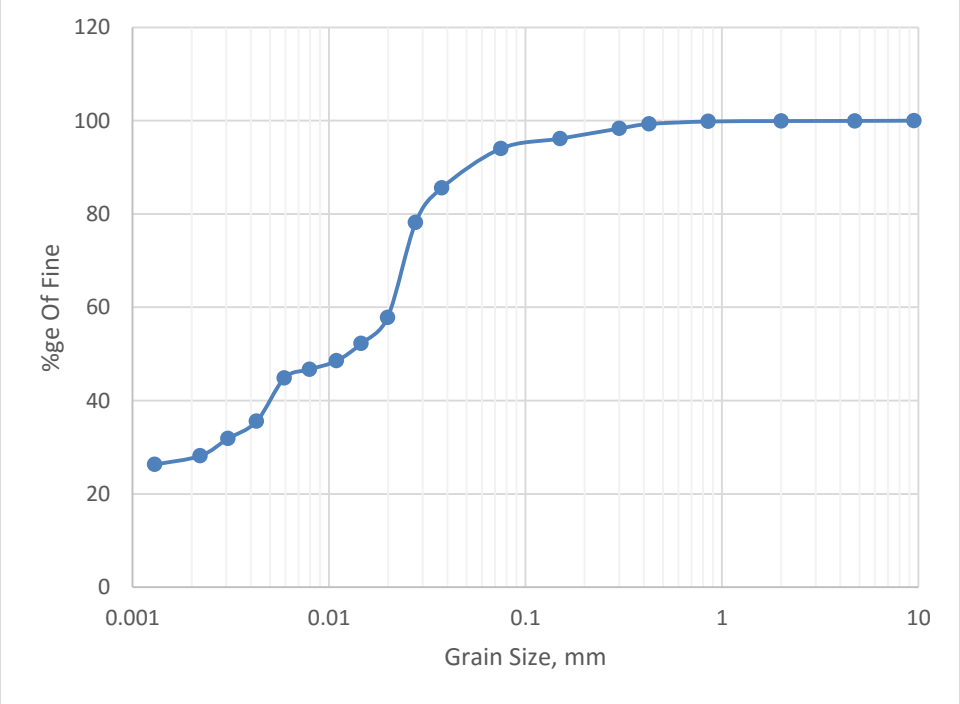

Combined Hydrometer and Sieve Analysis

APPENDIX E

Permeability Lab Test Result

TableE-1 Soil sample at the left and bottom side: - Falling head data sheet

Sample depth = 3m

Project Name: Nansabo District, Tullu Gola Peasant Association

Sample Number: L.S.T.P-1 and B.S.T.P-2

Sample Description: Gray to brownish- silt soil

L.S.T.P-1: Falling head data sheet			
Trial	01	02	03
Head, h_o (cm)	95.8	94.3	93.6
Head,h_1 (cm)	75.4	74.7	73.6
Time, t (s)	43	42	41
Temperature, T (^{o}c)	21	20	20
Volume, (ml)	46	48	51
Height dropped(cm)	20.4	19.6	20
Permeability at T^{o}c, K_T	$1.65*10^{-04}$	$1.64*10^{-04}$	$1.73*10^{-04}$
R_t for T	0.9761	1.0000	1.0000
Permeability at 20^{o}C, K_{20}	$1.61*10^{-04}$	$1.64*10^{-04}$	$1.73*10^{-04}$
Average K_{20} (cm/s)	**$1.66*10^{-04}$**		
B.S.T.P-2: Falling head data sheet			
Trial	01	02	03
Head, h_o(cm)	92.1	95.8	91
Head,h_1(cm)	61.2	70.4	67.8
Time, t (s)	36	39	41
Temperature, T (^{o}c)	21	20	20
Volume, (ml)	70	67	64
Height dropped(cm)	30.9	25.4	23.2
Permeability at T^{o}c, K_T	$3.51*10^{-04}$	$2.44*10^{-04}$	$2.22*10^{-04}$
R_t for T	0.9761	1.0000	1.0000
Permeability at 20^{o}C, K_{20}	3.43E-04	$2.44*10^{-04}$	$2.22*10^{-04}$
Average K_{20}(cm/s)	**$2.70*10^{-04}$**		

Table E-2 Soil sample at the right and top side:-Falling head data sheet

Sample depth = 3m

Project Name: Nansabo District, Tullu Gola Peasant Association

Sample Number: R.S.T.P-4 and T.S.T.P-3

Sample Description: Gray to brownish- silt soil

R.S.T.P-4: Falling head data sheet			
Trial	01	02	03
Head, h_o (cm)	89	96.3	91.6
Head,h_1 (cm)	56.9	66	59
Time, t (s)	67	58	54
Temperature, T (^{o}c)	20	20	20
Volume, (ml)	46	48	51
Height dropped (cm)	32.1	30.3	32.6
Permeability at T^{o}c, K_T	$1.25*10^{-04}$	$1.22*10^{-04}$	$1.52*10^{-04}$
R_t for T	1.0000	1.0000	1.0000
Permeability at 20^{o}C, K_{20}	$1.25*10^{-04}$	$1.22*10^{-04}$	$1.52*10^{-04}$
Average K_{20} (cm/s)	**$1.33*10^{-04}$**		
T.S.T.P-3: **Falling head data sheet**			
Trial	01	02	03
Head, h_o (cm)	84	89	94
Head,h_1 (cm)	67	66	73
Time, t (s)	54	48	62
Temperature, T(^{o}c)	21	20	20
Volume, (ml)	48	46	53
Height dropped(cm)	17	23	21
Permeability at T^{o}c, K_T	$1.23*10^{-04}$	$1.84*10^{-04}$	$1.20*10^{-04}$
R_t for T	0.9761	1.0000	1.0000
Permeability at 20^{o}C, K_{20}	$1.20*10^{-04}$	$1.84*10^{-04}$	$1.20*10^{-04}$
Average K_{20} (cm/s)	**$1.41*10^{-04}$**		

APPENDIX F

Unconfined Compression Strength Lab Test Result

Table F-1 Soil sample at the Right side: - Unconfined Compression Strength Test Data Sheet

Soil sample at the Right side: - USC Test Data Sheet

Sample depth = 3m

Project Name: Nansabo District, Tullu Gola Peasant Association

Sample Number: R.S.T.P-3

Sample Description: Gray to brownish-silt soil

Qu	381.0394		kN/m^2
Cu	190.5197		Kpa
ms	156.757		g
ds	37.5		m
hs	75		m
mc	9.773		g
mcws	98.786		g
Mcds	78.763		g
mw	20.023		g
mds	68.99		g
w%	29.02305		%
density	0.001893	1.893361	Kg/m^3
unit weight		18.57387	kN/m^3
dry unit weight		14.39578	kN/m^3

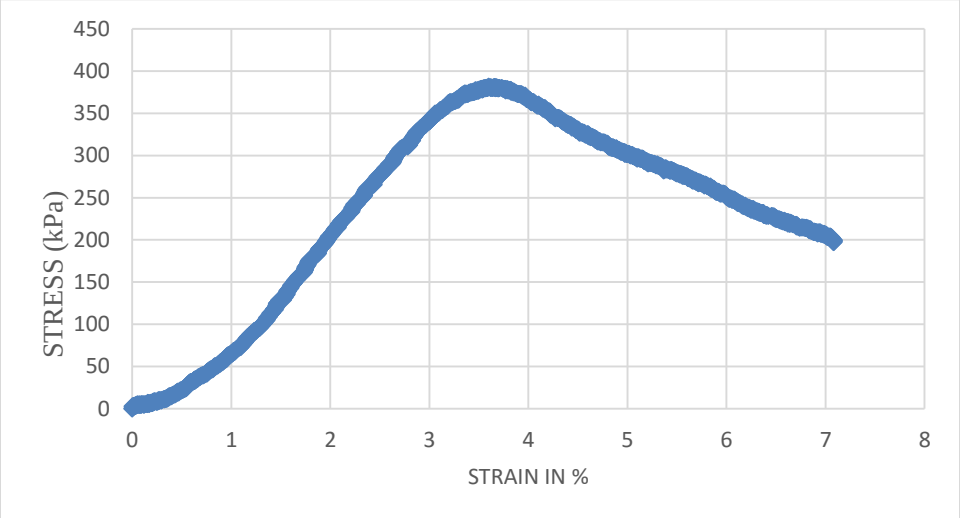

Table F-2 Soil sample at the Top side: - USC Test Data Sheet

Soil sample at the Top side: - USC Test Data Sheet

Sample depth = 3m

Project Name: Nansabo District, Tullu Gola Peasant Association

Sample Number: T.S.T.P-3

Sample Description: Gray to brownish-silt soil

qu	102.4601		kN/m^2
cu	51.23005		Kpa
ms	152.892		g
ds	37.5		m
hs	80		m
mc	36.52		g
mcws	158.876		g
Mcds	127.333		g
mw	31.543		g
mds	90.813		g
w%	34.73401		%
density	0.001731	1.731261	
unit weight		16.98367	kN/m^3
dry unit weight		12.60533	kN/m^3

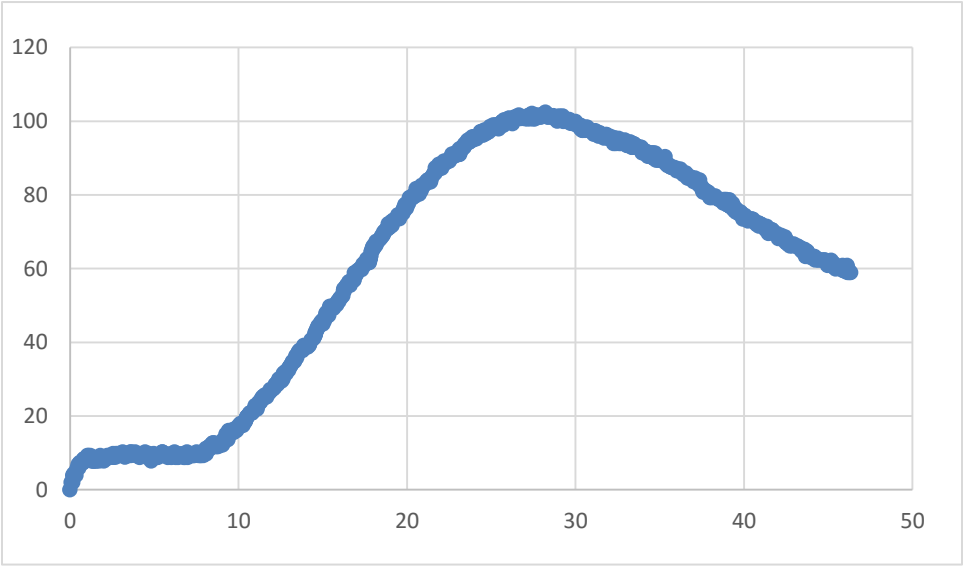

APPENDIX G

Consolidation Lab Test Result

Table G-1 Soil sample at the Right side: -Consolidation Test Data Sheet

Soil sample at the Right side: - Consolidation Test Data Sheet

Sample depth = 3m

Project Name: Nansabo District, Tullu Gola Peasant Association

Sample Number: T.S.T.P-3

Sample Description: silty soil

Time	Deformation @ 1kg	Deformation @ 2kg	Deformation @ 4kg	Deformation @ 8kg	Deformation @ 16kg	Unloading @ 8kg	Unloading @ 4kg	unloading @ 2kg	unloading @ 1kg
0.00	0.02	0.190	1.182	3.068	5.156	8.192	8.142	8.052	7.152
0.10	0.130	1.07	2.094	4.028	7.02	8.198	8.132	8.028	7.132
0.25	0.136	1.078	2.124	4.102	7.064	8.174	8.112	8.024	7.128
0.50	0.142	1.088	2.142	4.138	7.096	8.17	8.108	8.022	7.124
1.00	0.146	1.1	2.158	4.168	7.124	8.166	8.106	8.018	7.122
2.00	0.152	1.108	2.172	5	7.158	8.164	8.102	8.016	7.12
4.00	0.156	1.12	2.188	5.026	7.188	8.162	8.1	8.012	7.118
15.00	0.164	1.136	3.012	5.064	8.052	8.156	8.09	8.004	7.112
30.00	0.168	1.144	3.022	5.088	8.092	8.152	8.082	7.196	7.104
60.00	0.172	1.15	3.032	5.106	8.122	8.148	8.076	7.188	7.096
120.00	0.176	1.156	3.042	5.12	8.148	8.146	8.068	7.176	7.084
240.00	0.182	1.166	3.052	5.132	8.17	8.144	8.062	7.168	7.07
480.00	0.188	1.174	3.06	5.144	8.192	8.142	8.056	7.16	7.062
1440.00	0.190	1.182	3.068	5.156	8.192	8.142	8.052	7.152	7.05
								7.152	7.05
t2 = 4t1	0.006	0.008	0.030	0.074	**0.044**	0.024	0.020	0.004	0.004
	0.010	0.022	0.034	0.066	0.060	0.008	0.006	0.006	0.006
	0.010	**0.020**	0.030	0.862	0.062	0.006	**0.006**	0.006	**0.004**
	0.010	0.020	**0.030**	**0.858**	0.064	**0.004**	0.006	**0.006**	**0.004**
Do	**0.126**	**1.068**	**2.128**	**3.310**	**6.976**	**8.170**	**8.114**	**8.024**	**7.126**
D100	0.19	1.18	2.95	5.1	8.2	8.142	8.056	7.2	7.066
D50%	0.158	1.124	2.539	4.205	7.588	8.156	8.085	7.612	7.096
t50%	**2**	**4**	**6**	**1**	**7**	**6**	**40**	**20**	70

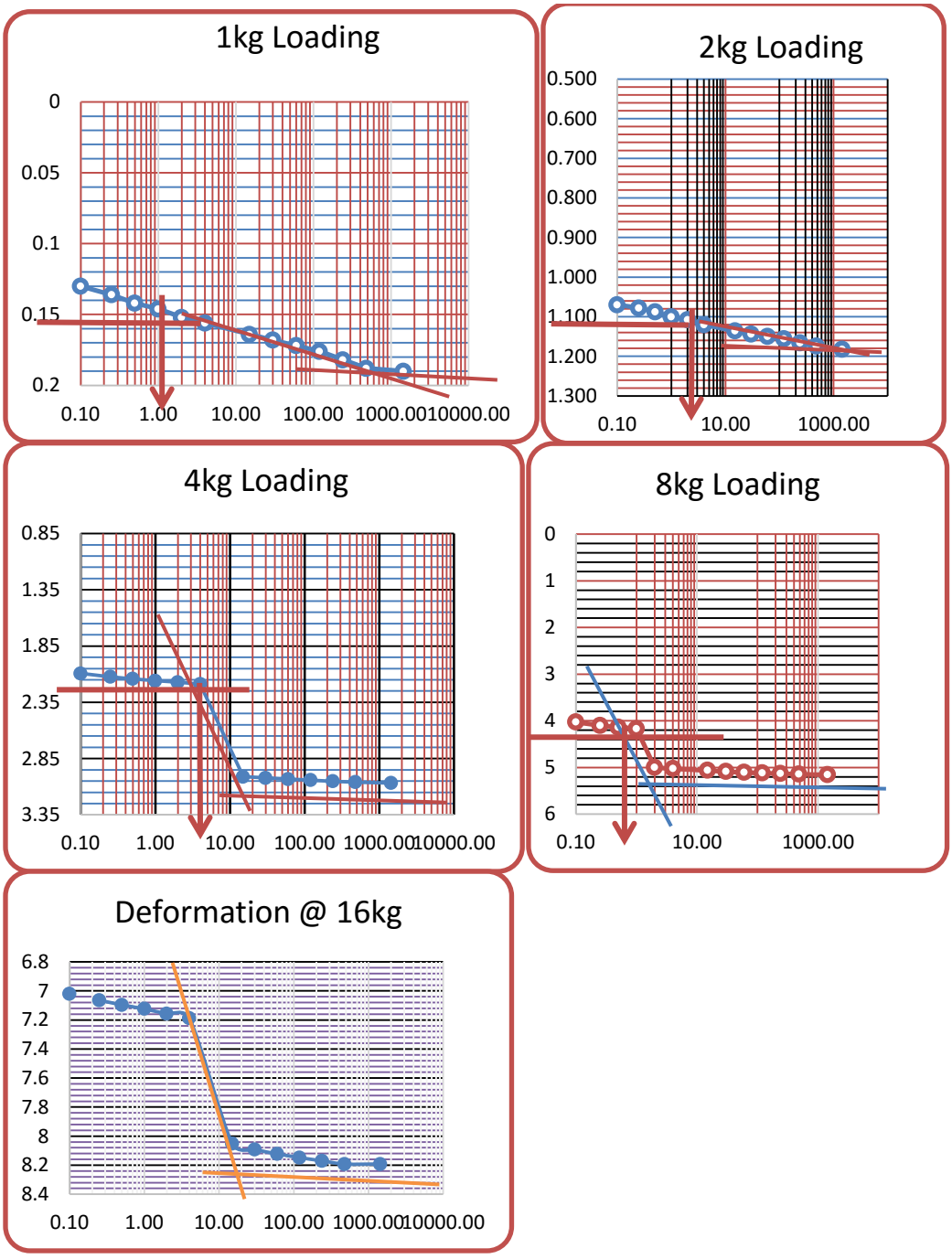
1kg Loading
0
0.05
0.1
0.15
0.2
0.10
1.00
10.00
100.00
1000.00
10000.00
2kg Loading
0.500
0.600
0.700
0.800
0.900
1.000
1.100
1.200
1.300
0.10
10.00
1000.00
4kg Loading
0.85
1.35
1.85
2.35
2.85
3.35
0.10
1.00
10.00
100.00
1000.00
10000.00
8kg Loading
0
1
2
3
4
5
6
0.10
10.00
1000.00
Deformation @ 16kg
6.8
7
7.2
7.4
7.6
7.8
8
8.2
8.4
0.10
1.00
10.00
100.00
1000.00
10000.00

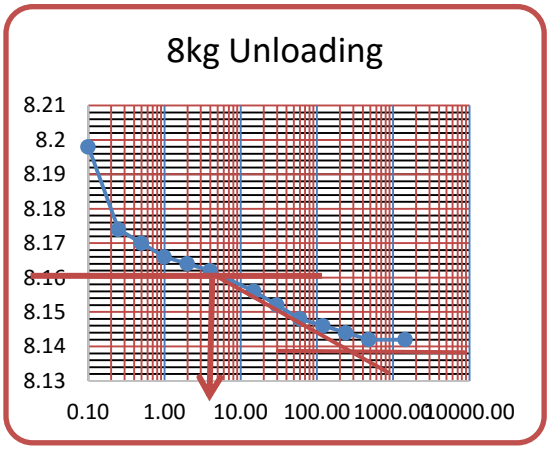
8kg Unloading
8.21
8.2
8.19
8.18
8.17
8.16
8.15
8.14
8.13
0.10
1.00
10.00
100.00
1000.00
10000.00

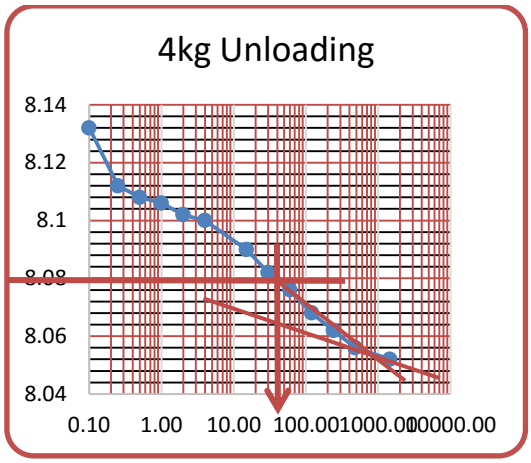
4kg Unloading
8.14
8.12
8.1
8.08
8.06
8.04
0.10
1.00
10.00
100.00
1000.00
10000.00

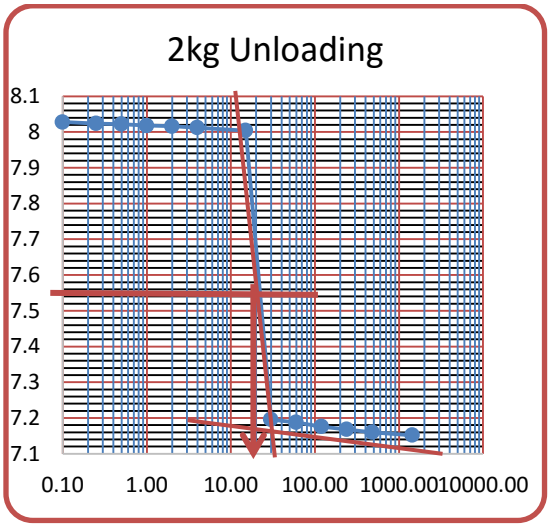
2kg Unloading
8.1
8
7.9
7.8
7.7
7.6
7.5
7.4
7.3
7.2
7.1
0.10
1.00
10.00
100.00
1000.00
10000.00

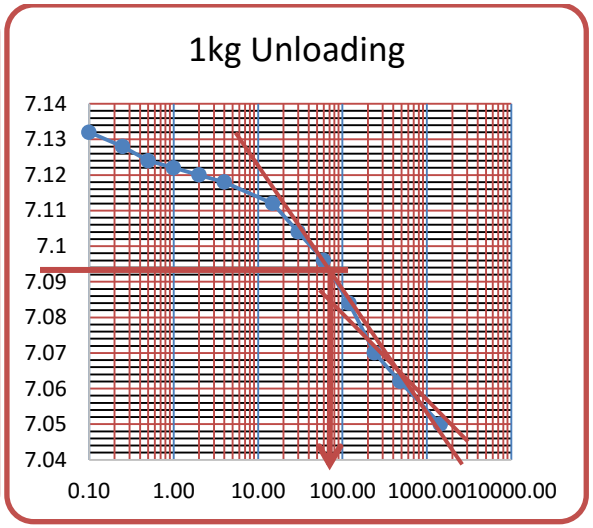
1kg Unloading
7.14
7.13
7.12
7.11
7.1
7.09
7.08
7.07
7.06
7.05
7.04
0.10
1.00
10.00
100.00
1000.00
10000.00

APPENDIX H

Table H-1 Soil sample at the Right side: - Triaxial Test Data Sheet

Soil sample at the: left and top side

Sample depth = 3m

Project Name: Nansabo District, Tullu Gola Peasant Association

Sample Number: R.S.T.P-4 and T.S.T.P-3

Sample Description: silty soil

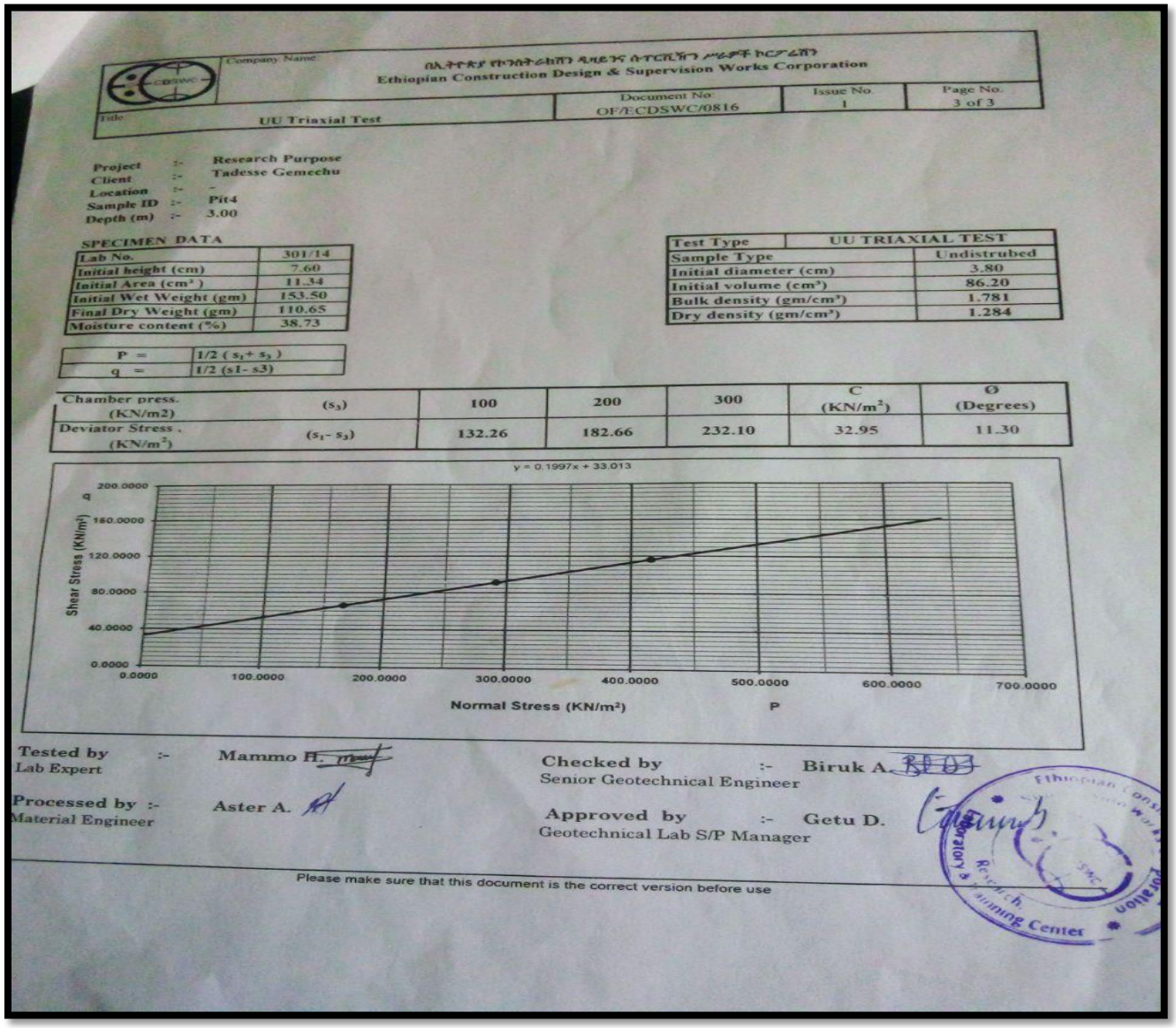

Company Name: በኢትዮጵያ የኮንስትራክሽን ዲዛይንና ሱፐርቪዥን ሥራዎች ኮርፖሬሽን
Ethiopian Construction Design & Supervision Works Corporation

Title	Document No	Issue No	Page No
UU Triaxial Test	OF/ECDSWC/0816	1	3 of 3

Project :- Research Purpose
Client :- Tadesse Gemechu
Location :- -
Sample ID :- Pit4
Depth (m) :- 3.00

SPECIMEN DATA

Lab No.	301/14
Initial height (cm)	7.60
Initial Area (cm²)	11.34
Initial Wet Weight (gm)	153.50
Final Dry Weight (gm)	110.65
Moisture content (%)	38.73

Test Type	UU TRIAXIAL TEST
Sample Type	Undistrubed
Initial diameter (cm)	3.80
Initial volume (cm³)	86.20
Bulk density (gm/cm³)	1.781
Dry density (gm/cm³)	1.284

P =	1/2 (s_1+ s_3)
q =	1/2 (s1- s3)

Chamber press. (KN/m2)	(s_3)	100	200	300	C (KN/m²)	Ø (Degrees)
Deviator Stress , (KN/m²)	(s_1- s_3)	132.26	182.66	232.10	32.95	11.30

Tested by :- Mammo H. — Lab Expert
Checked by :- Biruk A. — Senior Geotechnical Engineer
Processed by :- Aster A. — Material Engineer
Approved by :- Getu D. — Geotechnical Lab S/P Manager

Please make sure that this document is the correct version before use

Company Name

በኢትዮጵያ የኮንስትራክሽን ዲዛይንና ሱፐርቪዥን ሥራዎች ኮርፖሬሽን
Ethiopian Construction Design & Supervision Works Corporation

Title	Document No	Issue No	Page No
UU Triaxial Test	OP/ECDSWC/0816	1	2 of 3

Project :- Research Purpose
Client :- Tadesse Gemechu
Location :- -
Sample ID :- Pit3
Depth (m) :- 3.00

SPECIMEN DATA

Lab No.	300/14
Initial height (cm)	7.60
Initial Area (cm^2)	11.34
Initial Wet Weight (gm)	155.30
Final Dry Weight (gm)	118.80
Moisture content (%)	30.72

Test Type	UU TRIAXIAL TEST
Sample Type	Undistrubed
Initial diameter (cm)	3.80
Initial volume (cm^3)	86.20
Bulk density (gm/cm^3)	1.802
Dry density (gm/cm^3)	1.378

P =	1/2 (s_1+ s_3)
q =	1/2 (s1- s3)

Chamber press. (KN/m2)	(s_3)	100	200	300	C (KN/m^2)	Ø (Degrees)
Deviator Stress , (KN/m^2)	(s_1- s_3)	186.07	292.12	395.17	26.77	18.95

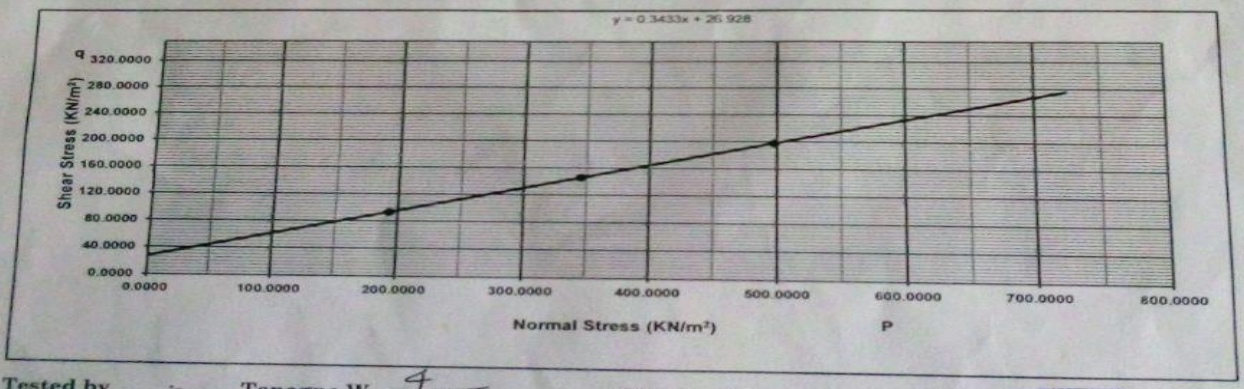

Tested by :- Tenagne W. — WA+M
Lab Expert

Checked by :- Biruk A.
Senior Geotechnical Engineer

Processed by :- Aster A.
Material Engineer

Approved by :- Getu D.
Geotechnical Lab S/P Manager

Please make sure that this document is the correct version before use

Company Name

በኢትዮጵያ የኮንስትራክሽን ዲዛይንና ቁጥጥር ሥራዎች ኮርፖሬሽን

ETHIOPIAN CONSTRUCTION DESIGN & SUPERVISION WORKS CORPORATION

Title: Geotechnical Laboratory Testing Report	Document No: OR/ECDSWC/0996	Issue No: 1	Page No: 1 of 2

Client Ref	-
Date Received	16/09/2021
Reported on	30/09/2021

Lab No. :-300/14-301/14
Submitted by :- Tadesse Gemechu
Project :- Research Purpose
Station :- -
Test Requested :- Triaxial Shear Test (UU).
Reported to :- Tadesse Gemechu

No.	Test Type	Standard Test Methods	Soil Samples Test Result	
			Lab No: 300/14 ID: Pit 3 Depth (m): 3.00	Lab No: 301/14 ID: Pit 4 Depth (m): 3.00
1	Triaxial Shear Test (UU)	ASTM D2850		
	C (kPa)		26.77	18.95
	Φ (Degree)		32.95	11.30

REMARK: The samples were collected & submitted to the laboratory by Client.

Processed by :- Aster A.
Material Engineer

Checked By :- Biruk A.
Senior Geotechnical Engineer

Approved By :- Getu D.
Geotechnical Lab. Q/R Manager

Ethiopian Construction Design & Supervision Works (ECDSWC) Research & Training Center

Among the major services rendered by the Geotechnical and Material Laboratory Testing s/processes of Ethiopian Construction Design & Supervision Works Corporation are
•**In Geotechnical Laboratory** -Testing the engineering properties of Soil Mechanics and Rock Mechanics.
•**In Material Testing Laboratory** - Testing the engineering properties of various Construction materials, such as Aggregates, Asphalts/Bitumen/, Cements, Rocks, Water, Reinforcement steel bars, Hollow Blocks, Bricks, Ceramics, Tiles,Asphalt & Concrete Core Tests, Concrete Mix Designs, Asphalt Mix Designs, Sampling of the soil and construction materials, and so on.

Please make sure that this document is the correct version before use.

APPENDIX I

Swelling Free Lab Test Result

Table F-1 Soil sample: - Data Sheet For Swelling Free Lab Test Result

Soil sample at the: right, left, top and bottom side

Sample depth = 2, 2.5, 2, 2 m

Project Name: Nansabo District, Tullu Gola Peasant Association

Sample Number: L.S.T.P-1, B.S.T.P-2, T.S.T.P-3 and R.S.T.P-4

Sample Description: Gray to brownish-silt soil

Designation	Depth(m)	Volume of sample in kerosene(ml)	Volume of sample in water(ml)	Free swell (%)
L.S.T.P-1	2	12	15	25
B.S.T.P-2	2.5	12	15	25
T.S.T.P-3	2	12	16	33.33
R.S.T.P-4	2	13	17	30.77